


2011

Performance Enhancement Using Cross Layer Approaches in Wireless Ad Hoc Networks

Murad Khallid

University of South Florida, sayf_k2000@yahoo.com

Follow this and additional works at: <http://scholarcommons.usf.edu/etd>

 Part of the [American Studies Commons](#), and the [Electrical and Computer Engineering Commons](#)

Scholar Commons Citation

Khallid, Murad, "Performance Enhancement Using Cross Layer Approaches in Wireless Ad Hoc Networks" (2011). *Graduate Theses and Dissertations*.

<http://scholarcommons.usf.edu/etd/3180>

This Dissertation is brought to you for free and open access by the Graduate School at Scholar Commons. It has been accepted for inclusion in Graduate Theses and Dissertations by an authorized administrator of Scholar Commons. For more information, please contact scholarcommons@usf.edu.

Performance Enhancement Using Cross Layer Approaches in Wireless Ad Hoc Networks

by

Murad Khalid

A dissertation submitted in partial fulfillment
of the requirements for the degree of
Doctor of Philosophy
Department of Electrical Engineering
College of Engineering
University of South Florida

Major Professor: Ravi Sankar, Ph.D.
Richard D. Gitlin, Sc.D.
Sudeep Sarkar, Ph.D.
Kandethody M. Ramachandran, Ph.D.
In-ho Ra, Ph.D.

Date of Approval:
March 3, 2011

Keywords: directional medium access control, cooperative scheduling, Rayleigh fading,
relay communication, polarization

Copyright © 2011, Murad Khalid

DEDICATION

To my lovely wife, children, my brother and parents

ACKNOWLEDGEMENTS

I am truly indebted to my supervisor, Dr. Ravi Sankar, for his guidance, support, impeccable patience, and constant encouragement during my Ph.D. study at USF. I am extremely grateful to Dr. Richard D. Gitlin, Dr. Sudeep Sarkar, Dr. Ramachandaran Kantethody and Dr. In-ho Ra for serving in my committee; and for their precious time and invaluable suggestions. I would also like to acknowledge Dr. Salvatore D. Morgera, Dr. Paris Wiley, Gayla Montgomery, Irene Wiley, and Becky Brenner from the Electrical Engineering Department at USF who have always been very helpful, supportive and kind. I owe much to Dr. In-ho Ra for his technical advice and fiscal support during my Ph.D. research at USF. I am also grateful to my dear friends and colleagues at the Interdisciplinary Communication Networking and Signal Processing (ICONS) group. I am particularly grateful to my dearest friends; Ismail Bütün, Dr. Kun Li, Dr. Xuan Hung Le, Yufeng Wang, Mukesh Agrawal and Raja Prasad, for their support, collaboration and encouragement. I am also thankful to all my friends in WCSP group for enlightening discussions and support.

Words are not enough to express my deepest gratitude to my wife, to my brother Dr. Humayun Khalid, to my mother and to my parents-in-law for their relentless support, encouragement and supplications.

In the end, the ultimate reality is that this would not be possible without the Will of God.

I pray to God to pave our way to ultimate knowledge and help us use it for the real benefit of mankind.

TABLE OF CONTENTS

List of Tables	v
List of Figures	vi
Abstract	x
CHAPTER 1 INTRODUCTION	1
1.1 Wireless Ad hoc Networks	1
1.2 Challenges and Constraints in Ad hoc Networks.....	4
1.3 Research Motivation	5
1.4 Contributions and Organization of this Dissertation.....	6
CHAPTER 2 A CROSS LAYER FRAMEWORK	11
2.1 Introduction	11
2.2 Literature Review and Motivation	13
2.3 Proposed Conceptual Framework	16
2.3.1 Awareness Descriptors and Parameters.....	18
2.3.2 Functional Architecture	20
2.3.3 Optimization Cycle	21
2.3.4 Awareness Optimizer.....	22
2.4 Cross Layer Framework Optimization.....	23
2.4.1 Simulation Scenario for Ad hoc Network	25
2.5 Concluding Remarks	30
CHAPTER 3 FINITE HORIZON SCHEDULING IN WIRELESS AD HOC NETWORKS	31
3.1 Introduction and Motivation	31
3.2 Literature Review.....	33
3.3 System Model and Assumptions.....	36

3.3.1	Network Model	36
3.3.2	Queue and Channel Behavior	38
3.3.3	Window Requirement	40
3.4	Two-User Optimal Policy	41
3.4.1	SR Versus Linear Optimal Strategy	44
3.5	Proposed SR Scheduling Strategy.....	47
3.6	Simulation Results and Discussion	47
3.7	SR Performance Limitations	51
3.8	Proposed GR Scheduling Scheme and Simulation Results	52
3.9	GR Soft Throughput Guarantee	55
3.10	Concluding Remarks.....	57

CHAPTER 4 COOPERATIVE RELAY BASED MAC PROTOCOLS FOR
WIRELESS AD HOC NETWORKS

	WIRELESS AD HOC NETWORKS	59
4.1	TWO-RELAY BASED COOPERATIVE MAC PROTOCOL.....	59
4.1.1	Introduction and Related Work	59
4.1.2	System Model	62
4.1.3	Proposed 2rcMAC Protocol.....	64
4.1.3.1	IEEE 802.11 MAC Protocol Overview	64
4.1.3.2	Basic Idea of 2rcMAC Protocol	65
4.1.3.3	2rcMAC Protocol Details	66
4.1.3.4	NAV Adaptation in 2rcMAC Protocol	72
4.1.3.5	2rcMAC Framing and Logical Addressing	75
4.1.3.6	Node Density and Relay Management	77
4.1.4	Comparative Analysis and Discussion	79
4.1.5	Performance Evaluation.....	82
4.1.5.1	Simulation Setup.....	83
4.1.5.2	Simulation Results and Discussion.....	85
4.2	COHERENCE TIME BASED COOPERATIVE MAC PROTOCOL.....	89
4.2.1	Proposed IrcMAC Protocol	90
4.2.1.1	IrcMAC Protocol Details.....	90
4.2.1.2	NAV Adaptation in IrcMAC Protocol.....	93

4.2.1.3	IrcMAC Framing and Logical Addressing	95
4.2.1.4	IrcMAC Relay Management.....	96
4.2.2	Performance Evaluation.....	97
4.2.2.1	IrcMAC Simulation Results and Discussion	97
4.2.2.2	Impact of Coherence Time on Performance	101
4.3	Concluding Remarks	103
CHAPTER 5	DIRECTIONAL COMMUNICATION IN WIRELESS AD HOC NETWORKS	105
5.1	Introduction.....	105
5.2	Throughput Performance Issues in Directional Communication.....	105
5.3	Description of DMAC Protocol	111
5.4	Simulation Results and Discussion	116
5.4.1	Simulation Scenario.....	116
5.4.2	Simulation Parameters	117
5.4.3	Simulation Results	119
5.5	Concluding Remarks.....	121
CHAPTER 6	ADAPTIVE DMAC PROTOCOL WITH INTEGRATED DESTINATION DISCOVERY FOR WIRELESS AD HOC NETWORKS	123
6.1	Introduction and Motivation	123
6.2	Literature Review	124
6.3	Proposed ADMAC Protocol	125
6.4	Analysis.....	131
6.5	Results and Discussion.....	135
6.6	Concluding Remarks.....	139
CHAPTER 7	POLARIZATION BASED DMAC PROTOCOL FOR WIRELESS AD HOC NETWORKS.....	141
7.1	Introduction and Motivation	141
7.2	Outdoor Propagation and Preliminaries	144
7.2.1	Polarization Background	145

7.2.2	Outdoor Propagation Environment.....	146
7.2.3	Polarization Diversity Antenna.....	148
7.3	Analysis.....	148
7.3.1	Directional System Model.....	149
7.3.2	Bound for \tilde{N}_v	151
7.3.3	Approximate Bound for P_s	154
7.4	Proposed Polarization Based DMAC Protocol.....	157
7.4.1	Idle Mode.....	162
7.4.2	Reception Mode.....	163
7.4.3	Transmission Mode.....	163
7.5	Simulation Results and Discussion.....	164
7.6	Concluding Remarks.....	171
CHAPTER 8 CONCLUSION AND FUTURE DIRECTIONS.....		173
8.1	Main Contributions.....	173
8.2	Future Directions.....	176
REFERENCES.....		178
APPENDICES.....		190
	Appendix A.....	191
	Appendix B.....	193
	Appendix C.....	194
ABOUT THE AUTHOR.....		End Page

LIST OF TABLES

Table 3.1	Simulation parameters	48
Table 3.2	Jain's fairness index comparison	51
Table 4.1	Simulation parameters	84
Table 5.1	Simulation parameters	118
Table 6.1	Simulation parameters	135
Table 7.1	Parameter list	155
Table 7.2	Simulation parameters	165

LIST OF FIGURES

Figure 1.1	Hybrid ad hoc network.....	3
Figure 1.2	Illustration of cross layer information exchange	6
Figure 2.1	Proposed cross layer framework.....	18
Figure 2.2	Optimization cycle	23
Figure 2.3	Awareness optimizer.....	24
Figure 2.4	Ad hoc network scenario	25
Figure 2.5	Average RTS packets transmission	26
Figure 2.6	Average packets retransmission due to ACK timeout	26
Figure 2.7	Average DuPACK packets received.....	27
Figure 2.8	Average number of RERR packets.....	27
Figure 2.9	Average time spent in queue.....	28
Figure 3.1	Timing sequence illustration.....	38
Figure 3.2	Two-user probability of transmission comparison between linear and SR schemes with $w = 30$, $P_{g_t}^{(1)} = P_{g_t}^{(2)} = 1$, and $\Delta = 0$	46
Figure 3.3	Aggregate throughput per finite horizon.....	50
Figure 3.4	Aggregate throughput scalability (Each node transmits 100 packets)	50
Figure 3.5	Average throughput variance per window	51
Figure 3.6	Aggregate throughput performance for SR and GR at 5 dB and 7 dB of channel asymmetry	55

Figure 4.1	Cooperative ad hoc network illustration	63
Figure 4.2	RR frame format	71
Figure 4.3	Message sequence for two best relays scenario	71
Figure 4.4	Message sequence for one or no best relay scenario	72
Figure 4.5	Message sequence for no relay response scenario	72
Figure 4.6	2rcMAC NAV update mechanism for one best relay scenario.....	75
Figure 4.7	Frame format for 2rcMAC protocol	77
Figure 4.8	Average relay node statistics with rates greater than 1 Mbps.....	79
Figure 4.9	Average relay node statistics with rates greater than source- destination rates	79
Figure 4.10	Saturation throughput comparison as a function of distance for 2rcMAC	88
Figure 4.11	Average delay for successful packet transmission for 2rcMAC.....	88
Figure 4.12	Network saturation throughput for 2rcMAC	89
Figure 4.13	Message sequence for the best relay scenario for IrcMAC	93
Figure 4.14	IrcMAC NAV update mechanism for best relay scenario	95
Figure 4.15	Saturation throughput comparison as a function of distance for IrcMAC	100
Figure 4.16	Average delay for successful packet transmission for IrcMAC	101
Figure 4.17	Network saturation throughput for IrcMAC	101
Figure 4.18	Impact of coherence time on saturation throughput for IrcMAC	103
Figure 5.1	Illustration of directional versus omni-directional communications	107
Figure 5.2	Percentage of failure factors in directional communication	110
Figure 5.3	Finite state machine for DMAC.....	114
Figure 5.4	Directional channel reservation mechanism	116

Figure 5.5	Simulation scenario snapshot.....	117
Figure 5.6	Throughput performance omni versus directional	121
Figure 5.7	Throughput performance omni versus directional for reduced distance	121
Figure 6.1	Source node flow control for ADMAC	130
Figure 6.2	Transmitter (T) and Receiver (R) search span illustration.....	131
Figure 6.3	Illustration of cases for search span estimation	131
Figure 6.4	Total average throughput as a function of transmission probability for $\alpha = 60^\circ$ and $v = 10, 20, 30, 70$ (m/s)	136
Figure 6.5	Total average throughput as a function of transmission probability for $\alpha = 30^\circ$ and $v = 10, 20, 30, 70$ (m/s)	137
Figure 6.6	Total average throughput as a function of transmission probability for $\alpha = 10^\circ$ and $v = 10, 20, 30, 70$ (m/s)	137
Figure 6.7	Total average throughput as a function of nodes for $\alpha = 60^\circ$ and $v = 10, 20, 30, 70$ (m/s)	138
Figure 6.8	Total average throughput as a function of nodes for $\alpha = 30^\circ$ and $v = 10, 20, 30, 70$ (m/s)	138
Figure 6.9	Total average throughput as a function of nodes for $\alpha = 10^\circ$ and $v = 10, 20, 30, 70$ (m/s)	139
Figure 7.1	Depiction of depolarization in urban/suburban propagation environment	146
Figure 7.2	Signal losses and impairments through channel	147
Figure 7.3	System model for interference analysis	150
Figure 7.4	Lower bound for probability of success in directional antenna case	156
Figure 7.5	Interference example.....	158
Figure 7.6	Receiver flow chart.....	159
Figure 7.7	Transmitter flow chart.....	160

Figure 7.8	Node average throughput performance for 8 nodes.....	166
Figure 7.9	Node average throughput performance for 16 nodes.....	166
Figure 7.10	Node average throughput performance for 24 nodes.....	167
Figure 7.11	Node average throughput performance for 32 nodes.....	167
Figure 7.12	Node average throughput for 8, 16, 24, and 32 nodes at 1.95 Mbps	168
Figure 7.13	Comparison of average delay for 8 nodes.....	170
Figure 7.14	Comparison of average delay for 16 nodes.....	170
Figure 7.15	Comparison of average delay for 24 nodes.....	171

ABSTRACT

Ad hoc network is intrinsically autonomous and self-configuring network that does not require any dedicated centralized management. For specialized applications such as, military operations, search-and-rescue missions, security and surveillance, patient monitoring, hazardous material monitoring, 4G (4th Generation) coverage extension, and rural communication; ad hoc networks provide an intelligent, robust, flexible and cost-effective solution for the wireless communication needs.

As in centralized wireless systems, ad hoc networks are also expected to support high data rates, low delays, and large node density in addition to many other QoS (Quality of Service) requirements. However, due to unique ad hoc network characteristics, spectrum scarcity, computational limit of current state-of-the-art technology, power consumption, and memory; meeting QoS requirements is very challenging in ad hoc networks. Studies have shown cross layer to be very effective in enhancing QoS performance under spectrum scarcity and other constraints.

In this dissertation, our main goal is to enhance performance (e.g., throughput, delay, scalability, fairness) by developing novel cross layer techniques in single-hop single-channel general ad hoc networks. Our dissertation mainly consists of three main sections. In the first section, we identify major challenges intrinsic to ad hoc networks that affect QoS performance under spectrum constraint (i.e., single channel). In the later parts of the dissertation, we investigate and propose novel distributed techniques for ad hoc networks

to tackle identified challenges. Different from our main goal, albeit closely related; in the first section we propose a conceptual cross layer frame work for interaction control and coordination. In this context, we identify various functional blocks, and show through simulations that global and local perturbations through parametric correlation can be used for performance optimization.

In the second section, we propose MAC (Medium Access Control) scheduling approaches for omni-directional antenna environment to enhance throughput, delay, scalability and fairness performance under channel fading conditions. First, we propose a novel cooperative ratio-based MAC scheduling scheme for finite horizon applications. In this scheduling scheme, each node cooperatively adapts access probability in every window based on its own and neighbors' backlogs and channel states to enhance throughput, scalability and fairness performance. Further, in the second section, we propose two novel relay based MAC scheduling protocols (termed as 2rcMAC and IrcMAC) that make use of relays for reliable transmission with enhanced throughput and delay performance. The proposed protocols make use of spatial diversity due to relay path(s) provided they offer higher data rates compared to the direct path. Simulation results confirm improved performance compared to existing relay based protocols.

In the third section, we make use of directional antenna technology to enhance spatial reuse and thus increase network throughput and scalability in ad hoc networks. In this section, we introduce problems that arise as a result of directional communication. We consider two such problems and propose techniques that consequently lead to throughput, delay and scalability enhancement. Specifically, we consider destination location and tracking problem as our first problem. We propose a novel neighbor discovery DMAC

(Directional MAC) protocol that probabilistically searches for the destination based on elapsed time, distance, average velocity and beam-width. Results confirm improved performance compared to commonly used random sector and last sector based directional MAC protocols. Further, we identify RTS/CTS collisions as our second problem which leads to appreciable throughput degradation in ad hoc networks. In this respect, we investigate and propose a fully distributed asynchronous polarization based DMAC protocol. In this protocol, each node senses its neighborhood on both linear polarization channels and adapts polarization to enhance throughput and scalability. Throughput and delay comparisons against the basic DMAC protocol clearly show throughput, scalability and delay improvements.

CHAPTER 1

INTRODUCTION

1.1 Wireless Ad hoc Networks

The age of ubiquitous communication and pervasive computing is here. Indeed applications of wireless ad hoc networks in the realms of military operations; unmanned airborne surveillance missions, search-and-rescue operations, scientific monitoring of habitat and environment, simple peer-to-peer communication, 4G cellular network extension, home networking, social networking, external and internal patient monitoring, security, and intelligent transportation services, clearly remind us that wireless communication and ad hoc networking has undoubtedly become indispensable part of our lives (see [1] and refs. therein).

Over the last few years, extensive academic research in ad hoc networks and technological development on many fronts, for instance: Bluetooth, Zigbee, Hiperlan, and IEEE 802.11 systems; modulation/coding, multiple antenna, and multiuser detection techniques; MAC, routing; and access security protocols have attracted global industrial and commercial interests in wireless ad hoc networks. Today, we witness unprecedented popularity of wireless ad hoc network in the form of traditional mobile ad hoc networks (MANET), hybrid ad hoc networks, wireless sensor networks (WSN), wireless mesh networks (WMN) and vehicular ad hoc networks (VANET) [2].

Ad hoc network consists of nodes that communicate over a common wireless channel in an autonomous and distributed manner. The nodes in the network dynamically self-organize without any pre-existing infrastructure. Ad hoc networks can generally be classified as traditional ad hoc networks, hybrid ad hoc networks, sensor networks, mesh networks and vehicular ad hoc networks.

- 1) Traditional Ad hoc Network: Traditional ad hoc network nodes are fully autonomous with no dedicated controlling or managing entity, and more importantly they are not designed for specific application in mind. Although, a few nodes can temporarily assume a partial supervisory role, but they all follow the basic paradigm of data transfer in a fully distributed and cooperative manner [3], [4]. Traditional ad hoc networks have primarily been cherished by the academic research community, but interestingly research and funding in traditional ad hoc networks domain has further spurred major developments towards real world wireless ad hoc networks.
- 2) Hybrid Ad hoc Network: Hybrid ad hoc network consists of autonomous nodes that communicate with each other in a multi-hop topology, and in addition, can communicate with the cellular network either directly or indirectly via other nodes as shown in Fig. 1.1. The main advantage of this hybrid approach is increased coverage in areas where it is costly or impractical to install base stations [5].
- 3) Sensor Network: Sensor network typically consists of a large collection of low cost and small size transceiver nodes that are stationary. It is mainly used for industrial monitoring, environmental monitoring, habitat monitoring, patient's health monitoring (e.g., body sensor networks), etc. In sensor network, each sensor node senses and collects data and then forwards it to one or more data sinks [6].

- 4) Mesh Network: Wireless mesh network consists of two types of nodes: clients and routers [7]. Nodes behaving as routers are stationary and have stable power supply. One or more router nodes may have wireless access to the internet gateway. The client nodes have limited power supply and are typically mobile. Application of mesh network includes local area networks (LANs) and metropolitan area networks (MANs). Mesh network is particularly beneficial for establishing wireless communication capability in rural areas.
- 5) Vehicular Ad hoc Network: In vehicular ad hoc network communication takes place between vehicles. The vision is to equip each car with transceiver so that hundreds of car can spontaneously form an ad hoc network. Major applications include car safety, nearby attractions and parking information, etc., [8, 9].

In the following section we highlight critical challenges as pertains to the ad hoc networks.

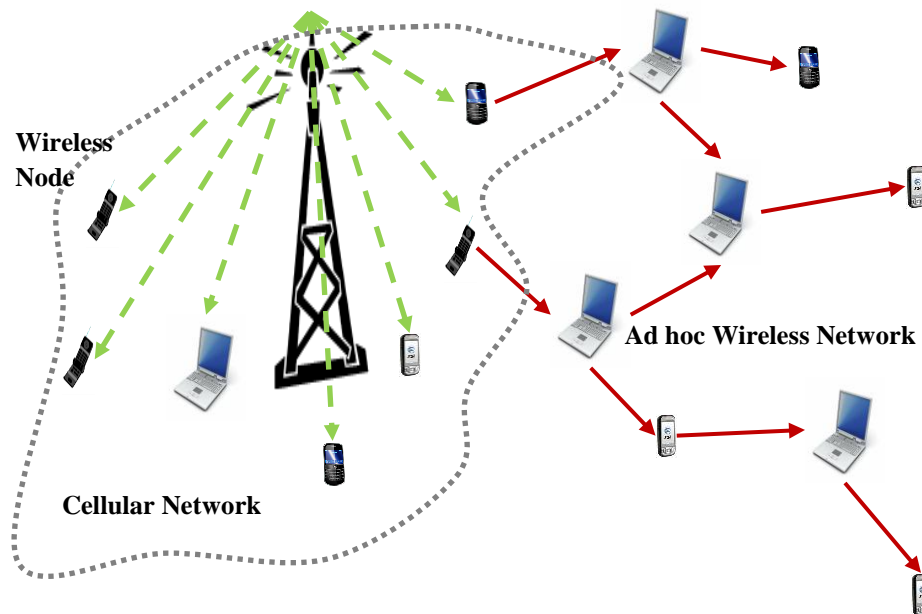


Figure 1.1 Hybrid ad hoc network

1.2 Challenges and Constraints in Ad hoc Networks

Increasing deployment of ad hoc network for different applications is due to its inherent advantageous characteristics: such as, self-configuration, mobility, multi-hop behavior, no single point of failure, autonomous behavior, infrastructureless operation, ease of deployment, and low cost. However, the benefits and flexibility of ad hoc networks inevitably introduce many design challenges and constraints:

- 1) Dynamic topology due to nodes' mobility leads to packet losses, network partition, and network instability due to frequent route disconnections
- 2) Broadcast nature of wireless link leads to unavoidable interference and thus causes packet errors
- 3) Limited bandwidth of wireless links lead to lower QoS compared to wired links
- 4) Heterogeneous nodes with different capabilities (e.g., air interfaces) create further challenges
- 5) Limited battery power
- 6) Network connectivity depends on transmission power, nodes density, and dynamic topology
- 7) Network reliability and robustness depends on autonomous nodes' behavior, node density, network load, topology changes, and link disconnections
- 8) Network security is critical since wireless links are prone to eavesdropping
- 9) Network scalability presents a daunting challenge for QoS delivery (for example, throughput or delay guarantees, etc.), network management, and security

Specific to some aforementioned challenges in wireless ad hoc networks, it is shown that with existing technologies, per node throughput decays as $\frac{c}{n^{1.68}}$, where n is the

number of nodes and c is a constant [10, 11]. It is shown in [12] that with IEEE 802.11 technology, MANETs are practically beneficial up to 2-3 hops and up to 10-20 nodes. [13] has shown that multi-hop throughput degradation is closely coupled to MAC contentions. [14] theoretically shows that throughput per node improves with mobility in ad hoc networks. However, the underlying assumption is that the source transmits to the destination only when they are very close to each other (reduces interference), the probability of which is extremely low. This also points to the fact that to maintain network connectivity, low power transmission for interference reduction is not a viable option [3, 4].

Thus, finding solutions to the aforementioned challenges (to enhance ad hoc network performance) have become the holy grail for researchers. However, it is known that there is no one solution to the above problems. Specific solutions for specific problems are sought by the researchers. Seminal research contributions harnessing interactions from physical layer to higher layers (known as cross layer approach) have shown significant performance gains in enhancing network performance [15]. In this regard, cross layer framework and design coupling approaches using multiple channels, directional communication, and MIMO (Multiple-Input-Multiple-Output) antenna technology have also been investigated to enhance various network performance metrics (i.e., throughput, delay, fairness, scalability, energy consumption, etc.) [16, 17].

1.3 Research Motivation

Traditional OSI (Open System Interconnect) layered approach does not provide significant gains in performance due to limited exchange of standardized primitives between adjacent layers [18]. As previously mentioned, ad hoc network performance is

severely limited due to its inherent characteristics. In particular, MAC performance begins to dwindle under high node density, heavy load and channel fading conditions. Cross layer approaches are known to provide significant performance improvement (see Fig. 1.2). Based on this motivation, work in this dissertation commonly explores cross layer information and design coupling techniques across physical and MAC layers to improve throughput, delay and scalability performance under heavy load and channel fading conditions.

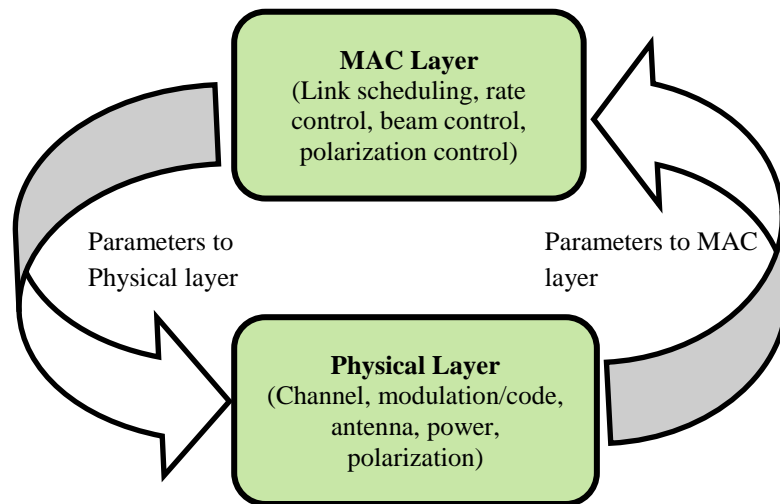


Figure 1.2 Illustration of cross layer information exchange

1.4 Contributions and Organization of this Dissertation

Cross layer approaches can be roughly classified as information coupling, design coupling, layer merging, vertical coupling, and interlayer architectures [16]. In the main body of this dissertation, our work primarily focuses on information and design coupling approaches. In the context of this dissertation; information coupling implies that information from physical layer is made available to MAC layer for performance

improvement, and design coupling implies that MAC protocol is designed to accommodate physical layer capabilities; for instance, directional antenna beam-forming, etc.

In Chapter 2, we propose a conceptual cross layer framework based on vertical layer architecture for performance enhancement [19]. Primary contribution is the functional architecture of the vertical layer which is primarily responsible for cross layer interaction management and optimization. The second contribution is the use of optimization cycle that comprises awareness parameters collection, mapping, classification and the analysis phases. The third contribution is the decomposition of the parameters into local and global network perspective for performance optimization. We have shown through simulations how parameters' variations can represent local and global views of the network and how we can set local and global thresholds to perform opportunistic optimization.

In Chapter 3, a simple ratio-based (SR) cooperative scheduling scheme with minimal signaling to enhance network throughput, scalability and fairness for single hop single channel wireless ad hoc network is presented [20, 21]. In the proposed scheme, finite horizon is divided into multiple shorter windows consisting of data transmission and cooperation windows. Nodes adapt access probability thresholds cooperatively in each cooperation window for subsequent data transmissions. Through analysis users' thresholds are shown to be time variant for throughput maximization with fairness in each window. Simulation results clearly show that compared with non-cooperative random access strategy (e.g., CSMA/CA), SR scheme achieves stable throughput and is scalable in terms of the number of nodes. SR fairness index performance is better in case

of symmetric and asymmetric channels compared to non-cooperative random access strategy. Further, we modify SR scheme to GR (General Ratio) scheme that balances between fairness and throughput by giving precedence to nodes with relatively best channels and reasonable backlogs or nodes with reasonable channel states and larger backlogs [21]. In GR Scheme, nodes cooperatively adapt access probabilities in each window based on the ratio of weighted backlog to the total weighted backlogs. It is shown that under asymmetric channel conditions GR improves throughput compared to SR scheme.

Cooperative communication paradigm promises improved throughput and delay performance by effective use of spatial diversity in wireless ad hoc networks. In Chapter 4, we propose two novel cooperative MAC protocols termed as 2rcMAC and IrcMAC [22, 23]. The 2rcMAC protocol makes use of two cooperating nodes to achieve superior throughput and delay performances, compared with the existing cooperative MAC protocols. The secondary relay path is invoked as a backup path for better transmission reliability and higher throughput through the relay path. IrcMAC is a single relay protocol that uses channel coherence time and instantaneous signal-to-noise ratio (snr) of source-to-relay, relay-to-destination and source-to-destination links; to reliably choose between single relay path or direct path for enhanced throughput and delay performances. Moreover, handshaking and single bit feedbacks resolve contentions among relay nodes in close proximity at the time, and further provides source node with rate information on source-to-destination, source-to-relay and relay-to-destination links. Performance gains achieved by the 2rcMAC and IrcMAC protocols under fast fading condition over the existing cooperative MAC protocols are compared and discussed. Results clearly show

that 2rcMAC and IrcMAC protocols significantly outperform CoopMAC I ([84, 85]) and UtdMAC ([87]) in terms of throughput, delay and scalability performances.

Seminal work using directional antennas in wireless ad hoc networks has clearly demonstrated throughput improvement due to effective spatial reuse [24]. Chapter 5 serves as a prelude to contributions in Chapters 6 and 7. In Chapter 5, directional MAC (DMAC) protocol is introduced and DMAC throughput performance is compared to omni-directional communication under heavy load and increased density conditions with no power control [25, 26]. Directional antenna throughput is shown to degrade drastically and approach omni-directional performance level at high traffic rates. Further, in Chapter 5, major problems that are introduced due to directional antennas are expounded upon in detail. Specifically, neighbor discovery and RTS (request-to-send)/CTS (clear-to-send) collisions problems in ad hoc networks are tackled in Chapter 6 and 7 using cross layer design coupling approach.

In Chapter 6, novel DMAC protocol with integrated neighbor discovery is developed to improve throughput performance in wireless ad hoc networks [27]. Under heavy load, high mobility and narrow beam-width conditions, frequent updates are required to track the destinations. However, frequent updates may degrade the effective throughput of the network. Proposed Adaptive Directional MAC (termed ADMAC) protocol with integrated destination discovery estimates destination's possible search span and then initiates transmission in that search span direction. Average throughput performance is compared between last sector (LS), random sector (RS) and search span approaches. Average throughput results show an improvement of up to 40 % and greater than 400 %, when compared to the LS and the RS based DMAC protocols, respectively.

In Chapter 7, RTS/CTS collisions are reduced under high density and heavy load conditions. We propose a fully distributed DMAC protocol that cooperatively makes use of polarization diversity in low-mobility urban/suburban outdoor wireless ad hoc network environment [28]. In the proposed cooperative polarization based DMAC protocol (PDMAC), each node directionally senses on both vertical and horizontal polarizations and adapts polarization that minimizes overall interference in the ad hoc network. Analysis is performed to establish relationship between vertically and horizontally polarized nodes in the network. Further, a theoretical lower bound is derived for probability of successful transmission to show capacity improvement as a function of cross polarization ratio (CPR). Simulation results confirm from 2 % (for 8 nodes) up to 400 % (for 32 nodes) improvement in average per node throughput at traffic rate of 1.95 Mbps when compared to the traditional DMAC protocol. Moreover, our study clearly shows that the average throughput difference increases with increasing node density when compared to the traditional DMAC protocol.

In Chapter 8, we summarize our contributions from Chapters 2-7 and then propose recommendations for future work.

CHAPTER 2

A CROSS LAYER FRAMEWORK

2.1 Introduction

Cross layer approach has undoubtedly proven itself as a promising step forward in wireless network performance optimization. Recent trends in wireless networks allow users with heterogeneous service requirements to communicate effectively in a dynamic resource-limited environment. Each user has their own set of end-to-end QoS requirements that the wireless network must satisfy. To cater to multiple user service requirements every bit of available resource has to be used in an optimal manner. The quest for optimization consequently leads to establishing and harnessing the richer interactions between the OSI layers of the communication stack. Each layer of the OSI protocol stack has to perform a specific set of functions and depending upon the user service requirement each function needs to adapt based on the information from the other layers. For instance, if the mobile user in a centralized wireless network has a stringent throughput requirement; the MAC layer can dynamically adapt the modulation and coding based on the channel feedback from the Physical (PHY) layer to optimize user's throughput. The Network (NET) layer can, in turn, assign appropriate channel so that the interference is minimized for the user on that channel. Another example that has been cited in numerous papers ([15-17, 29]) is that of the TCP window reset in Transport (TRAN) layer. It is shown that the TCP window size resets to unity when the signal

fading results in packet errors. The TCP misinterprets ACK delay due to retransmissions (on account of signal fading) as the sign of congestion in the network and consequently resets its transmission rate window. It is shown that if the TCP gets insight into congestion by using the Explicit Congestion Notification (ECN) bit or the Explicit Loss Notification (ELN) bit, then it can easily distinguish the actual cause of delay and, therefore, avoid resetting its transmission window. This clearly depicts that many layers can interact concurrently and exchange their protocol variables to squeeze out better performance in every possible way to achieve the optimal performance goal.

Many wireless networks like ad hoc networks, sensor networks and third-generation (3G) cellular networks require real time adaptations for dynamic network conditions and changing user requirements. Furthermore, recent development in multi-antenna and multi-packet capture technologies requires the OSI layered architecture to be flexible enough to fully utilize the potential of the above technologies.

Indeed the temptation of using the cross layer interaction for performance optimization is irresistible. However, the long term consequences of unbridled cross layer interaction schemes in a heterogeneous wireless environment, can lead to a chaotic collection of disparate cross layer techniques that may not interoperate flexibly. This obviously requires us to think how far we want to go beyond the layered architecture or how much of a trade-off is acceptable so that the performance and interoperability objectives are achieved. So far, the research community has mainly focused on interactions between various combinations of non-adjacent layers to meet specific performance goals. Thus, to date there are still a number of unresolved questions in this realm of cross layer optimization and many issues that remain unexplored. Some important open questions are

related to the monitoring of the parameters that trigger interactions; type of trigger event; statistical significance of the trigger; trigger relationship to performance goals; generation and control of interactions; standardization of cross layer framework and interactions.

2.2 Literature Review and Motivation

Generally, cross layer research contributions can be categorized into cross layer design surveys ([15, 16, 29, 30]), design coupling approaches ([17, 31-38]), cross layer architecture for information sharing ([18, 39]), and cross layer interaction characterization and modeling ([40-42]). A broad level definition and classification of cross layer designs, type of cross layer couplings and challenges related to cross layer design were presented in [16]. However, it only provides high level glance into cross layer architecture and framework. The authors in [29] highlighted the importance of reference architecture with respect to long term performance goals, ease of modification, stability and reliability. It convincingly points out that cross layer approach to optimization can lead to unintended conflicts between various performance requirements of different layers. Furthermore, cross layer modifications are not easy and require understanding of interactions between parameters and so tracing and debugging code becomes very difficult. A survey of cross layer optimization solutions related to third-generation (3G) wireless mobile networks was presented in [15]. The paper adopts a vertical layer approach with security, QoS, mobility and link adaptation layers as the vertical layers that are visible to the standard OSI layers. It characterizes various types of interactions and signaling into inter-layer, intra-layer control messages within the host and between different hosts. However, it does not discuss existing cross layer frameworks that control and manage all the interactions and signaling in a stable manner. An

exhaustive survey of cross layer approaches related to sensor networks can be found in [30]. Papers reviewed are based on design coupling approaches, where pairs of PHY, MAC, NET and TRAN layers interact to optimize certain performance goals. However, it lacks any discussion on generic cross layer framework architecture.

A small set of contributions related to cross layer design coupling approach are presented in [31-38]. In [31], PHY layer capture and multi-packet reception capability in conjunction with MAC layer to improve throughput and delay performance of the wireless network is presented. In [32], a PHY-MAC cross layer interaction is exploited to optimize throughput and delay. It introduces a new multiple-input-multiple-output (MIMO) based MAC protocol extension to 802.11a that enables multi antenna terminals to communicate with each other in multiplexing mode and/or diversity mode in a low correlation wireless propagation environment. In [33], cross layer interaction between MAC and NET network layers is exploited. It proposes throughput increase via interference based routing protocol that chooses routes with minimal interference using spatial proximity of transmitters. In [34], a design coupling approach using PHY, MAC and NET layer interactions for a centralized multi-hop wireless network is developed to minimize end-to-end latency. In [35], a PHY-MAC cross layer interaction is used to optimize end-to-end throughput and energy efficiency for a set of pre-defined routes in a multi-hop wireless network. The authors in [36] propose the MAC, NET and TRAN layer interactions to optimize the throughput based on congestion price input. The algorithm is based on using the congestion metric to reduce congestion which impacts the throughput of a multi-hop route. A cross layer approach to optimize network lifetime, delay and energy consumption by jointly using routing and scheduling in a TDMA wireless ad hoc

network is presented in [37]. The scheme is based on utility function optimization which is defined as a weighted function of queue length, transmission power and node's utilization. The authors in [38] propose a cross layer approach to minimize energy consumption for transmission by joint scheduling, routing and using power control in a fixed TDMA wireless network.

In [18, 39, 43], a cross layer information sharing approach, in which modular architecture is preserved, is presented. In [18] cross layer framework is generic and somewhat close to our proposed framework. It is based on local and neighbor state information which is then collectively used to optimize based on performance criteria. However, managing or switching between different network applications and requirements is not clearly discussed. A cross layer framework for multimedia application in Ad Hoc networks can be found in [39]. The Framework is based on interaction between the middleware and the routing layers only. Middleware layer provides the QoS requirement to the routing layer for optimal route selection and the routing layer shares node location information with the middleware layer to provide data availability information. However, it lacks generic mechanism for controlling and managing interactions. In [43], another information sharing architecture in which a Network Status Layer is used as a repository to share parameters between layers is proposed. In contrast to the aforementioned contributions, our work defines a vertical layer architecture which is much more intelligent than just being a repository, with general functionalities as awareness parameters monitoring, mapping, classification and stochastic optimization using local and global network perspectives.

Characterization of interactions and their inherent stochastic behavior provide invaluable insight into protocol design and cross layer adaptation. But, unfortunately other than the contributions made available in [40-42], there is very little to be found. In [40], cross layer interaction models and the cross layer interaction arrays for three broad classes of cross layer atomic actions are defined. It provides a comprehensive list of interactions for various types of events and triggers. However, it does not address interaction management and control to achieve the required QoS. In [41], the authors interestingly point out that the stochastic behavior of the network is a combination of protocol dynamics and statistical behavior. Using methods insensitive to the correlation between dynamical and stochastic behavior, network performance characteristics can be accurately predicted to effectively use cross layer optimization. An exhaustive analysis of interactions between the MAC and the NET layers under varying packet injection rate, node's speed and mobility conditions was given in [42]. Results clearly show that under varying conditions different combination of protocols must be invoked at MAC and NET layer for optimal performance.

Despite many years of contributions in cross layer realm, not much consolidation is seen in terms of cross layer framework standardization and interoperability. This serves as the main motivation for our work. In this chapter, we propose a conceptual cross layer framework that can co-exist with the legacy systems and maintain modularity and stability.

2.3 Proposed Conceptual Framework

We propose a vertical layer based cross layer framework as shown in Figure 2.1. The vertical layer is not just a repository for the standard OSI layers to share parameters, but

provides a complete parameter exchange between layers in an intelligent and controlled manner. Modification to the existing protocols is required to create control and data information path between the horizontal and the vertical layers. The main idea is to design the vertical layer independent of the horizontal OSI layers and control the interactions through this intelligent vertical layer. Thus, the vertical layer can be thought of as the control engine (brain) behind the cross layer interactions which makes this framework modular, intelligent and adaptive. Some salient functions of the vertical layer framework are described as under:

- 1) Vertical layer is aware of the outside network(s) state, aware of the user, and aware of the internal state
- 2) Vertical layer communicates with the horizontal layers through V-SAP (Vertical Service Access Points) primitives
- 3) Vertical layer monitors interactions between horizontal layers
- 4) Vertical layer activates or deactivates any combinations of protocols in horizontal layers
- 5) Vertical layer monitors and changes protocol parameters depending upon outside network state, user state, and system state
- 6) Vertical layer performs optimization to make accurate adaptations
- 7) Vertical layer uses Awareness Knowledge and Policy Database to determine network type, policies, and performance goals; select appropriate protocols, and optimize performance
- 8) Vertical layer learns and updates Awareness Knowledge and Policy Database

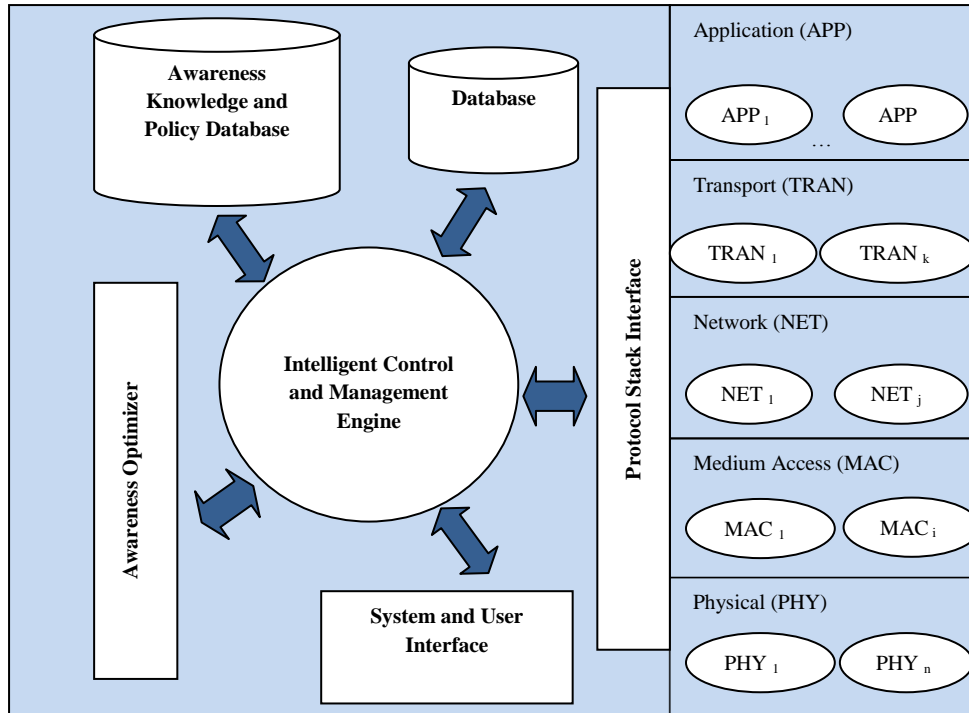


Figure 2.1 Proposed cross layer framework

The aforementioned vertical layer functions provide for a framework to adapt if the network environment changes or if a new service network becomes available.

2.3.1 Awareness Descriptors and Parameters

In this section we introduce awareness parameters related to vertical cross layer framework as shown in Appendix A. Awareness parameters are like state variables that comprise of many parameters as defined in the summary column of the table in Appendix A. The awareness parameters contain information about the local and global views of the network dynamics, channel and environment information, user requirements and behavior information, and internal system information. This information has to be extracted from the awareness parameters and mapped to awareness descriptors for proper information classification and database storage. Awareness descriptors are used by the awareness optimizer for decisions. The idea of awareness is mainly derived from

cognitive radio domain [44]. However, awareness introduced in [44] is primarily focused on location awareness related information. We know from wireless network environment that location awareness is just one piece of useful information in addition to other awareness descriptors, such as: system awareness, user awareness, RF awareness, protocol stack awareness, network awareness, application awareness, topographical awareness, and meteorological awareness.

Systems awareness used in the framework provides useful information about the node's self-awareness aspect. It may include battery life, bugs in the system, looping in the system, RF capabilities and limitations. In many network applications battery life is extremely important, since it has to be considered along with other performance goals and awareness monitoring. The system awareness descriptor encompasses energy and system interrupt awareness parameters. User awareness represents information regarding user behavior in time and location, and user generated commands. RF awareness provides information gathered from the PHY layer of the protocol stack. It contains RF state and Antenna mode awareness parameters. Protocol stack awareness defines monitoring of MAC, NET and TRAN layers' parameters and messages for performance optimization. Network awareness represents the type of network service available in the area, mode of service and capabilities, and security and encryption policies of the network. Application awareness contains information about user application requirements and its security and encryption constraints. Topographical awareness and meteorological awareness provide information about the terrain environment and climatic condition relative to the user location.

Furthermore, antenna mode awareness parameters define single antenna or multi-antenna configurations. The resultant RF awareness descriptor defines the channel characteristics and the antenna configuration, but does not provide any information about the climatic condition which can have detrimental propagation effects. Thus, in order to make an intelligent decision multiple awareness descriptors have to be jointly analyzed for performance enhancement.

2.3.2 Functional Architecture

The proposed cross layer framework is based on intelligent vertical layer architecture for interactions control and management. The vertical layer consists of six functional blocks: Intelligent Control and Management Engine (ICME), Protocol Stack Interface, System and User Interface, Database, Awareness Knowledge and Policy Database, and Awareness Optimizer.

The ICME is the brain of interactions control. It is primarily responsible for monitoring all awareness parameters, monitoring interactions between OSI layers, selecting protocols and tuning protocol parameters based on awareness optimizer decisions. The ICME communicates with the system, user and the OSI layers via the System, User and the Protocol Stack Interfaces, respectively. Protocol Stack Interface has the capability to receive and send any type of information from and to any protocol in a particular layer within the OSI protocol stack, respectively. Since, the communication can be with multiple layers at a time, therefore, V-SAP packet format needs to be defined with proper address, control and data sections. However, the interface definition is not within the scope of this work. The vertical cross layer framework contains two logical databases. The Awareness Knowledge and Policy Database contain pre-stored thresholds and cases

to be used for decision making. For example, for Network Awareness it may contain information about different types of networks, available services and modes of operation, security policies, and relevant protocols. As another example, User Awareness may contain information about user's time and location trend and user's application services history. This can prove very useful in pre-emptive adaptations where network dynamics change rapidly. The last functional block is the Awareness Optimizer which uses awareness parameters for optimization decisions.

2.3.3 Optimization Cycle

As explained before, the main purpose of the vertical cross layer framework is performance optimization. The modularity and standardized interaction between the OSI layers are maintained in this framework (see Fig. 2.1). The optimization performed by the vertical cross layer framework is based on three phases as depicted in Figure 2.2. The first phase is the monitoring phase, where all the internal and external events are constantly monitored. The rate of monitoring will actually depend on the application. Interested readers are referred to [15, 41] for a non-standardized list of interactions and events. In the monitoring phase, all awareness parameters are gathered in real time and stored in the database. The events trigger the optimization phase, where all the awareness parameters and awareness descriptors are classified and jointly analyzed. The comparison with the pre-stored cases and thresholds and optimization approach leads to decision output. The decision output triggers adaptation phase. In adaptation phase, the parameters belonging to the respective protocols and layers are tuned for performance enhancement. After the adaptation phase the optimization cycle repeats the monitoring phase. As seen in Figure 2.2, awareness learning phase represents updating of the Awareness Knowledge

and Policy Database if new cases or thresholds are learned during the optimization cycle. It must be kept in mind that awareness learning phase is not where the optimization cycle ends. Rather, it is invoked in parallel with the adaptation phase for learning purpose only.

2.3.4 Awareness Optimizer

In this section we introduce the functional block architecture of the Awareness Optimizer as shown in Figure 2.3. We propose three functional blocks within the Awareness Optimizer. The block shown in dotted line merely illustrates interaction with the Awareness Knowledge and Policy Database for strategies and is not part of the Awareness Optimizer. The function of Awareness Mapper is to map awareness parameters into awareness descriptors for categorization purpose. For instance, Awareness Mapper may extract information about the antenna operating in a multiplexing mode and the RF environment as the dense urban and utilize it as the RF awareness descriptor. This RF awareness descriptor is used by the classifier to generate local view of the network. The Awareness Classifier uses the awareness descriptors to extract performance goals, constraints, local and global view of the network. The local view comprises awareness parameters that provide information about the single hop neighbors where as global view comprises awareness parameters that provide information over multiple hops in the network. The Stochastic Awareness Analyzer block analyzes stochastic behavior of the local and global views of the network. The purpose is to determine the time scale of local and global perturbations. Then based on the local and global views; user behavior, awareness parameters, goals and constraints; the Stochastic Awareness Analyzer may search for best pre-stored strategies (e.g., heuristic optimization) to make decisions for the choice of protocols and parameters.

2.4 Cross Layer Framework Optimization

As emphasized before that vertical cross layer framework relies on Awareness Optimizer and Awareness Knowledge and Policy Database to make intelligent cross layer decisions. The computational complexity of the Awareness Optimizer can be reduced by pre-storing thresholds, cases and precedence. To clarify further, the pre-stored cases should address some of the following questions.

- 1) Is the RF environment urban, suburban or rural?
- 2) What should be the antenna mode?
- 3) What type of network service is available and what are its policies?
- 4) What are the security requirements for the network service?
- 5) Which protocols to invoke for available network services?

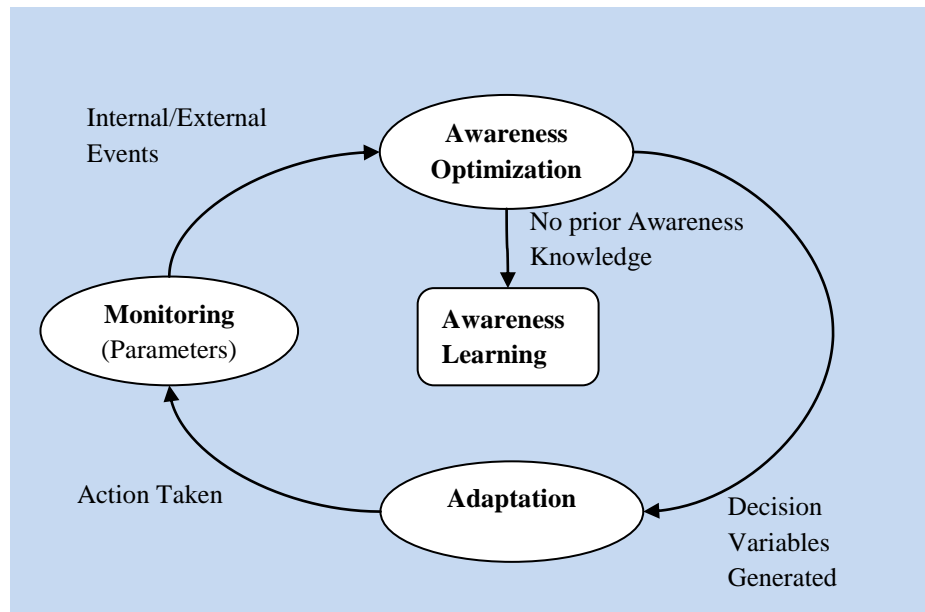


Figure 2.2 Optimization cycle

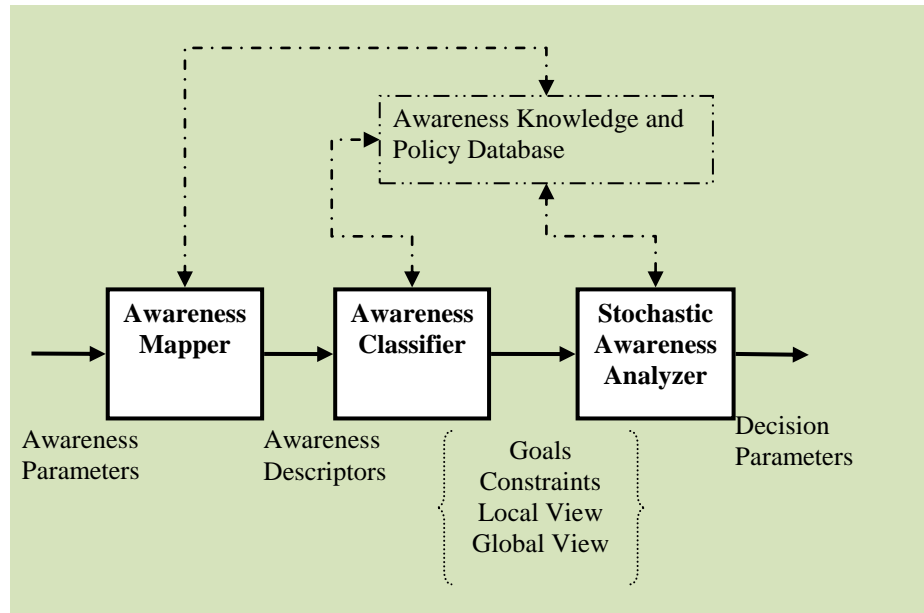


Figure 2.3 Awareness optimizer

- 6) What are the user's next location and corresponding service need?
- 7) What are the goals and constraints for the required applications?
- 8) What should be preferred modulation and coding for the required goals and constraints?
- 9) Is it a local or global perturbation?
- 10) Is the local or global perturbation critical or significant?
- 11) What should be adapted in case of particular local or global perturbations?
- 12) What should be adapted in case of medium or low battery energy?
- 13) What applications type to be switched in case of certain type of local or global perturbations?

It is worth mentioning that multi-objective optimization techniques can be used to enhance performance, but at the expense of increased computational complexity.

Although, discussion on optimization methods is beyond the scope of this work; yet, we believe that pre-stored thresholds, cases and scenarios can reduce computations and conflicts in complex scenarios.

2.4.1 Simulation Scenario for Ad hoc Network

Through simulation of an ad hoc network scenario, we illustrate how the Awareness Optimizer (described in section 2.3.4) can make a decision about the criticality of local and global perturbations. The local and global perturbation information can be obtained through implicit or explicit messages as briefly discussed in [15]. Subsequently, the Awareness Optimizer can isolate the stochastic perturbations into local or global perturbations and make appropriate decisions based on the goals and constraints.

The simulation was performed in QualNet 4.0 environment. In the simulation 100

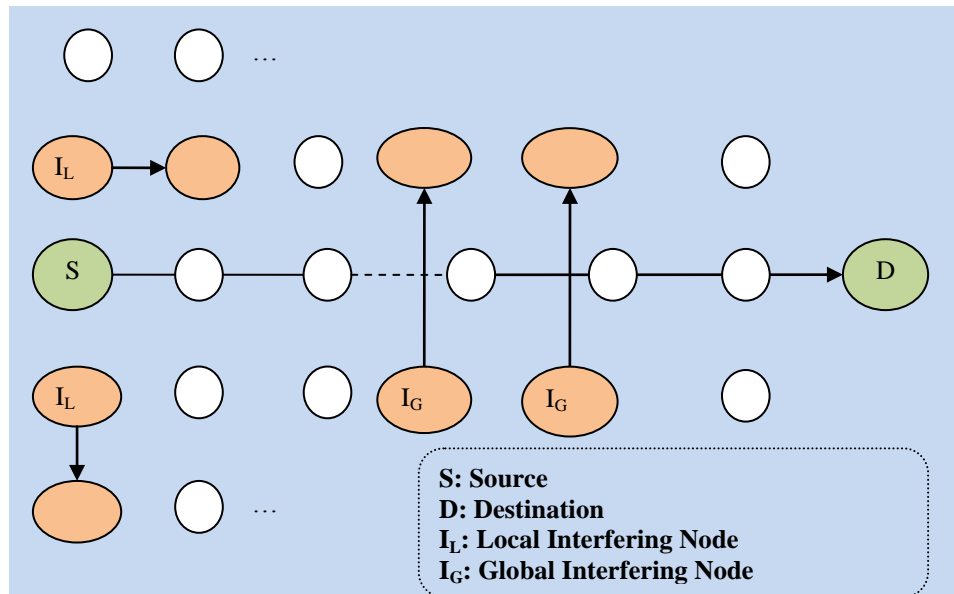


Figure 2.4 Ad hoc network scenario

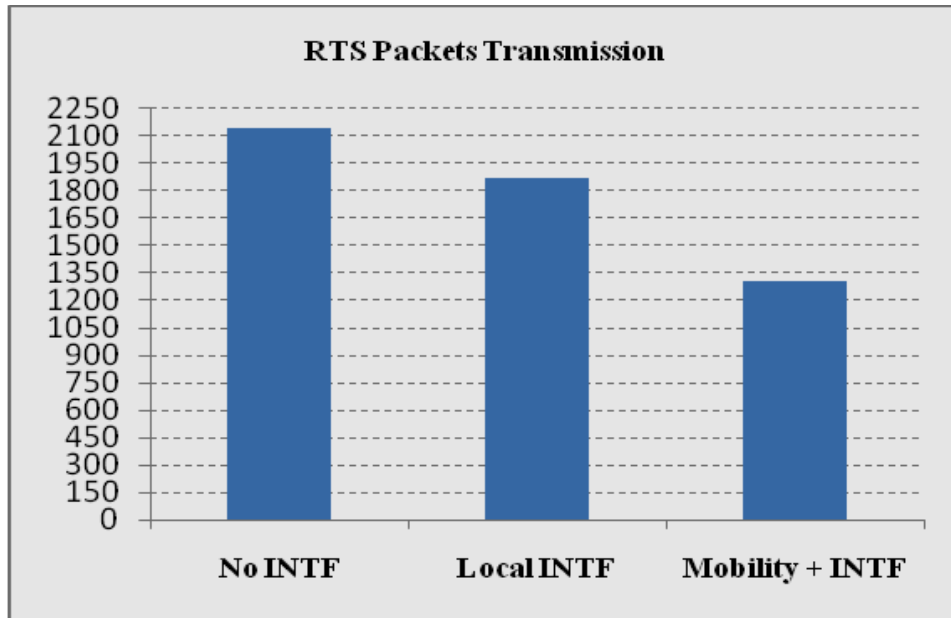


Figure 2.5 Average RTS packets transmission

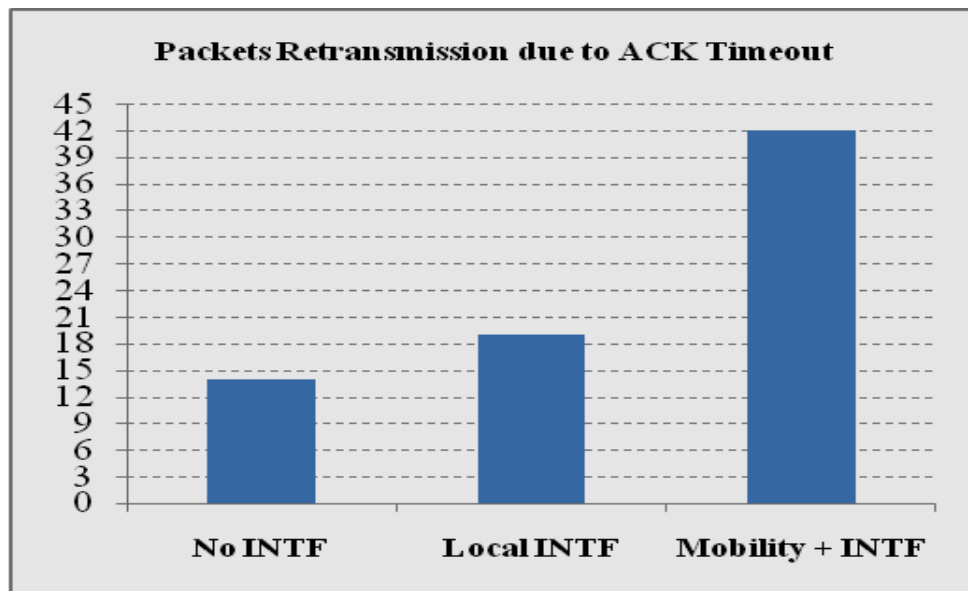


Figure 2.6 Average packets retransmission due to ACK timeout

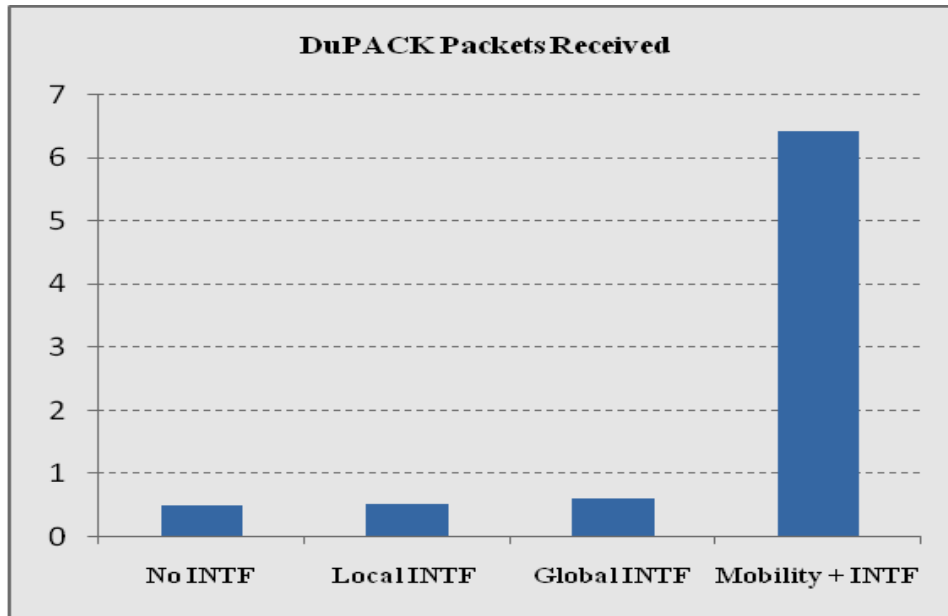


Figure 2.7 Average DuPACK packets received

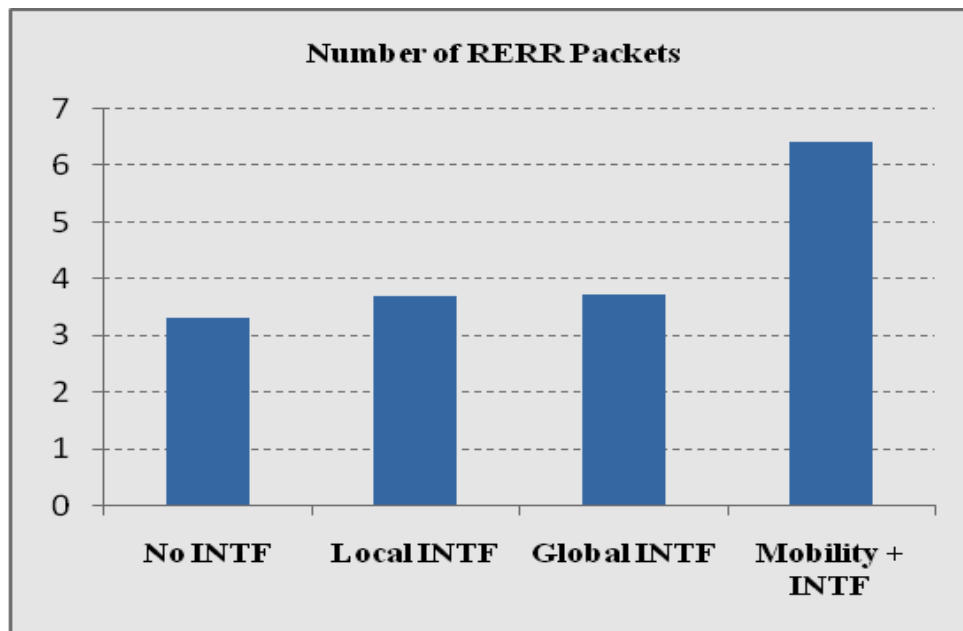


Figure 2.8 Average number of RERR packets

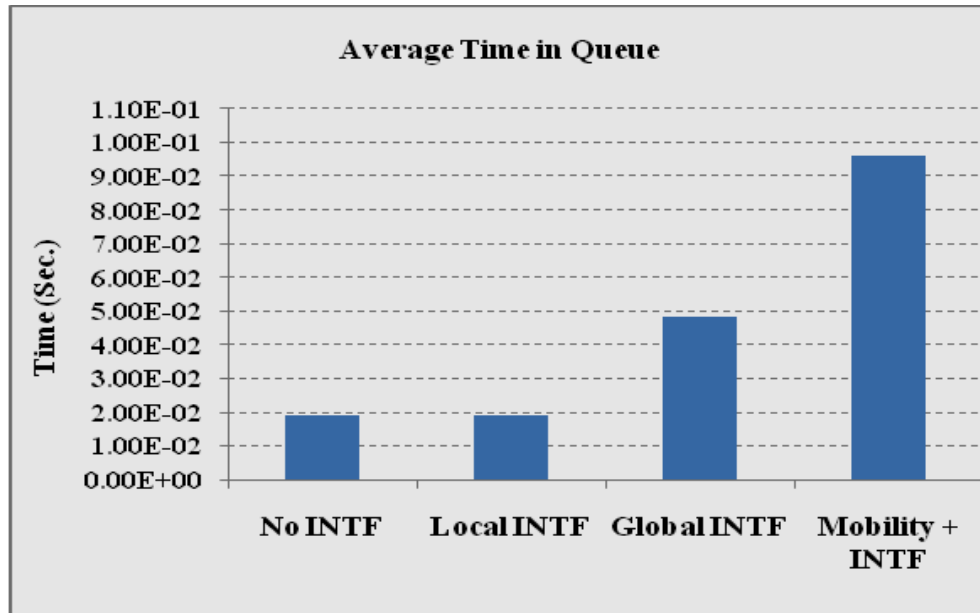


Figure 2.9 Average time spent in queue

nodes were placed in a grid format in an area of 1500x1500 m². A single File Transfer Protocol (FTP) multi-hop session was established between the source node and the destination node as designated by 'S' and 'D' letters in Figure 2.4. The routing protocol used was Dynamic Source Routing (DSR) and the MAC protocol was the standard IEEE 802.11b. The simulations were conducted in four separate steps. In the first step, only FTP sessions were activated with no mobility and without any local or global interference. In the second step, only local interference was created by creating independent sessions as designated by 'I_L.' The effects on parameters were observed at the source node 'S.' In the third step, only global interference was created by creating independent sessions as designated by 'I_G.' The global interfering nodes were placed in such a manner so that they interfere with intermediate hops of the FTP session. This global interference has no direct effect on the link at the source (S) or the destination (D) node. In the fourth step, mobility was introduced along with the local and global interferences. Random waypoint mobility model was used with a pause time of 30

seconds and a random speed of 0-10 meters/second. The observed parameters were averaged over ten independent runs for each step, where each run is for the duration of 600 seconds.

The parameters were observed at the MAC, NET and TRAN layers. As shown in Figures 2.5-2.9, a select number of parameters for the above four steps are picked to illustrate the global and local perturbations. It is clear from Figures 2.5-2.9, when local interference (Local INTF) is introduced, RTS transmissions and packet retransmissions at MAC layer show a significant change compared to DuPACK (DuPlicate ACK), RERR (Route ERRor) and Time in Queue parameters at TRAN and NET layers. This means that a node can sense its local neighborhood environment based on MAC parameters. On the other hand, when only global interference (Global INTF) is introduced, DuPACK, and RERR parameters do not show any significant change compared to no interference (No INTF) situation. However, Average Time in Queue parameter shows a significant change. This means that a node can get good indication of global interference through this parameter. This information can be explicitly communicated through piggy backing, or through control protocol like Internet Control and Message Protocol (ICMP). However, to explicitly gather local and global information through control protocols increase network load is observed during the simulation (due to scope irrelevance results are not shown). It must be understood that if local or global interference is increased by adding more interfering nodes the absolute values shown in Figures 2.5-2.9 will change, but the general behavior will remain the same. Moreover, if local interference increases the source node will get an indication of link contention at the MAC level, but at the source node the Average Time in Queue at NET level will also be affected. An explicit

means (i.e., in-band or out-of-band control information) can be used to get the Average Time in Queue and other parameters' information regarding the global situation. It is also obvious from Figures 2.5-2.9 that mobility and interference combined (Mobility + INTF), affects all the parameters appreciably. This implies that correlating changes in the parameters can give a good indication of mobility at the local or global level. In essence, the point we are trying to make is that the local perturbations that affect parameters at the NET and TRAN layers can be separated from the global perturbations at the NET and TRAN layers. As stated before, the Awareness Optimizer can use this separated local and global views to make intelligent decisions.

2.5 Concluding Remarks

In this work we have proposed a vertical cross layer framework. The key contributions are functional vertical cross layer architecture, concept and identification of awareness parameters for performance optimization, functional architecture and behavior of Awareness Optimizer, optimization cycle for the cross layer optimization, and the concept of local and global optimization approach. Simulations are done to understand parameters behavior under interference and mobility to isolate local and global perturbations.

CHAPTER 3

FINITE HORIZON SCHEDULING IN WIRELESS AD HOC NETWORKS

3.1 Introduction and Motivation

Extensive research has been done in the area of wireless opportunistic scheduling, where multiuser time varying channel environment is exploited to schedule users to satisfy their QoS requirements [45, 46]. However, one fundamental requirement is timely feedback from users on a separate channel, so that multiuser diversity can be effectively used to enhance users' QoS requirements. In centralized wireless networks, central controller (base station) has relevant information (channel statistics and QoS requirement) of all the users to make optimal scheduling decisions. However, in wireless ad hoc network environment, users autonomously contend for the channel resource(s) based on sensing their local environment or limited exchange of signaling to gather local information. Thus, distributed network environment creates unique challenges; such as, time varying channel conditions, random channel contention among users, interference between distant users, limited resources, imprecise network information, dynamic topology, etc., for users to effectively schedule transmissions to achieve optimal throughput and latency performance. Specifically, multimedia streaming users with short term throughput and latency requirements face greater challenges to meet such stringent QoS requirements [47]. The QoS assurance problem becomes even more formidable in a distributed ad hoc network where users have multiple QoS requirements. Clearly, lack of

central controller leads to reduced QoS performance and this obviously necessitates some form of control in ad hoc networks [48].

Furthermore, end-to-end multi-hop flow in an ad hoc network is fundamentally limited by the single hop constraints. [13] shows that multi-hop congestion and throughput performance are closely coupled to MAC contentions. Hence, it is apparent from the above discussion that we need some form of MAC level control and coordination in short term opportunistic scheduling for enhanced performance.

This provides a major motivation for our work to devise a partially controlled opportunistic scheduling method for distributed networks to optimize network throughput in a finite horizon (short term). A scheduling method to maximize short term throughput in a centralized network for a single channel resource (downlink) was proposed in [49]. Each user is scheduled opportunistically in a frame such that starvation time does not exceed two consecutive frames. In distributed environment with single channel constraint, it is difficult to fully control slot assignment opportunistically for all the users due to heavy signaling and user coordination requirements. However, if users cooperate and coordinate transmissions we can achieve partial control over network performance [50]. One major issue that arises out of this coordination between users in a single channel distributed environment is that signaling to exchange information can create extra load on the network traffic and thus, potentially reduce throughput. As such, in this work we address two questions:

- 1) How to establish partial control in a distributed ad hoc network with minimal signaling between users?

- 2) What is the finite horizon scheduling strategy to enhance throughput, improve scalability and fairness performance of the network in an interference limited and time varying channel environment?

We consider a slotted environment in which users contend for slots in a probabilistic manner. The main idea of this research is to divide the finite horizon duration into a number of shorter time-scale windows in which probabilistic control actions are taken to improve throughput, scalability and fairness performance.

3.2 Literature Review

Over the last decade, significant work has been done in opportunistic scheduling for wireless networks. Contributions and ideas in centralized scheduling (downlink) have been extensively adopted for scheduling in distributed networks. Therefore, we categorize our overview of prior art as centralized and distributed scheduling techniques. An in-depth survey of earlier centralized wireless scheduling schemes, such as channel-state dependent packet scheduling (CSDPS), class-based scheduling (CBS), weighted fair queuing (WFQ), channel independent fairness (CIF), and many variants of the algorithms are discussed in [51]. Many new scheduling techniques are derived from the combination of the above algorithms for realistic wireless channels. Many of these algorithms use channel states to make long term or short term performance guarantees. The proposed wireless scheduling schemes provide various degrees of performance guarantees, including short-term and long-term fairness bounds. However, their focus is mainly limited to scheduling in centralized networks.

A scheduling scheme based on picking user with maximum signal-to-noise ratio (SNR) in a time slot was proposed in [52]. [53] proposed a scheduling scheme based on picking

user with maximum normalized SNR. This method gives higher priority to users with higher instantaneous and lower average SNR. A proportional fairness scheduling (PFS) algorithm for HDR/CDMA (High Data Rate/Code Division Multiple Access) system, where the product of throughput delivered to all the users is maximized was proposed in [54]. The PFS provides long term throughput maximization with poor delay performance for data services which is analyzed in detail in [55]. A modified largest weighted delay first (M-LWDF) method for real time applications which is throughput optimal and is stable in terms of queue backlog was proposed in [56, 57]. User with largest product of weighted channel rate and packet wait time is scheduled first at the expense of increased queuing delays for other users.

However, this proposed scheme is designed for HDR/CDMA fixed wireless network where each slot is accessible without any possibility of contention. A throughput optimal exponential scheduling scheme that modifies M-LWDF by giving more weight to queue when delay differences between users is large and shifts to PFS when delay differences are small was proposed in [58]. In [59] PFS bias is discussed with respect to asymmetric fading and a new score based scheduler is proposed for fixed wireless network.

A frame work for opportunistic scheduling to maximize wireless system performance to satisfy QoS requirements was proposed in [60]. The paper investigates scheduling problems with respect to temporal and utilitarian fairness requirements and derives optimal solution to be index-based policy. A weighted throughput based scheduling for HDR throughput optimization that basically schedules user with maximum rate-reward product was proposed in [61]. The scheme is roughly a combination of PFS and M-LWDF techniques using on-line iterative weight adjustment algorithm to compensate for

observed deviations from the target throughput. Our work is close to this paper in terms of dynamic weight adaptation. However, in our work we calculate myopic weights based on relative backlog ratios in each window to minimize backlog differences and improve throughput, fairness and scalability performance.

Furthermore, our work significantly differs in terms of defining finite horizon multiple window framework for backlog minimization in wireless ad hoc networks. In [62], opportunistic scheduling policy for short-term fairness constraint is proposed for HDR/CDMA system. Furthermore, a large volume of scheduling schemes can be found in [63-67] and the references therein.

In distributed networks, significant contributions are discussed hereafter. A dynamic control strategy to achieve optimal fairness for heterogeneous multi-hop network was proposed in [68]. The strategy decouples into separate algorithms for flow control, routing and scheduling, and resource allocation. However, the paper only discusses long-term optimal data rate performance in multi-hop ad hoc wireless networks. A cooperative rate adaptation (CRA) and QoS aware opportunistic scheduling schemes to reduce overall energy consumption in a multiuser ad hoc network was proposed in [50]. This paper loosely relates to our work in terms of cooperative strategy. An opportunistic scheduling for single hop ad hoc network using optimal stopping framework was proposed in [46]. It mainly considers scheduling from network centric aspect and shows that optimal strategy is a threshold-based policy. However, this paper deals with throughput maximization for infinite horizon only. In contrast, we consider throughput maximization in finite horizon using multiple stopping framework. Plethora of work in transmission policies using

Markov decision process (MDP) for infinite horizon can be found in [69, 70] and the references therein.

3.3 System Model and Assumptions

Consider wireless ad hoc network environment where users in a small cluster share and randomly contend for a single channel. We assume that all the users are homogeneous. In this context, it means that all the users have the same kind of application. Further, users' finite horizons end at the same time T .

3.3.1 Network Model

Consider slotted system, where time slot synchronization is assumed to be provided by the virtual leader ([71], Section I in [72]). We further assume for simplicity that slot size is large enough to accommodate request-to-send (RTS), clear-to-send (CTS) type of control packets and data packet along with propagation delays as shown in Figure 3.1. Hence, if a user successfully transmits in a slot it implies that the user has successfully exchanged RTS and CTS signals, and has transmitted the data as well. The RTS and CTS signals in the context of this paper represent exchange of control information between the nodes; provides information to other neighboring nodes, and further help avoid any hidden node problems. Users use CPW (cooperation window) phase to retrieve information and attain slot synchronization. It is also assumed that topology does not change during the data transmission window.

In our system model, finite horizon T refers to a deadline for i_{th} user to transmit $\eta_t^{(i)}$ amount of data remaining at t_{th} window, where t is defined to be in the range $[1, T]$. Thus, a finite horizon consists of T number of data transmission windows, where each window comprises w slots. Further, each data transmission window is separated by a

“Cooperation Window,” which marks the end of the current window and the start of the new window (see Fig. 3.1). The “Cooperation Window” (CPW) duration can be extremely short compared to the window size w since it broadcasts total traffic information to the users/nodes. The CPW duration is about two slots and consists of many micro slots for information dissemination and synchronization. We define the duration of the data transmission window and the CPW as one cycle. In this network model, the virtual leader has the responsibility of providing periodic slot timing during the CPW phase and it further defines the start of a new data transmission window. The virtual head also uses this CPW to provide total traffic information η_{tot} at the t_{th} window to the users so that users can contend for slots in this new data transmission window with updated thresholds for network performance improvement. This also requires that new users in a cluster can initiate communication only at the beginning of the new window, once they have informed the cluster head of their backlogs.

The question that still remains to be answered is how does cluster head know about the total traffic information. Actually, we assume here that when a user joins the cluster it

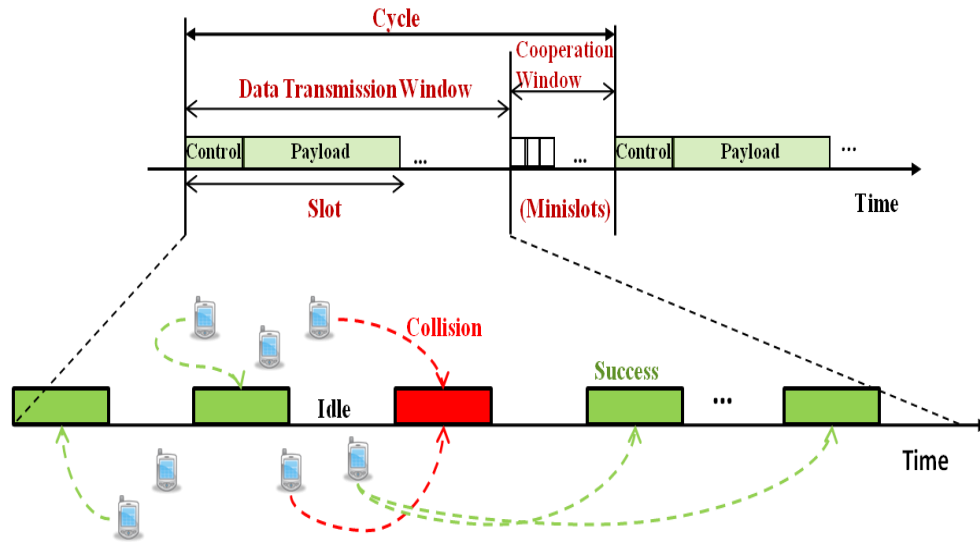


Figure 3.1 Timing Sequence Illustration

informs the cluster head with a single registration packet (may include data amount to be transmitted within T windows) which should not be larger in size than the RTS type packet. Thus, in an ideal case, the virtual head is aware of users entering and the total pending traffic of the users. This helps provide partial control in wireless ad hoc distributed network. The partial control also creates room for coordination between the users.

3.3.2 Queue and Channel Behavior

Assume that network has been operational for some time. Consider that each user fills up the lower queue with data packets that have to be transmitted within the finite horizon T . The queue is not filled by higher level queue until the lower level queue is emptied. This way we are only concerned with the amount of data remaining in the lower level queue rather than the arrivals in the upper level queue within the finite horizon. We can think of the higher level queue as the network layer queue and the lower level queue as the data link layer queue. The lower queue state then represents the amount of data that

needs to be transmitted within the finite horizon T . For the i_{th} user in the t_{th} data transmission window (t is a discrete time at the start of the window), the queue state is denoted by $\eta_t^{(i)} = [0, 1, \dots, U]$. The queue state evolves as $\eta_t^{(i)} = \eta_{t-1}^{(i)} - \lambda_{t-1}^{(i)}$, where $\lambda_{t-1}^{(i)}$ is the random number of slots out of w slots on which user i transmitted in the $t-1$ window. We will refer to λ as the rate in subsequent sections.

The probability of $\lambda_t^{(i)}$ successfully transmitted slots out of w slots for user i in t_{th} window is given by,

$$P(\lambda_t^{(i)}) = \binom{w}{\lambda_t^{(i)}} (P_{s_t}^{(i)})^{\lambda_t^{(i)}} (1 - P_{s_t}^{(i)})^{w - \lambda_t^{(i)}}. \quad (3.1)$$

Next we need to define probability of success $P_{s_t}^{(i)}$ for user i in the t_{th} window. A user successfully transmits in a slot when no other neighboring user transmits in that same slot and the channel is in a good state; or when other neighboring nodes transmit but relatively their channels are in bad states (diversity gain). For simplicity, we assume that the channel is stationary over the data transmission window and it follows a 2-state channel model (see [73] and refs. therein). It is further assumed that users' statistics are independent and identically distributed (i.i.d.), and the process is ergodic so that pathwise statistics is sufficient. The probability that the channel is good in a slot depends on receiver signal-to-interference (SIR) threshold of the user [73]. The channel fading is invariant over the slot duration, but it varies from slot to slot in a given window. So, the probability that a user i is successful in a given slot in the t_{th} window is given by,

$$P_{s_t}^{(i)} = \tau_t^{(i)} * P_{g_t}^{(i)} * \left\{ \prod_{\substack{j=1 \\ j \neq i}}^n (1 - \tau_t^{(j)} P_{g_t}^{(j)}) \right\}. \quad (3.2)$$

Where, $P_{g_t}^{(i)}$ is the i_{th} user probability that channel is in a good state in a slot in the t_{th}

window. $\tau_t^{(i)}$ is the probability that the i_{th} user transmits in a randomly chosen slot. The probability of the i_{th} user channel being in a good state in the t_{th} window is given by $P_{g_t}^{(i)} = \int_{\gamma_t^{(i)}}^{\infty} f_t^{(i)}(r)dr$. Where, $\gamma_t^{(i)}$ is the SIR threshold for the i_{th} user in the t_{th} window and $f_t^{(i)}(r)$ is the density function for the SIR. Distribution for $f_t^{(i)}(r)$ is a bit complicated and is based on the ratio of users' Rayleigh distributed signal fading. Plugging (3.2) into (3.1) gives us the probability of $\lambda_t^{(i)}$ successfully transmitted slots which also defines the state transition probability. It is apparent that for any i_{th} user, if we need we can vary the probability of transmission $\tau_t^{(i)}$ in the slot to control the probability of success $P_{s_t}^{(i)}$ in the network for enhanced throughput, scalability and fairness performance. Note that n in (3.2) is the number of contending users and is given by $n = \pi A^2 \rho$, where A is the coverage area and ρ is the node density.

3.3.3 Window Requirement

As mentioned before, we divide finite horizon into T windows, where each data transmission window consists of w slots. The virtual head provides for the timing synchronization as explained previously. The main reason for having windows is to control and coordinate random contentions in a cooperative manner over window-based time scales so that network throughput, fairness and scalability is improved in each window until the horizon is reached. We consider worst case situation, where random maximal scheduling for a specific single-hop interference model touches lower bound and achieves only 50 % throughput [74]. Actual data transmission window size may depend on the number of slots the system remains synchronized, the number of slots over which the average channel state remains constant and the total average backlog. We

assume that the window size is short enough to satisfy synchronization and average channel state requirements. Hence, if we wish to allocate each of the n users at least $\bar{\eta}$ number of slots on the average in the window, then the window size w should satisfy, $w \geq 2 n \bar{\eta}$. From implementation point of view, this provides approximate lower bound for the window size based on the number of users and the average backlog per user in a window.

3.4 Two-User Optimal Policy

For finite horizon problems, backward induction is used recursively to evaluate the optimal sequence of actions given the states information of users in the system. However, backward induction technique renders itself impractical due to unpredictability of channel and high computational complexity [75]. The structure of our problem is of control limit policy form [76, Chap 4], whereby each user starts and continues random transmissions when below its rate limit and stops when it reaches the required rate limit in a window.

Users contend for slots in a window based on their backlogs and channel states. Thus, multiuser diversity is created due to diverse channel and queue states between the users. In order to exploit the diversity and enhance network throughput (minimize network backlog), fairness and scalability performance opportunistically in a finite horizon T , users dynamically adapt and coordinate the access probabilities in a slot based on their own weighted backlogs and the total weighted backlog at the start of every data transmission window. This means that each user opportunistically transmits in a certain number of slots based on the rate threshold setting in a window.

Consider two users in t_{th} window with large backlogs $\eta_t^1 > w$ and $\eta_t^2 > w$. Assume network has been operational for some time and all users are precisely synchronized. Our

objective is to minimize backlogs in the $t + 1$ window, or maximize throughput for both the users in the window as follows;

$$\min \{E[\eta_t^1 - \lambda_t^1]^+ + E[\eta_t^2 - \lambda_t^2]^+\}, \text{ where } [x - y]^+ = \max(x - y, 0). \quad (3.3)$$

For large backlogs, $\eta_t^1 - \lambda_t^1$ and $\eta_t^2 - \lambda_t^2$ are always positive, and therefore, $\min \{E[\eta_t^1 - \lambda_t^1]^+ + E[\eta_t^2 - \lambda_t^2]^+\} \approx \min \{E[\eta_t^1 - \lambda_t^1] + E[\eta_t^2 - \lambda_t^2]\}$. Taking expectation (average) we reduce our objective function to $\min\{\sum_0^w \eta_t^1 P(\lambda_t^1) + \sum_0^w \eta_t^2 P(\lambda_t^2) - \sum_0^w \lambda_t^1 P(\lambda_t^1) - \sum_0^w \lambda_t^2 P(\lambda_t^2)\}$. Since η_t^1 and η_t^2 are known at the start of the t_{th} window, and both $P(\lambda_t^1)$ and $P(\lambda_t^2)$ are binomial distributions, the objective function then simplifies to $\min\{\eta_t^1 + \eta_t^2 - wP_{s_t}^1 - wP_{s_t}^2\}$. Hence, our final objective function that needs to be minimized with the fairness constraint takes the form,

$$\begin{aligned} & \min\{\eta_t^1 + \eta_t^2 - wP_{s_t}^1 - wP_{s_t}^2\}, \\ & \text{subject to } (\eta_t^1 - \eta_t^2 - wP_{s_t}^1 + wP_{s_t}^2)^2 \leq \Delta^2. \end{aligned} \quad (3.4)$$

Where, $\Delta \ll w$ is the backlog difference bias. The Lagrangian using Kuhn-Tucker theorem is then given by,

$$\begin{aligned} L(\tau_t^1, \tau_t^2, \mu) &= \eta_t^1 + \eta_t^2 - w * P_{g_t}^{(1)} * \tau_t^1 (1 - P_{g_t}^{(2)} \tau_t^2) - w * P_{g_t}^{(2)} \tau_t^2 (1 - P_{g_t}^{(1)} \tau_t^1) - \\ & \mu \left\{ \Delta^2 - [\eta_t^1 - \eta_t^2 - w * P_{g_t}^{(1)} \tau_t^1 (1 - P_{g_t}^{(2)} \tau_t^2) + w * P_{g_t}^{(2)} \tau_t^2 (1 - P_{g_t}^{(1)} \tau_t^1)]^2 \right\}, \text{ where } \mu \geq 0. \end{aligned}$$

Then taking derivative of L with respect to τ_t^1 and τ_t^2 gives us,

$$\begin{aligned} \frac{\partial L}{\partial \tau_t^1} &= 0 \xrightarrow{\text{yields}} 2\mu * \left[\eta_t^1 - \eta_t^2 - wP_{g_t}^{(1)} \tau_t^1 (1 - P_{g_t}^{(2)} \tau_t^2) + wP_{g_t}^{(2)} \tau_t^2 (1 - P_{g_t}^{(1)} \tau_t^1) \right] = \\ & \frac{wP_{g_t}^{(2)} \tau_t^2 P_{g_t}^{(1)} - wP_{g_t}^{(1)} (1 - P_{g_t}^{(2)} \tau_t^2)}{wP_{g_t}^{(1)}}, \end{aligned}$$

$$\text{and } \frac{\partial L}{\partial \tau_t^2} = 0 \xrightarrow{\text{yields}} 2\mu * \left[\eta_t^1 - \eta_t^2 - wP_{g_t}^{(1)} \tau_t^1 (1 - P_{g_t}^{(2)} \tau_t^2) + wP_{g_t}^{(2)} \tau_t^2 (1 - P_{g_t}^{(1)} \tau_t^1) \right] =$$

$$\frac{wP_{g_t}^{(2)} (1 - P_{g_t}^{(1)} \tau_t^1) - wP_{g_t}^{(1)} P_{g_t}^{(2)} \tau_t^1}{wP_{g_t}^{(2)}}.$$

For $\mu \geq 0$, the point at which objective function is minimum satisfies $P_{g_t}^{(1)} \tau_t^1 + P_{g_t}^{(2)} \tau_t^2 =$

1. For the case when the constraint is inactive, i.e., $\mu = 0$, the optimal probabilities are

given by, $\tau_t^{*1} = \frac{1}{2P_{g_t}^{(1)}}$ and $\tau_t^{*2} = \frac{1}{2P_{g_t}^{(2)}}$. It is noteworthy that when the solution lies inside

the constraint region, the transmission probabilities are independent of the backlogs (η_t^1

and η_t^2). However, an interesting case arises when the constraint is active, i.e., $\mu > 0$ and

the minimum that is achievable is at the constraint boundary. To determine optimal

transmission probabilities in this case we substitute $P_{g_t}^{(2)} \tau_t^2 = 1 - P_{g_t}^{(1)} \tau_t^1$ into the

complementarity condition given by $\mu \left\{ \Delta^2 - [\eta_t^1 - \eta_t^2 - wP_{g_t}^{(1)} \tau_t^1 (1 - P_{g_t}^{(2)} \tau_t^2) +$

$wP_{g_t}^{(2)} \tau_t^2 (1 - P_{g_t}^{(1)} \tau_t^1)]^2 \right\} = 0$. A minor simplification gives us the optimal values of τ_t^{*1}

and τ_t^{*2} . Therefore, user 1 and user 2 set their *linear optimal transmission probabilities* in

each slot as,

$$\tau_t^{*1} = \frac{1}{2P_{g_t}^{(1)}} + \frac{(\eta_t^1 - \eta_t^2) - \Delta}{2wP_{g_t}^{(1)}},$$

$$\text{and } \tau_t^{*2} = \frac{1}{2P_{g_t}^{(2)}} - \frac{(\eta_t^1 - \eta_t^2) - \Delta}{2wP_{g_t}^{(2)}}.$$

Note that an offset adds to the optimal transmission probabilities compared to the case

when constraint is inactive. This allows us to pick a user who is relatively unfortunate, or

resource starved. It is important to understand that for finite horizon throughput

maximization with fairness, the random access probability is increased when a user is

behind its share of resource. Further note that the optimal values of $\tau_t^{*(1)} \geq 0$ and $\tau_t^{*(2)} \geq 0$ should satisfy $P_{g_t}^{(1)} \tau_t^{*(1)} + P_{g_t}^{(2)} \tau_t^{*(2)} = 1$. Ideally, we would prefer to set the bias (Δ) to a negligible value or zero. Thus, optimal probabilities of success are given by, $P_{S_t}^{*(1)} = \left(\frac{1}{2} + \frac{\eta_t^1 - \eta_t^2 - \Delta}{2w}\right)^2$ and $P_{S_t}^{*(2)} = \left(\frac{1}{2} - \frac{\eta_t^1 - \eta_t^2 - \Delta}{2w}\right)^2$. The optimal stopping rates for user 1 and user 2 are $\lambda_t^{*(1)} = w\tau_t^{*1}$ and $\lambda_t^{*(2)} = w\tau_t^{*2}$, respectively. It is obvious from optimal transmission probability equations that when user 2 backlog is greater than user 1 then $P_{S_t}^{*(2)} > P_{S_t}^{*(1)}$, and when user 1 and user 2 have equal backlogs then $P_{S_t}^{*(2)} = P_{S_t}^{*(1)}$.

In realistic ad hoc networks with more than two users, it becomes very complex to find backlog differences based optimal values and therefore such approach becomes infeasible. Hence, in section 3.5 we first propose a simple ratio-based (SR) scheduling scheme where users only need to know the total backlog in the network which can be easily obtained during the CPW phase. The access probabilities in our SR scheduling scheme depend on the relative backlogs' ratios only as opposed to backlog differences in a linear scheme.

3.4.1 SR Versus Linear Optimal Strategy

For SR scheme, the transmission probability for the i_{th} user in the t_{th} window is given by $\tau_t^{*(i)} = \frac{\eta_t^i}{\sum_{k=1}^n \eta_t^k}$ and the probability of success for the i_{th} user comes out to be as,

$$P_{S_t}^{*(i)} = \frac{P_{g_t}^{(i)} \eta_t^{(i)} \left\{ \prod_{\substack{j=1 \\ j \neq i}}^n (\sum_{k=1}^n \eta_t^{(k)} - \eta_t^{(j)} P_{g_t}^{(j)}) \right\}}{\left[\sum_{k=1}^n \eta_t^{(k)} \right]^n}, \text{ for } n \geq 2 \text{ (see Appendix B). In Fig. 3.2, we}$$

compare the SR scheme and linear scheme under identical conditions when users' backlog difference increases from 0 to 30. Fig. 3.2 shows that when the backlog

difference is 15 (50% of the window size), user 1 gets 75% of the slots in the window relative to user 2 for the linear scheme, while for the ratio-based scheme user 1 gets about 65% of the slots. We observe that SR reduces the backlog difference more conservatively compared to the linear scheme. However, SR is far simpler to implement than linear optimal strategy. Also, noteworthy in SR is that we don't need channel information for symmetric links (average channel conditions are same). Any random channel variations (fast fading) or temporary bad channel conditions that affect user's success rate in a window shows up as an increase in user's backlog in the following window. Consequently, thresholds are adapted accordingly and coordinated between the users to compensate for any change in relative backlogs (see proposition). Next proposition states the threshold requirement for maximizing network throughput (minimizing backlog) in a fair manner.

Proposition 3.1: The myopic stopping strategy is a time variant threshold which improves network throughput with fairness.

Proof: Consider the probability of success under the same channel conditions ($P_{g_t}^{(1)} \approx P_{g_t}^{(2)}$) for two users. Suppose each user has a backlog η_t^1 and η_t^2 at the start of window t .

Further assume that $\frac{\eta_t^1}{\eta_t^2} = \alpha$ such that $\alpha \gg 1$. After minor simplification, users are set to

achieve the probability of success as $P_{s_t}^{*(1)} \approx \left\{ \frac{\alpha}{1 - P_{g_t}^{(1)}} \right\} P_{s_t}^{*(2)}$. This implies that we expect

$\lambda_t^{(1)} > \lambda_t^{(2)}$. However, due to slot contentions and channel fading assume that user 1

achieves the same random rate as user 2, i.e., $\lambda_t^{(1)} = \lambda_t^{(2)} = \lambda$ and assume that $\lambda \leq \eta$.

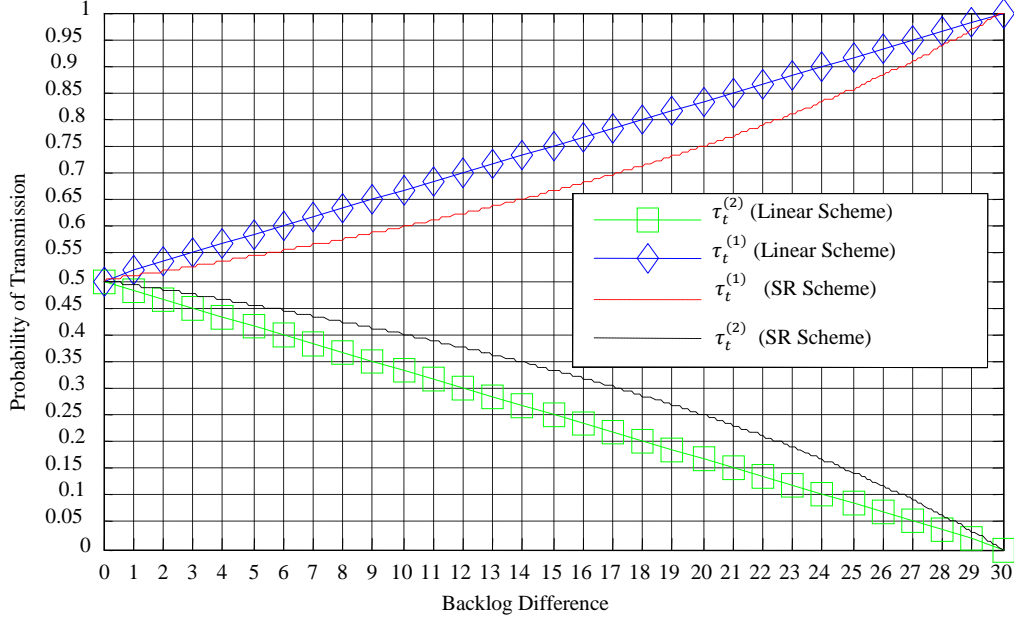


Figure 3.2 Two-user probability of transmission comparison between linear and SR schemes with $w = 30$, $P_{g_t}^{(1)} = P_{g_t}^{(2)} = 1$, and $\Delta = 0$

Then the new backlogs for user 1 and 2 become $\frac{\eta_{t+1}^1}{\eta_{t+1}^2} = \frac{\eta_t^1 - \lambda_t^{(1)}}{\eta_t^2 - \lambda_t^{(2)}} \approx \frac{\alpha - (\lambda/\eta_t^2)}{1 - (\lambda/\eta_t^2)} \approx \frac{\alpha}{1 - (\lambda/\eta_t^2)}$.

Since, $1 - (\lambda/\eta_t^2) < 1$ this implies that $\frac{\eta_{t+1}^1}{\eta_{t+1}^2} > \alpha$. So as the backlog gap widens between

user 1 and 2, so does the threshold gap increase to $\frac{P_{s_{t+1}}^{*(1)}}{P_{s_{t+1}}^{*(2)}} > \frac{P_{s_t}^{*(1)}}{P_{s_t}^{*(2)}}$. This proves that the

thresholds will change in the next window if users' backlog ratio changes in the next window. Hence, it is very intuitive that as the backlog of one user increases due to severe fading on its link compared to other users, the optimal threshold setting would be to give more weight to that user with bad link in the next window. This will maximize network throughput with fairness in a finite horizon.

3.5 Proposed SR Scheduling Strategy

Consider small cluster based homogeneous environment. Homogeneous environment in the context of this scheme means that all users belong to the same class with same priorities. The ratio-based scheduling strategy for a user i in the t_{th} window entails the following steps:

- 1) Calculate the weight for the t_{th} window given by $\tau_t^{*(i)} = \frac{\eta_t^i}{\sum_{k=1}^n \eta_t^k}$.
- 2) Set the stopping rate (target rate) in the t_{th} window to $\lambda_t^{*(i)}(\tau_t^{*(i)}) = w\tau_t^{*(i)}$.
- 3) Transmit packets in slots until the threshold rate $\lfloor \lambda_t^{*(i)}(\tau_t^{*(i)}) \rfloor$ (round to nearest integer) is achieved or the slots in the current window finish.
- 4) Repeat Steps 1-3 in every window.

3.6 Simulation Results and Discussion

A single hop time-slotted distributed wireless environment in a finite horizon T is simulated to validate the performance of SR scheduling scheme. CPW duration is assumed to be 1-2 slots (which is further subdivided into micro slots for synchronization and traffic information dissemination) compared to the data transmission window. Our SR scheme is compared with the non-cooperative random access scheduling scheme (abbreviated as Non-Coop) as the bench mark. In non-cooperative random access scheme, all users transmit at a fixed access probabilities without adapting thresholds (access rates) in each window up to the finite horizon. Aggregate throughput comparison is made under no fading and independent Rayleigh fading channel conditions. Further, scalability, average throughput variance per window and Jain's fairness index comparisons between two schemes are made under independent Rayleigh fading channel

conditions. It is noteworthy that in no fading condition, only slot contentions determine successful transmission and under Rayleigh fading channel condition contentions and relative SIR determines successful transmission. We assume that fast fading does not change during the slot duration and furthermore average received signal occasionally varies from window to window during the finite horizon. Details of the simulation parameters are listed in Table 3.1.

Simulation is run more than 1000 times so that data is averaged over 3,000,000 slots. Fig. 3.3 shows the comparison results of SR and non-cooperative random access schemes. In non-cooperative random access scheme all nodes set their rates at the start of the finite horizon duration and no transmission probability adaptation is performed. Since the rates are set for the finite horizon duration the non-cooperative scheme with fading achieves a maximum aggregate throughput of 1300 packets at the total data rate of 3600 packets per horizon. This corresponds to about 43% utilization within the finite horizon duration of 3000 slots. Fig. 3.3 shows that the non-cooperative scheme fails to meet the total data rate requirement even when the total data rate required is 50% (i.e., 1600 packets) of the finite horizon duration. This is due to the fact that it sets its transmission probability based on the finite horizon duration.

Table 3.1 Simulation parameters

Parameter	Value
Finite horizon duration (T)	3000 slots
Slot duration	1 ms
Transmitting nodes	4
Channel access	Random
Frequency	2.4 GHz
Doppler shift	80 Hz
Window duration	100 slots
Node data rate per horizon	100-1300 packets
SIR threshold	10 dB

Hence, in each window it does not achieve maximum aggregate throughput. On the other hand, SR scheme myopically adapts access probabilities in each window to maximize aggregate throughput with fairness. For total data rate from 2800 to 4400 packets per horizon, SR scheme performs as well as the non-cooperative scheme. When the total data rate is below 2800 or above 4400 packets, the performance of SR scheme is better than the non-cooperative scheme.

As expected, SR scheme does not achieve maximum aggregate throughput of 1300 packets, but on average remains within 1.6% of the maximum aggregate throughput for fading case. Fig. 3.4 compares the scalability performance of the two schemes for fading case only. The SR scheme's aggregate throughput clearly scales well with the number of nodes. The reason is that we adapt transmission probabilities of all users in proportion to their relative backlogs and fading effects to maximize utilization in shorter time-scale window. Average throughput variance per window for the two schemes is compared in Fig. 3.5 for the feasible data rates of 1200, 2000 and 2800 packets. It is apparent that our SR scheme in addition to enhancing aggregate throughput within the finite horizon, also keeps the average throughput variance within 1 slot in the case of fading. To measure fairness we use Jain's fairness index [77]. For n nodes, the fairness index (f) is given by,

$$f = \frac{(\sum_{i=1}^n x_i)^2}{n \sum_{i=1}^n x_i^2}. \text{ Fairness index value of 1 indicates ideal fairness and } \frac{1}{n} \text{ indicates no}$$

fairness. In Table 3.2, Jain's fairness index calculated over the finite horizon clearly indicates that the proposed SR scheme fairness is relatively better than the non-cooperative scheme. Jain's fairness index being close to unity also indicates the max-min fairness behavior for the symmetric channel case in Rayleigh fading environment. For the

case, where 50 % of the users have average SIR 5 dB below the other users, the SR scheme remains fair compared to non-cooperative scheme. This is due to the reason that SR scheme minimizes the backlog gap between users in each window in addition to maximizing the utilization in each window.

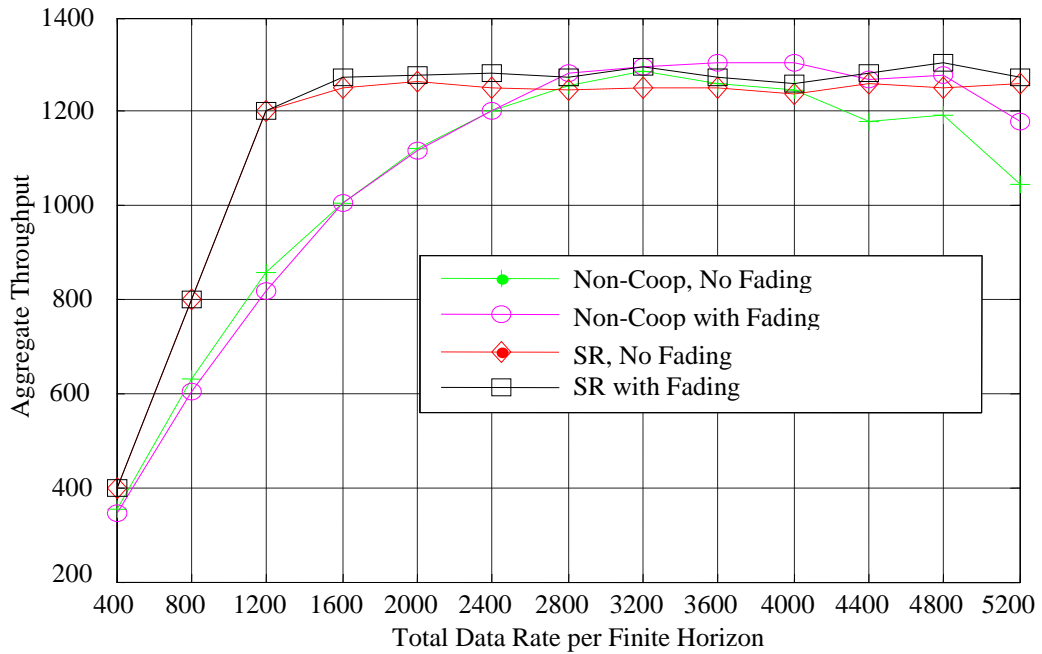


Figure 3.3 Aggregate throughput per finite horizon

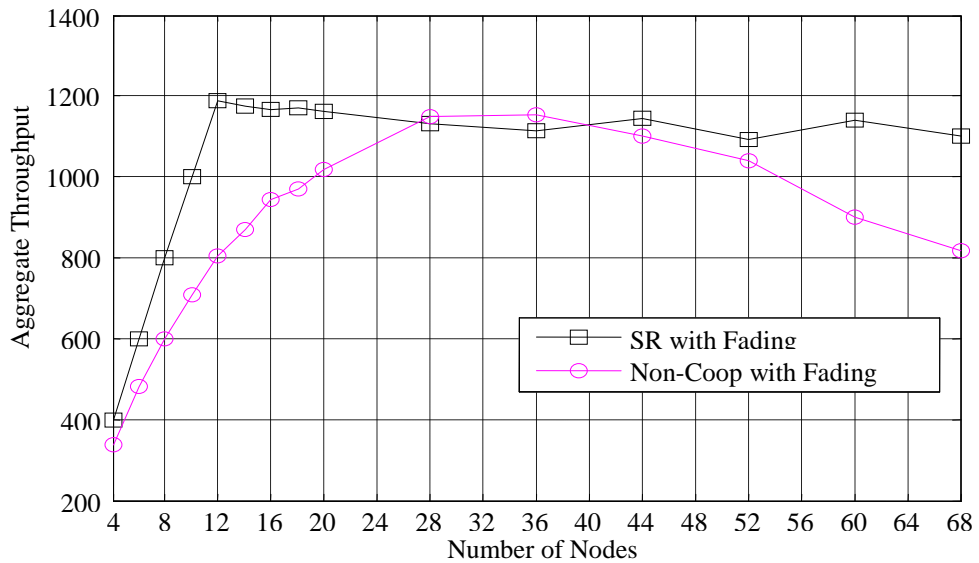


Figure 3.4 Aggregate throughput scalability (Each node transmits 100 packets)

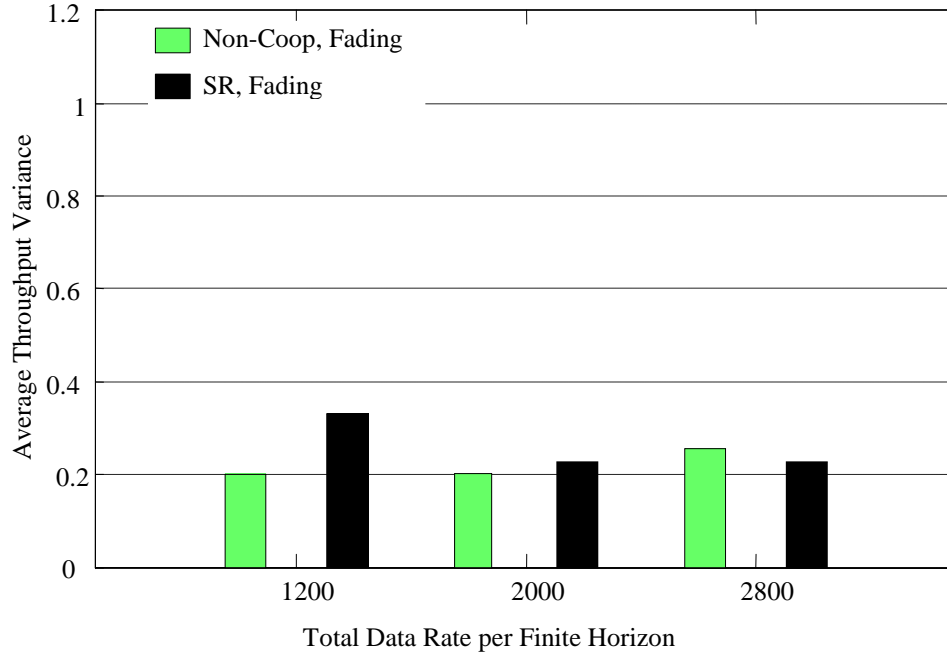


Figure 3.5 Average throughput variance per window

Table 3.2 Jain's fairness index comparison

Channel Behavior	Data Rate (packets per horizon)	SR Scheme (%)	Random Non-Cooperative (%)
Symmetric	1200	99.9	99.8
	2000	99.9	99.8
	2800	99.7	99.6
5 dB Asymmetry	1200	99.9	99.0
	2000	99.6	99.0
	2800	99.5	98.5

3.7 SR Performance Limitations

The SR algorithm performs well compared to non-cooperative random access scheme in terms of network throughput, scalability and fairness for symmetric channel conditions. In each window users adjust their access probabilities based on the relative

backlog weights only. When the channel condition gets bad for user i in a window, fewer packets are successfully transmitted relative to other users. As such, backlog of user i relatively increases in the next window which leads to increase in its access probability. Consequently, users cooperatively adapt access probabilities using multi-window approach to compensate for a user's occasional bad channel condition in a window. However, if a couple of users on average encounter bad channel conditions in every window, relative to other users, then the access probabilities for these users would continue to increase monotonically until the finite horizon is reached. This would lead to a significant network throughput degradation of the SR scheme. As such, user will consume a large amount of resource in every window and consequently may starve other users with better channel conditions. Since in many cases it may be desirable to trade fairness with short term throughput gains in the system, this necessitates users' channel states to be taken in to consideration along with the users' backlogs for setting the threshold rates as discussed in later sections.

3.8 Proposed GR Scheduling Scheme and Simulation Results

In this section, we present general ratio (GR) based scheme that adapts between fairness and throughput maximization. GR maximizes throughput under asymmetric channel conditions, and becomes fair under symmetric channel conditions. The general

transmission probability of i_{th} user is mathematically represented as, $\tau_t^{*(i)} = \frac{C_{it}\eta_t^{(i)}}{\sum_{k=1}^n C_{kt}\eta_t^{(k)}}.$

Where, C_{it} may represent a product of i_{th} user class and channel condition. In general, we can think of C_{it} as the trade-off parameter. If $C_{it} = C$, for all users then it is a fair system. However, if all C_{it} s depend on respective channel behaviors only then the system

shifts from fairness towards throughput maximization. Since, we consider homogeneous network where all users have the same class (or priority), the transmission probability of the i_{th} user simplifies to,

$$\tau_t^{*(i)} = \frac{\eta_t^{(i)} \times P_g^{(i)}}{\sum_{k=1}^n \{\eta_t^{(k)} \times P_g^{(k)}\}}, \text{ where } C_{it} = P_g^{(i)}. \quad (3.5)$$

Note, $P_g^{(i)}$ is the average normalized occurrence of a channel being in a good state.

Assume all users have same fixed SIR threshold. Then $P_g^{(i)}$ can be updated by each user i for every window using well-known exponential averaging technique based on the past history of the user (see section 6.4.3.1 of [78]).

Some centralized scheduling schemes (see [49, 51, 54, 57, 58, 60]) schedule user in a slot with maximum product of backlog and instantaneous channel rate. However, network dynamics and frequent feedback requirement of backlog and instantaneous channel rate makes it extremely difficult to have a deterministic level of slot control in a single channel ad hoc network. Following the same SR approach as in previous sections, each user in the GR scheme cooperatively adapts the access probability by taking the ratio of the product of its backlog and its channel state in a given window to the sum of products (of backlogs and channel states) of all the users in the ad hoc environment (see (3.5)). The sum of the products (of backlogs and channel states) of all the users is broadcast to the users by the virtual head that monitors the network. Note that users can easily provide their backlogs and channel states products information through control portion of the slot. The GR scheduling algorithm for user i in the t_{th} window entails the same steps as the SR scheme with the exception of $\tau_t^{*(i)}$ in (3.5).

Simulations are performed to demonstrate throughput degradation of the SR scheme. For simulation purpose we assume that the precise value of $P_g^{(i)}$ is known to the i_{th} user. Specifically, two cases are simulated: In the first case, 50 % users have an equal average SIR that is 5 dB below the other users in the network during the entire finite horizon duration. In the second case, the average SIR of the 50 % users is set 7 dB below the other users in the network. From Fig. 3.6, it is clear that for 5 dB channel asymmetry the SR scheme's aggregate throughput degrades by 2 % on the average, and for the 7 dB channel asymmetry it degrades by 4%. The reason for throughput degradation is due to the fact that the two users with consistent bad channels (i.e., with lower average SIR) cannot get rid of their backlogs and consequently lead to starvation of the other users with better channel conditions. The proposed GR scheme considers relative channel states of the users along with the backlogs to give higher precedence to users with relatively larger backlogs and reasonable channel states or users with the best channel states and reasonable backlogs. Note that when users' channels are symmetric then GR scheme transforms to SR scheme. The dotted lines in Fig. 3.6 clearly show aggregate throughput when GR scheme is employed in case of asymmetric channels. For 5 dB channel asymmetry, GR improves aggregate throughput by 1 % and for 7 dB channel asymmetry the aggregate throughput improves by about 2 %. Furthermore, it is noteworthy for SR and GR scheduling schemes, that each user always gets some share of slots in a window and is not starved unless its backlog and the channel state product is zero. Clearly, GR scheme seeks to exploit both multi-user diversity gains and provides a reasonable fairness.

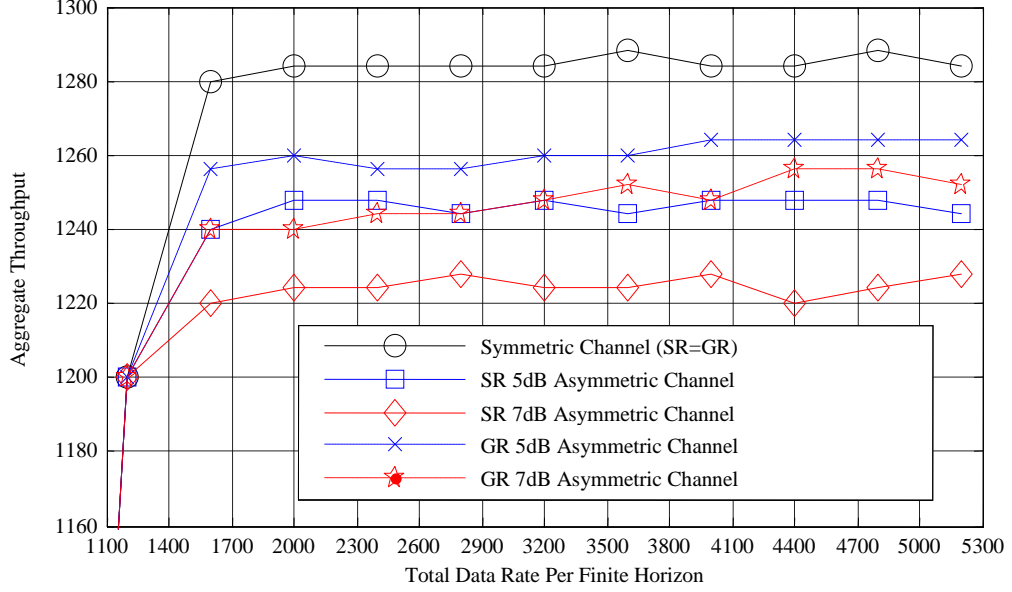


Figure 3.6 Aggregate throughput performance for SR and GR at 5 dB and 7 dB of channel asymmetry

3.9 GR Soft Throughput Guarantee

Generally, it is very complex to derive a closed form expression that shows the throughput guarantee of a scheduling technique in a finite horizon. However, we can use an approximate approach of [79] to derive an expression for the condition that guarantees soft throughput in a window. Soft throughput in the context of this section means that l_{th} user with required rate of η_l^i (backlog to be served in a window) is guaranteed to be served in a window l given that certain condition on probability of transmission (τ_l^{*i}) is met. We use from [79] the soft throughput guarantee violation probability concept to derive our expression. Assume user target rate of η_l^i per window and total sum of users' backlogs in a window is feasible such that $\eta_{ltot} = \sum_{i=1}^n \eta_l^i < w$. We define throughput guarantee in probabilistic terms as the probability that η_l^i amount of packets are guaranteed to be transmitted within the window l should be at least $1 - \epsilon$. Alternatively,

we define throughput guarantee violation probability as the probability that rate λ being less than η_l^i should not exceed ϵ , i.e.,

$$P(\lambda \leq \eta_l^i) \leq \epsilon, \quad (3.6)$$

where ϵ is a small positive number and $\eta_l^i = \eta_l^i - 1$. A user transmits λ sequence of packets randomly following Bernoulli trials. The probability that a user can have λ number of successful packet transmissions out of w possible Bernoulli trials has Binomial distribution given by, $P(\lambda) = \binom{w}{\lambda} P_s^{i\lambda} (1 - P_s^i)^{w-\lambda}$, where P_s^i is the probability of success (see (3.2)). Using Binomial distribution function, $P(\lambda \leq \eta_l^i)$ in (3.6) can be written as, $P(\lambda \leq \eta_l^i) = \sum_{\lambda=0}^{\eta_l^i} \binom{w}{\lambda} P_s^{i\lambda} (1 - P_s^i)^{w-\lambda}$. We now state a proposition that defines a condition on the probability of success P_s^i such that throughput violation probability does not exceed ϵ .

Proposition 3.2: A sufficient condition for $P(\lambda \leq \eta_l^i) \leq \epsilon$ to be true requires the probability of success to satisfy the following approximate condition,

$$P_s^i \geq \frac{(\eta_l^i - 1) + \sqrt{[\frac{w}{2} * \ln(\frac{1}{\epsilon})]}}{w}. \quad (3.7)$$

Proof: We will avoid subscripts and superscripts for convenience. We have shown that $P(\lambda \leq \eta_l) = \sum_{x=0}^{\eta_l} \binom{w}{x} P_s^{(x)} (1 - P_s)^{w-x}$. For sufficiently large window size of w slots, Hoeffding's inequality (see [80] and refs.) under the condition $\eta_l \leq wP_s$, yields the upper bound for $P(\lambda \leq \eta_l)$ as,

$$P(\lambda \leq \eta_l) \leq e^{\frac{-2*(wP_s - \eta_l)^2}{w}}. \quad (3.8)$$

Using throughput guarantee violation probability we roughly bound (3.8) as,

$$e^{\frac{-2*(wP_s-\hat{\eta}_l)^2}{w}} \leq \epsilon. \text{ Taking natural log of both sides and simplifying leads to, } \frac{w}{2} * \ln\left(\frac{1}{\epsilon}\right) \leq$$

$(wP_s - \hat{\eta}_l)^2$. Taking square root of both sides and manipulating the above equation finally proves the proposition 3.2.

Using proposition 3.2 we evaluate the soft throughput guarantee of our scheduling

strategy. Recall that probability of success is given by, $P_{st}^{(i)} = \tau_t^{(i)} * P_{gt}^{(i)} * \left\{ \prod_{j=1, j \neq i}^n (1 - \right.$

$\left. \tau_t^{(j)} P_{gt}^{(j)} \right\}$. Substituting P_s^i , $\tau_t^{(i)}$ and $\tau_t^{(j)}$ (using (3.5)) into (3.7) and simplifying gives us

sufficient condition for the backlog η_l^i to be served as,

$$\eta_l^i \geq \frac{\sqrt{\left[\frac{w}{2} \times \ln\left(\frac{1}{\epsilon}\right) \right] - 1}}{\left[\frac{w P_{gl}^{(i)2} \times \prod_{j=1, j \neq i}^n \left\{ \sum_{k=1}^n P_{gl}^{(k)} \eta_l^{(k)} - \eta_l^{(j)} P_{gl}^{(j)2} \right\}}{\left\{ \sum_{k=1}^n P_{gl}^{(k)} \eta_l^{(k)} \right\}^n} - 1 \right]}. \quad (3.9)$$

(3.9) is a soft condition in terms of minimum required backlog η_l^i for an i_{th} user out of the sum of products of backlogs and channel states in a window. Since GR scheduling scheme depends on the relative weights of the backlogs and channel states, therefore, intuitively higher relative backlog-channel product will guarantee higher transmission probability and smaller throughput violation probability.

3.10 Concluding Remarks

A novel approach of multi-window adaptation for throughput maximization with fairness in a finite horizon is presented for wireless ad hoc network. In the proposed SR scheme thresholds are myopically adapted for performance improvement in each window. The attractive feature of this scheme is that it only requires knowledge of the total backlog of all the users in a window. Simulation results clearly show that compared

to non-cooperative random access scheme, SR scheme achieves stable throughput performance, behaves fairly even under asymmetric channel conditions, and is highly scalable.

Further, it is shown that throughput performance of SR scheme degrades in asymmetric channel condition. The proposed GR scheme dynamically adapts between fairness and throughput maximization by considering channel states and the backlogs. It clearly outperforms the SR scheme in case of asymmetric channels. In the last part, we have derived a general sufficient condition for throughput guarantee using the GR scheduling scheme, which depends on the number of users, users' backlogs and channel states, and total sum of backlog-channel states product.

CHAPTER 4

COOPERATIVE RELAY BASED MAC PROTOCOLS FOR WIRELESS AD HOC NETWORKS

4.1 Two-Relay based Cooperative MAC Protocol

In this section, two-relay based cooperative MAC protocol, also termed as 2rcMAC, is presented.

4.1.1 Introduction and Related Work

Ever increasing demand for higher throughput and lower delay in wireless ad hoc networks led to an extensive research into newer techniques, algorithms and technologies. One such significant contribution is the notion of “Cooperative Communication” in ad hoc networks. Cooperative communication harnesses the broadcast nature of the wireless channel and uses spatial diversity of independent paths to mitigate channel impairments (mean path loss and fading), enhance throughput capacity of the network and reduce retransmission latency [81, 82]. In cooperative communication paradigm, nodes cooperate with the source and destination nodes at physical layer and/or MAC layer to improve throughput, delay, and coverage. Nodes cooperating at the physical layer receive packets and combine them together using different techniques (for example linear or random coding) for transmission to the destination nodes. Destination node can use multiple copies of the transmitted packet to decode with high reliability. Cooperation at physical layer has led to a specialized field of network coding [83].

Generally, for single hop ad hoc networks cooperative MAC protocols can be classified into two major categories: (1) protocols invoke relay node when transmission time via relay path is better than the direct path and (2) protocols invoke the relay node for back up transmission when direct transmission fails due to fading or interference. Cooperative communication is different from multi-hop communication in the sense that although source-destination pair can communicate directly at some rate, but the relay node is still invoked to achieve enhanced data rate. Nodes cooperating at MAC level simply relay received packets for improved throughput and coverage reliability. Specifically, MAC level cooperation improves performance when source-destination nodes are separated by a distance that prevents the source node from directly transmitting to the destination node at high data rates. Using any intermediate node that is appropriately located (and is willing to cooperate) can allow transmission at higher data rates compared to the direct transmission.

CoopMAC I protocol falls under category one and is most suitable for mobility conditions [84, 85]. It is based on slight modification of IEEE 802.11 distributed coordination function (DCF) that benefits from cooperation between nodes in infrastructure based wireless LAN (WLAN). CoopMAC I uses a table driven approach. Source node updates table entries by measuring path losses between source node and the relay nodes. Path losses are used to estimate possible rates using a rate lookup table. Further, the achievable rate between the relay node and the access point (AP) is obtained by listening to physical layer header transmissions between the relay and the AP. Once the source node has a packet to transmit, it compares the transmission times (using the relay table) between direct and indirect (via relay) transmissions and then picks the path

(direct path or indirect path) that maximizes the rate. However, note that CoopMAC I only uses either direct path or indirect path for packet transmission based on updated table. [86] extends CoopMAC I for ad hoc network environment. It is very similar to CoopMAC I approach, but adds some minor features in data and control planes. [87] is a category two cooperative MAC protocol, that opportunistically invokes the relay when direct transmission fails (termed hereafter as UtdMAC). UtdMAC does not invoke any particular relay which can support higher data rate to the destination, but assumes that the relay will cooperate if present. [88] proposes rDCF protocol that requires periodic broadcast of willing list by each node to its one-hop neighbors. Further, the protocol piggybacks the data rate information to its RTS (request to send) and CTS (clear-to-send) packets which adds more overhead and requires modifications to the legacy IEEE 802.11 MAC protocol. [89] proposes infrastructure based rpcf protocol, where a node reports to the AP with the sensed channel information. The AP then informs the node about the feasible rate for the relay through the polling packet.

It was shown in [87] that under Rayleigh fading conditions UtdMAC protocol outperforms CoopMAC I in terms of throughput. It is worth mentioning here that UtdMAC assumes that nodes have already agreed to cooperate and so does not consider relay management overhead when comparing results with the CoopMAC I protocol. Results show that UtdMAC performs better because it uses diversity of the relay path for backup transmissions. On the other hand, CoopMAC I picks either the direct path or the relay path for reduced transmission time and does not invoke diversity for backup transmission. Although, the relay path can provide higher data rate, but is more susceptible to transmission failure due to independent fading on source to relay and relay

to destination links. Hence, the relay path in CoopMAC I can provide higher throughput but with lower probability of packet success. In contrast, UtdMAC has higher probability of packet success due to backup relay path, but provides lower data rate depending upon source-destination separation. In essence, both CoopMAC I and UtdMAC protocols lack in providing higher throughput with higher probability of success under fading conditions.

Thus motivated, we propose 2rcMAC protocol that makes use of spatial diversity due to two best relay paths provided they offer higher data rates compared to the direct path. In case, only one relay path (better or worse compared to the direct path) is available the 2rcMAC protocol transmits directly to the destination node and uses relay for backup transmission. We will henceforth term it as Utd mode. When no relay is available for cooperation then direct transmission takes place.

4.1.2 System Model

We design cooperative MAC protocol for a single channel, single hop ad hoc network. Channel is assumed to be symmetric, so communication in either direction experiences the same channel fade. The system consists of source-destination pair separated by some distance (d) with uniformly distributed nodes that can serve as potential relays. Assume that source, destination and potential relay nodes are always within the communication range of each other when packets are transmitted at 1 Mbps. All nodes transmit at fixed power. The system model for a general cooperative network is shown in Fig. 4.1. Labels S , D , r_n represent source, destination, n^{th} relay node, and SD , Sr_3 , r_3D represent the source-destination, source-relay3 and relay3-destination links, respectively. Nodes passively listen and update relay table based on path loss estimation as in [84, 85].

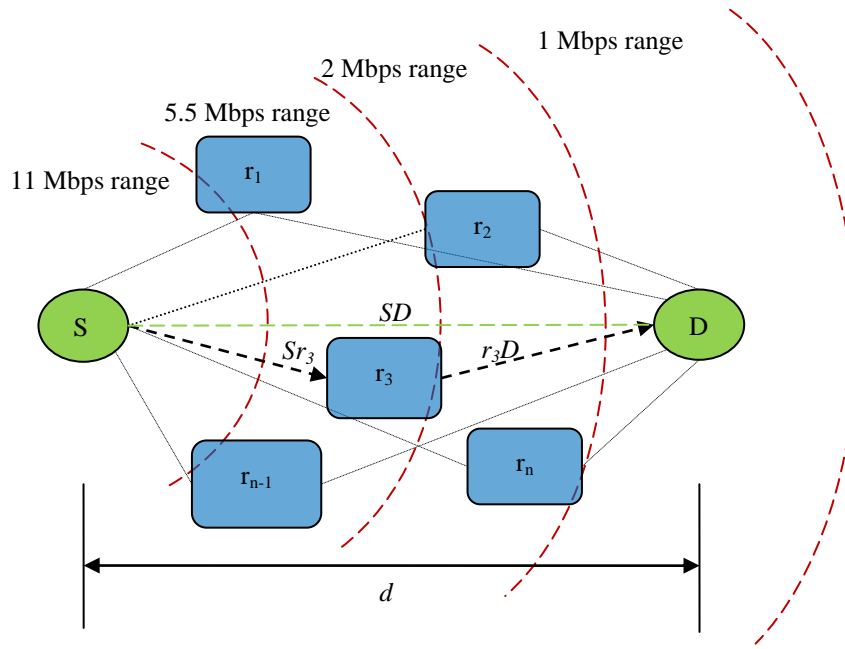


Figure 4.1: Cooperative Ad hoc Network Illustration

In this paper, we consider IEEE 802.11b physical layer which can support multiple data rates of 1, 2, 5.5 and 11 Mbps [90]. It uses direct sequence spread spectrum at a frequency of 2.4 GHz in ISM (Industrial Scientific and Medical) band. Different modulations techniques are used to achieve varying rates. Control packets and headers (RTS, CTS, PHY and MAC headers) are transmitted at a fixed rate of 1 Mbps. The achievable data rate between two nodes depends on the received SNR which is a function of many factors such as; distance, frequency, propagation environment, mobility, channel fading, and total noise at the receiver [91]. Data packets transmitted at a rate higher than the achievable rate cannot be correctly decoded due to increased BER (bit error rate) that consequently results in packet losses.

Further, we assume fast fading channel conditions. Each transmission cycle (see 4.1.3.1) and each link (for instance, SD , Sr_3 , and r_3D in Fig. 4.1) experience independent and identically distributed (i.i.d) Rayleigh fading.

4.1.3 Proposed 2rcMAC Protocol

In this section, we present an overview of IEEE 802.11 protocol, discuss the basic idea of the 2rcMAC protocol, present the details of the protocol, and finally explain the NAV (Network Allocation Vector) update mechanism and the framing used in 2rcMAC protocol. The proposed protocol is mainly based on IEEE 802.11 DCF protocol. Modulation techniques are chosen to maximize the transmission rate as a function of SNR.

4.1.3.1 IEEE 802.11 MAC Protocol Overview

Almost all of the proposed cooperative MAC protocols as discussed in Section 4.1.1 follow the basic IEEE 802.11 protocol procedures. In this section we provide a brief overview of the IEEE 802.11 DCF (distributed coordination function) protocol. Readers are referred to [90] for details. Source node wishing to transmit probes the channel by sensing it for DIFS (distributed interframe space) duration. If the channel is sensed idle, the source node backs-off randomly for a time period that is uniformly distributed between 0 and CW (contention window) and then transmits the RTS (request-to-send) packet to the destination, where, CW duration is contained within the interval $[CW_{min}, CW_{max}]$. The intended receiver (if not busy) after SIFS (short interframe space) duration responds by sending a CTS (clear-to-send) control packet to acknowledge the channel reservation. This handshake procedure takes care of two important issues: 1) Sender and receiver establish communication and initialize parameters; 2) the neighboring nodes that are in communication range of either the sender or the receiver avoid any transmission initiation during the ongoing session. Neighboring nodes update their NAV (network allocation vector) table for no transmission (termed as mute time) by

extracting information from the RTS or the CTS packet. Once the reservation is completed, the source node transmits the data packet after SIFS duration and then waits for acknowledgment (ACK) response from the destination. This completes one basic transmission cycle with the total duration of $RTS + SIFS + CTS + SIFS + DATA + SIFS + ACK$. If the channel is sensed busy during the DIFS period, the source node defers transmission. In case of packet transmission failure due to fading or collisions, source node after sensing for DIFS duration backs-off for a random duration that is uniformly distributed over the contention window interval $[0, CW_i]$, where, for the i^{th} retransmission attempt $CW_i = 2^i CW_{min}$ and $CW_i \in [CW_{min}, CW_{max}]$. This process is known binary exponential back-off.

4.1.3.2 Basic Idea of 2rcMAC Protocol

Fading conditions increase the probability of link failure. UtdMAC improves transmission reliability by using relay for backup transmission in case direct transmission fails between the source and the destination. UtdMAC throughput performance degrades appreciably when source-destination distance separation increases because only low rate direct transmission is possible. CoopMAC I improves throughput by choosing between direct path and relay path based on higher transmission rate. However, CoopMAC I does not provide any backup transmissions. Furthermore, relay path in CoopMAC I is highly susceptible to fading due to two independent links in a relay path transmission. In case of a transmission failure, CoopMAC I retransmits packet by repeating the transmission cycle as mentioned before. Generally, backup transmission requires lesser time than the new transmission cycle.

We propose the 2rcMAC protocol which makes use of two best relays to improve throughput and delay under fast fading conditions. We choose two best relays such that the total transmission time through first relay path plus the backup relay path (used for backup transmission) is less than the direct transmission time. The reason for such criterion is so that the mute time for other nodes in the network strictly remains less than the direct transmission time. Moreover, the use of backup path will provide better reliability compared to the CoopMAC I under fading conditions. Thus, as required by the 2rcMAC protocol, the total transmission time condition must satisfy,

$$\frac{1}{R_{Sr_1}} + \frac{1}{R_{r_1D}} + \frac{1}{R_{r_2D}} < \frac{1}{R_{SD}}.$$

We pick first best relay that offers combined rate better than the direct path rate, i.e.,

$$\frac{R_{Sr_1}R_{r_1D}}{R_{Sr_1}+R_{r_1D}} = \alpha R_{SD} \text{ (where, } \alpha \text{ can only take specific values greater than unity based on the}$$

IEEE 802.11b rates). Plugging the combined rate into the above transmission time condition leads to the transmission rate requirement for backup relay (relay 2), i.e.,

$$R_{r_2D} > \frac{\alpha R_{SD}}{\alpha - 1}.$$

To ascertain reliable reception at the backup relay, second condition that must be met requires $R_{Sr_2} \geq R_{Sr_1}$.

4.1.3.3 2rcMAC Protocol Details

In this section we explain the 2rcMAC protocol. In 2rcMAC protocol, nodes update the relay table using a passive listening approach as in [84-86]. However, node relay table in 2rcMAC is different as it only stores node's average rates with all the other nodes.

1) Idle Nodes always passively monitor transmissions in the neighborhood as in [84].

Nodes update the NAV tables for the duration of transmission. Relay table is updated with node ID, time of entry, and the average rate. The data rate (R) is estimated using

- path loss value (determined by subtracting received power from the fixed transmitted power) which is converted to the corresponding rate value using a physical mode table.
- 2) When the source node has a packet to transmit to the destination, it senses the channel for idleness. If the channel remains idle for the DIFS duration, the source then backs-off for a random duration as discussed in 4.1.3.1. Once the backoff counter reaches zero, the source then sends the RTS packet (at 1 Mbps) to the destination for channel reservation.
 - 3) If the RTS packet is decoded correctly at the destination node, it responds with the CTS packet after SIFS duration. In 2rcMAC, the CTS packet is transmitted before relays respond so that source and relays can confirm the presence of the destination node under fading conditions. Each relay node that receives both RTS and the CTS packets, responds in a relay response (RR) frame with a single bit feedback (at 1Mbps) to inform the source node of its presence and the rate capability. Generally, under heavy load and fast fading conditions relay nodes' dynamics necessitate relay information updates in real time. Furthermore, due to the presence of multiple relay nodes, collisions are also highly probable. As such, to manage relay contentions and retrieve rate information we introduce the RR frame. The RR frame is an 8-slot frame with 7 bits per slot. Optimal number of bits per slot can be investigated, but is not the focus of this research. Based on our simulations (for uniform placement of 500 nodes with varying source-destination distances from 20 meters to 120 meters) we found 7 bits to be sufficient for conflict resolution and information retrieval. Note that one conflict-free bit in a slot is sufficient to tap the relay. Each slot represents a different

rate category as shown in Fig. 4.2. For instance, the first two slots are for contention among relays with each relay having a combined rate of 1.46 Mbps ($\frac{2 \times 5.5}{2 + 5.5}$). The only difference between the first two slots is that the first slot is for relays with source to relay rate of 2 Mbps and relay to destination rate of 5.5 Mbps; whereas, it is reversed in the second slot. The last slot is for contention among relays such that each relay satisfies the combined rate requirement of 5.5 Mbps. In the last slot, since source to relay and relay to destination rates are same, therefore, no separate slot is needed. The duration of RR frame is fixed to $\sim 60 \mu\text{s}$. Each relay node remains precisely synchronized after receiving the CTS bits and knows the start bit time and the last bit time of the RR frame. A relay node based on its source-to-relay and relay-to-destination rates estimation chooses the appropriate rate slot and then sends a single bit feedback in a randomly picked bit interval location. Relays remain idle if they don't meet the rate requirements in the RR frame slots. We assume that the source node receives a single bit set to 1 when no collision takes place during a specific bit interval. Each relay node stores its bit interval location at which the response was sent to the source node (for example, a relay can send one bit feedback at the 54th bit interval location in the rate category slot (11,11) and store this location).

- 4) Once the relay responses are received during the RR frame, the source node searches for the two best relays (say, r_1 and r_2) in the same or different slots starting from the (11,11) rate category. Source node follows the steps below to find the two best relays:

- a. First find the best relay in the RR frame such that it offers a combined rate

$$(R_{C1} \equiv \frac{R_{Sr_1} \cdot R_{r_1D}}{[R_{Sr_1} + R_{r_1D}]}) \text{ greater than the source-destination rate,}$$

$$\text{i.e., } R_{C1} > R_{SD} .$$

- b. Calculate $\alpha = R_{C1}/R_{SD}$; where based on the allowed rates in the RR frame

notice that α can only attain certain values greater than one.

- c. Find second best relay that satisfies two conditions as follows: 1) $R_{r_2D} >$

$$\left(\frac{\alpha}{\alpha-1}\right) \cdot R_{SD} \text{ and 2) } R_{Sr_2} \geq R_{Sr_1} .$$

- 5) If two best relays are found in 4), then the source sends data to both the relays for eventual transmission to the destination node. The first picked best relay is always the first to transmit data to the destination. The source transmits at a compatible rate to this relay. Following data transmission completion by the first relay; if ACK transmitted directly to the source (at 1 Mbps) is overheard, the relays then clear their buffers. If no ACK is heard from the destination node, the second relay jumps in after relay timeout (RT) and retransmits the data. If no ACK is received after transmission by the second relay then relays clear their buffers and the source repeats the transmission cycle by retrying the failed data packet using exponential back-off process. In case, first relay did not receive the data packet due to fading then the second relay always jump in after relay timeout (RT) and transmits the data to the destination node. The two-best-relay message sequence is shown in Fig. 4.3 (note: dashed line shows backup path transmission).

- 6) In case, there is only one best relay (after receiving the RR frame) that offers combined rate better than the source-destination rate and all the other relays do not meet conditions in step (4c.), then the source picks the one best relay for backup path and transmits the packet directly to the destination node. In case of no ACK, the selected best relay jumps in and transmits the data packet. In case, the relay transmission fails as well, the source then repeats the transmission cycle. The one-best-relay message sequence is shown in Fig. 4.4.
- 7) If there is no best relay (received during the RR frame) with combined rate better than the source-destination rate, i.e., $R_{Sr_i} \cdot R_{r_iD} / (R_{Sr_i} + R_{r_iD}) \leq R_{SD}$ for $\forall i$, then the source picks any relay with maximum rate (or highest bit interval location in RR frame) as a backup path and transmits the packet directly to the destination node. In case of no ACK, the selected relay jumps in and transmits the data packet following the same message sequence as in Fig. 4.4.
- 8) In case, no relay feedback is received during the RR frame (due to collisions or due to absence of relays) then the source transmits directly to the destination without invoking any relay(s) as shown in Fig. 4.5.
- 9) The relay timeout (RT) is set larger than the SIFS duration to detect the beginning of ACK packet, but is much shorter than the DIFS duration. In this paper, we set RT to twice the SIFS duration.

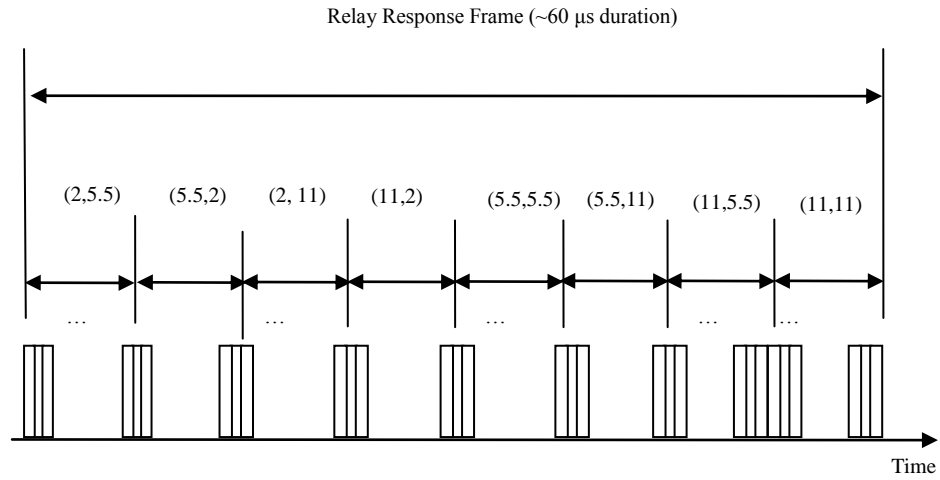


Figure 4.2: RR Frame Format

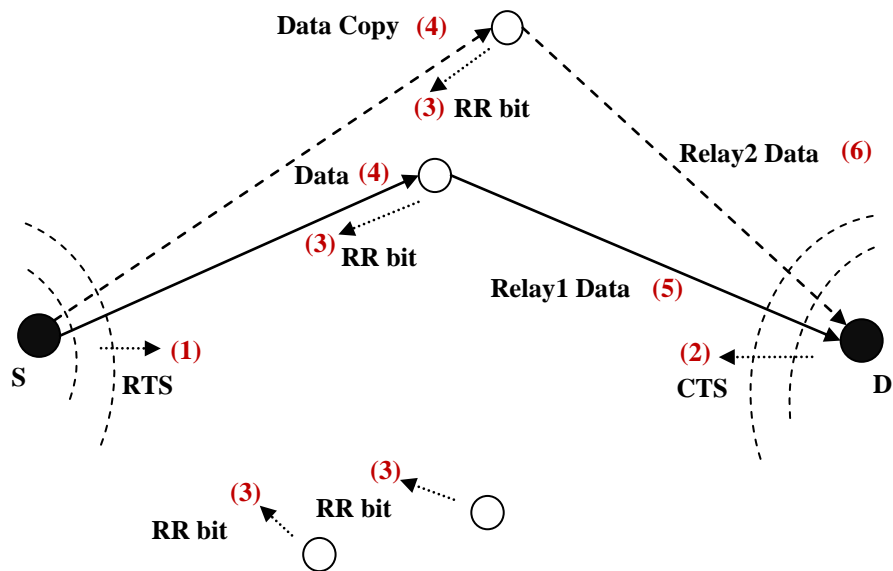


Figure 4.3: Message sequence for two best relays scenario

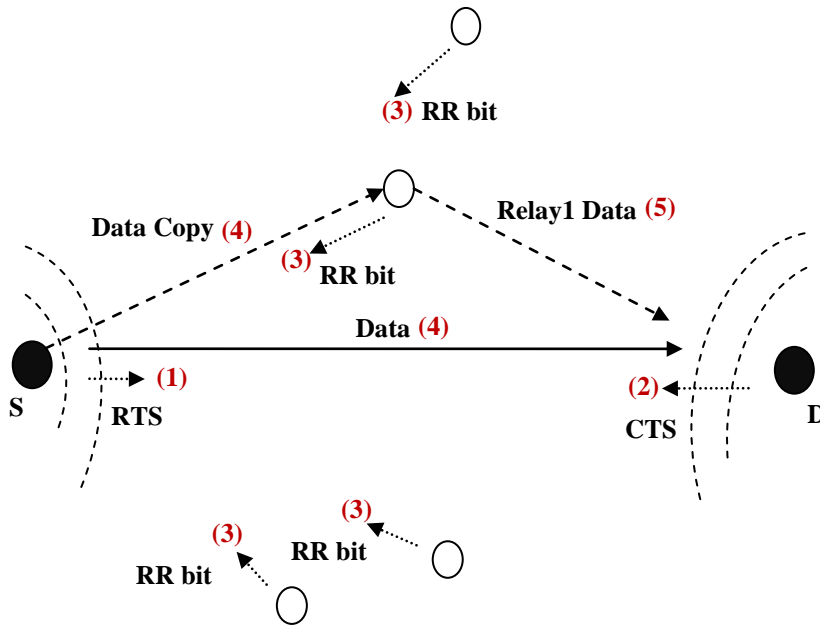


Figure 4.4: Message sequence for one or no best relay scenario

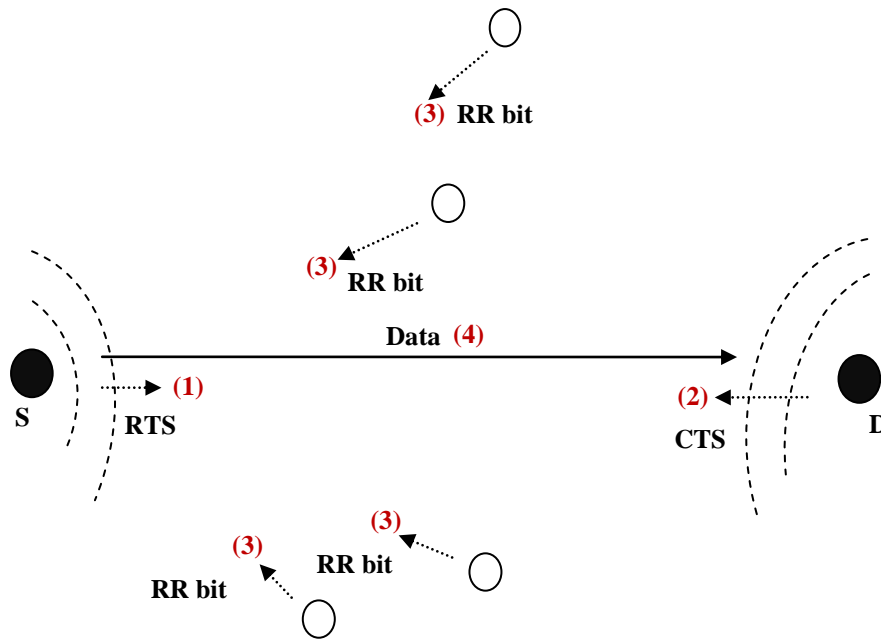


Figure 4.5: Message sequence for no relay response scenario

4.1.3.4 NAV Adaptation in 2rcMAC Protocol

The IEEE 802.11 DCF protocol uses virtual and physical carrier sensing to schedule transmission. Source node pre-calculates the transmission duration based on the packet length and fixed data rate. The duration fields in the RTS and CTS packets help the

neighbors set their NAV durations (used for physical and virtual sensing). In case of cooperative communications, the data rate is not fixed and depends on the relays' locations and channel conditions. Thus, the RTS and CTS duration fields cannot be precisely set until relay information becomes available at the source or destination node.

In 2rcMAC no additional signaling overhead is used to announce the transmission rates as in other protocols (see [84]). The neighboring nodes in 2rcMAC extract duration information from the RTS, CTS packets, and from MAC layer header which are transmitted at 1 Mbps. Thus, nodes are assumed to be at least in mutual communication or sensing range. Two points are worth mentioning under heavy load and fast fading conditions in ad hoc networks: 1) A particular relay may not be reachable due to fading or out of coverage range; and 2) multiple relays transmitting at the same time may result in contentions. The relay response (RR) frame with single-bit feedbacks provides relay rate information (R_{Sr} and R_{rD}) and also resolves collisions between the relays. From RR frame, the source may pick the available relay or relays for cooperation. Thus, only after RR frame the source and the neighbors can precisely know the data packet transmission duration. As such, this duration information is communicated through the duration field in the MAC header field.

In 2rcMAC protocol, the source sets the duration field in the RTS to $2SIFS + CTS + RR$ (ignore propagation delay for simplicity). The destination sets the CTS duration field to $2SIFS + RRF + Data_{RSD}$. Where, $Data_{RSD}$ is the duration of data transmission when source transmits payload data directly to the destination node at the rate of R_{SD} . In 2rcMAC protocol, we assume that the neighboring nodes are aware that the duration in the CTS packet is an estimate and so they monitor and extract information from the

header (see Fig. 4.7). Although, neighboring nodes can also extract information from the signal and length fields in the physical header, but for 2rcMAC we use duration field in the MAC header. We, henceforth, explain the NAV update mechanism for 2rcMAC protocol for one best relay scenario.

When source sends data to the destination then neighbors will update their NAVs to $Payload\ time + 2SIFS$ by extracting duration information from the MAC header. In case of direct transmission (one best relay case), the neighbors will start sensing for the DIFS duration after the NAV expires. In case of successful packet transmission, the neighbors will detect the ACK packet (medium busy) and will remain silent. However, if no ACK is transmitted (due to failure) then one best relay will jump in after RT timer (set to 2SIFS) expires and start transmitting. Thus, neighbors will detect the transmission of data packet again from the relay and will extract information from the MAC header to update their NAVs to $Payload\ time + SIFS + ACK$. Now suppose that data fails to reach both the destination and the backup relay node then the neighbors will not detect any relay transmission after the NAV expiration (i.e., $Payload\ time + 2SIFS$) and will continue carrier sensing for the DIFS duration for subsequent transmissions. Fig. 4.6 illustrates NAV update scheme in the case of one best relay retransmission.

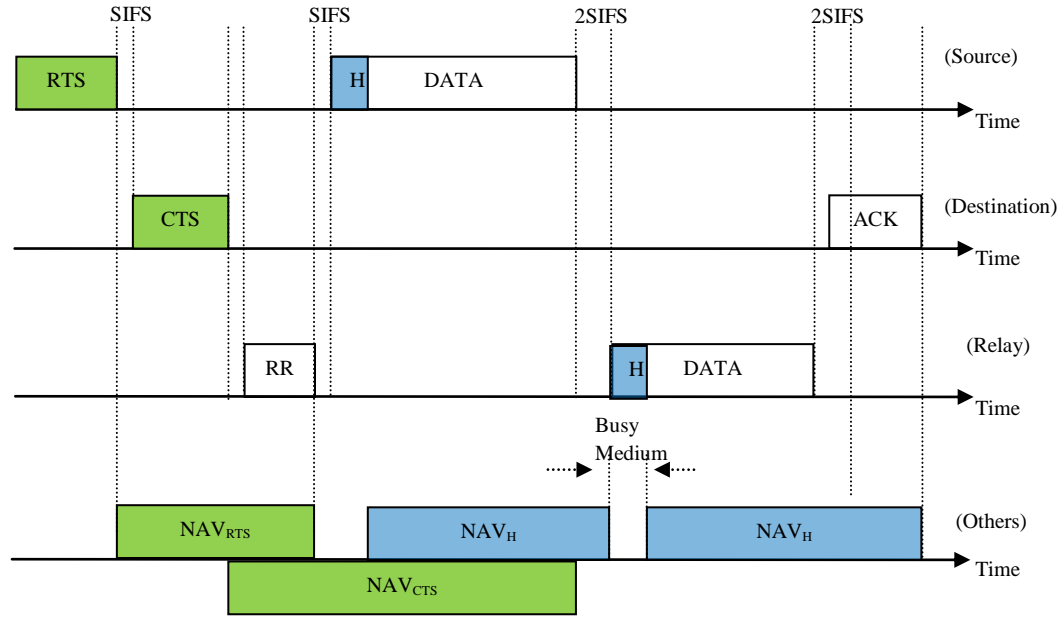


Figure 4.6: 2rcMAC NAV update mechanism for one best relay scenario

4.1.3.5 2rcMAC Framing and Logical Addressing

The 2rcMAC protocol uses IEEE 802.11b physical and MAC layer frames for unicast transmission as in Fig. 4.7. As discussed before, the PHY and MAC headers are transmitted at 1 Mbps, but the payload can be transmitted at varying rates of 1, 2, 5.5, and 11 Mbps. Since MAC header is transmitted at a lower rate of 1 Mbps so it can be used by the neighbors to update the NAV timer. In 2rcMAC protocol, multiple relays contend and respond during RR frame. If each relay broadcasts its address (to the source node and the destination node) then it will lead to extensive control overhead transmission. To avoid this unnecessary overhead transmission we use logical addressing in 2rcMAC protocol. We can use frame control and Address 4 fields in the MAC header to invoke one or two relays for help. If help from one or two relays is needed the Subtype field in the frame control is set accordingly for data type (see [90]). For example, Subtype field could be set to 1000 for one relay, 1001 for two relays, and 1111 for no relay help. Further, we use

first two octets of Address 4 to invoke specific relays as shown in Fig. 4.7. First Relay field identifies the relay that will transmit first, whereas the relay mentioned in the Second Relay field waits (until RT) for the first relay to start transmission. The two best relays that are picked from the RR frame, have unique bit interval location in the RR frame. For example, say that the first best relay that is picked transmitted one bit at the 52nd bit interval location and the second best relay transmitted at the 46th bit interval location. The source node changes the subtype field and then inserts these unique bit locations in the first relay and second relay fields. The contending relays always check the Subtype field and then the First Relay and Second Relay fields. Relays compare the Address 4 fields with their stored bit interval locations. If the match is found then the relay or relays transmit according to the 2rcMAC protocol. When the Subtype field is set to 1000 then only First relay field is used and the Second relay field octet is set to all zeros. When the relay transmits the data packet to the destination node it sets the Subtype field to 1111 so that no other relays are invoked.

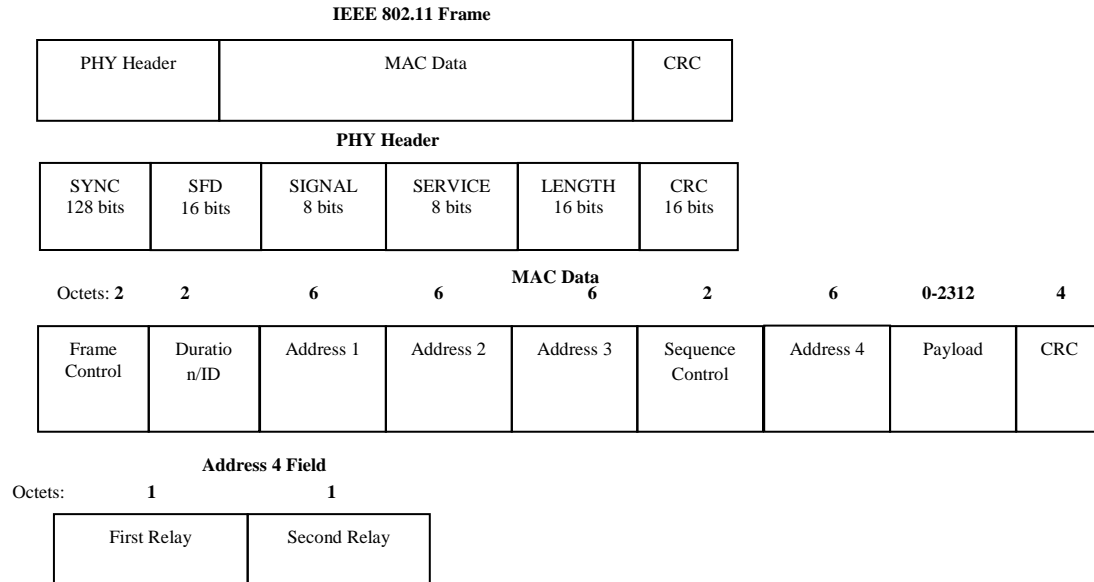


Figure 4.7: Frame format for 2rcMAC protocol

4.1.3.6 Node Density and Relay Management

Intuitively, as the node density increases the probability of finding relays also increase. This also necessitates managing relay contentions. UtdMAC assumes that a node (willing to behave as a relay) will listen passively and jump in when direct transmission (source to destination) fails. However, it does not address relay rate requirement and multiple relay transmissions and collisions. Managing relays require overhead which is not considered in UtdMAC. CoopMAC I partially addresses the relay contention issue by requesting a particular relay based on the stored relay rates in the table. This requires addition of three new fields in the RTS packet in CoopMAC I. However, the requested relay may not be reachable due to fading (mobility) and CoopMAC I may have no option but to transmit directly. Furthermore, in CoopMAC I handshaking, HTS message is transmitted by the requested relay to the source before CTS message is sent by the destination node. Therefore, it is likely that the destination node may not receive HTS packet due to fading and begin transmission of CTS packet while the HTS packet is being received by the

source node. This will lead to unnecessary collisions and waste precious bandwidth resource.

In contrast, 2rcMAC protocol fully exploits available relays and further resolves contention between relays under fading conditions as follows:

- 1) All nodes passively update tables for average rates;
- 2) RTS and CTS messages are exchanged before relays can respond. This way only relays that can decode both RTS and CTS packets respond in the RR frame;
- 3) each relay with combined rate greater than 1 Mbps can respond in RR frame;
- 4) each relay responds with a single bit at random bit interval location in an appropriate slot; and
- 5) source invokes relay(s) with logical addressing by using Address 4 field in IEEE 802.11 MAC header.

In short, 2rcMAC resolves possible relay contentions and further guarantees relay to destination connection under fading conditions.

Next, we show why relay conflict resolution is necessary in 2rcMAC. Fig. 4.8 shows the average number of relays with minimum combined rates greater than 1 Mbps as a function of source-destination separation for different node densities. Simulations were run 10,000 times under uniform node distribution. Notice that even for up to a distance separation of 100 m, more than two relays are present within the overlap area for different node densities. Fig. 4.9 shows the average number of relays with average combined rates better than the source-destination rate based on distance separations. Notice that on average for $d \leq 60$ m, relays with combined rates better than the source-destination rate are almost non-existent.

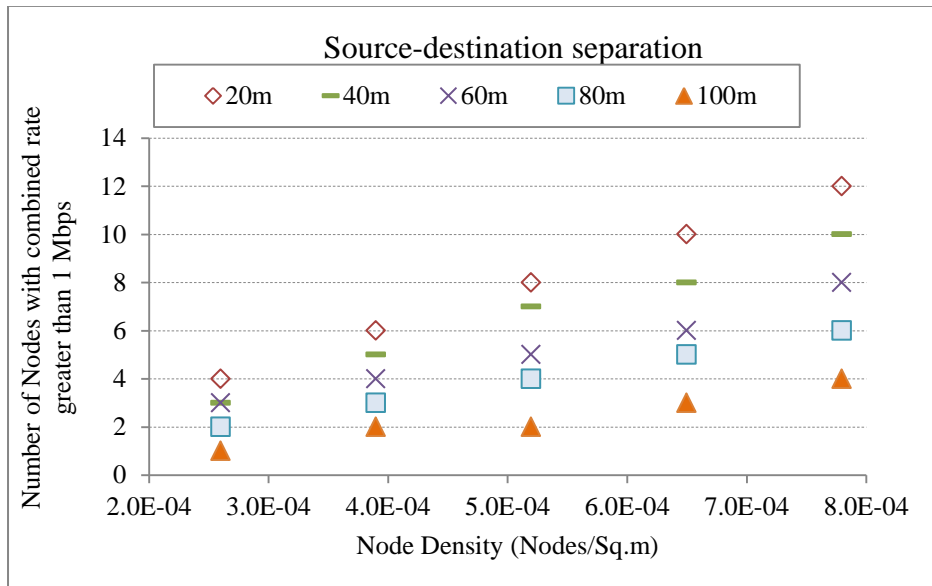


Figure 4.8: Average relay nodes statistics with rates greater than 1 Mbps

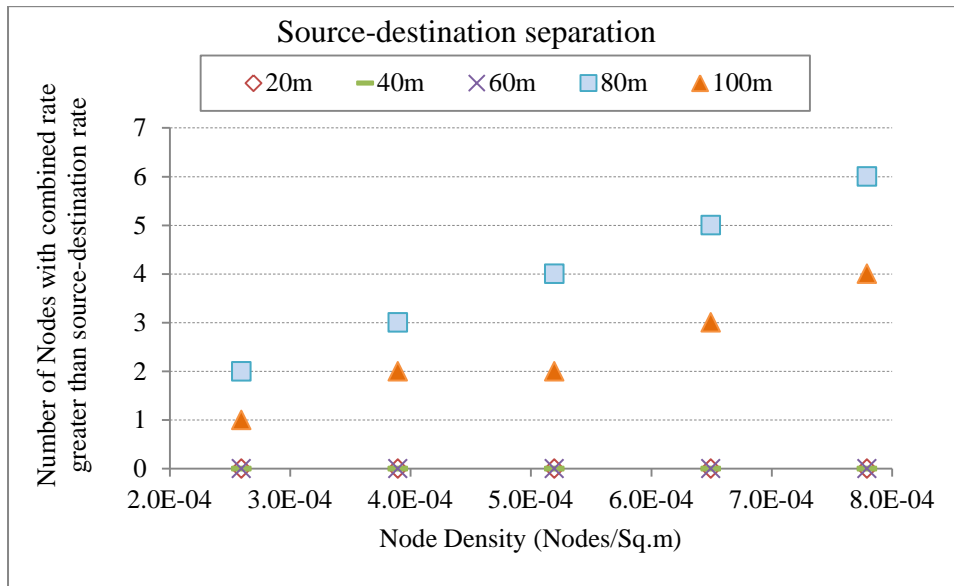


Figure 4.9: Average relay node statistics with rates greater than source-destination rates

4.1.4 Comparative Analysis and Discussion

In this section, we derive expressions for saturation throughput of UtdMAC, CoopMAC I and 2rcMAC protocols under fading conditions for IEEE 802.11b

specifications. For fading conditions, we define link probability of success as the probability of feasible (achievable) rate being greater than or equal to the actual transmission rate. P_{SD} , P_{Sr1} , and P_{r1D} represent link success probabilities of source-destination, source-to-relay1 and relay1-to-destination links, respectively. For UtdMAC that makes use of single relay for backup transmission, the probability of successful packet transmission is given by,

$$P_{s_utd} = P_{SD} + (1 - P_{SD}) \cdot P_{Sr1} \cdot P_{r1D} \quad (4.1)$$

CoopMAC I uses single relay path (indirect) only when it offers combined rate better than the source to destination rate, otherwise source to destination path (direct) is preferred for packet transmission. In reality, finding such relay nodes depends on the source-destination distance separation (or the overlapping area), node density, distribution of nodes, traffic load and many other factors. Let the probability of finding no best nodes be denoted by P_o . It is worth mentioning that the probability that no best nodes (with combined rates better than the source-destination rates) are available is a function of distance for a given node density. This was discussed in Section 4.1.3.6. Since CoopMAC I uses either direct path or indirect path the node probability of successful packet transmission is given by,

$$P_{s_coop} = P_o \cdot P_{SD} + (1 - P_o) \cdot P_{Sr1} \cdot P_{r1D} \quad (4.2)$$

2rcMAC protocol makes use of two best relays. If no best relay or one best relay is available it switches to Utd mode and if two best relays are available it transmits packets through first relay path ($Sr1 \rightarrow r1D$) and uses second relay path for backup transmission. Thus, the probability of successful packet transmission is given by,

$$P_{s_2rcmac} = (\dot{P}_2) \cdot \{P_{SD} + (1 - P_{SD}) \cdot P_{Sr1} \cdot P_{r1D}\} + (1 - \dot{P}_2) \{P_{Sr1} \cdot P_{r1D} + P_{Sr1} \cdot P_{r1D}\} \cdot P_{Sr2} \cdot P_{r2D} \quad (1 - (4.3))$$

where, \dot{P}_2 is the probability that two best relays are not available for higher rate transmission. Notice in (4.3) that the probability of success improves due to backup relay path compared to CoopMAC I. Later, we will use (4.1)-(4.3) for saturation throughput derivation.

Next, we extend the analytical results in [92] for cooperative MAC protocols under fading conditions. Assume saturation condition such that a node always has a packet to transmit. Let τ be the transmission probability of each node in a time slot and P_{s_x} be the probability of successful packet transmission for cooperative protocol x (where, x can be *UtdMAC*, *CoopMAC I* or *2rcMAC* as derived in (4.1)-(4.3)). For n active nodes, the probability that at least one node transmits in the time slot for protocol x is given by [93], $P_{tr_x} = 1 - (1 - \tau \cdot P_{s_x})^n$. Then the probability of successful transmission given that at least one node transmits is given by, $P_{trs_x} = \frac{n \cdot \tau \cdot (1 - \tau \cdot P_{s_x})^{n-1}}{P_{tr_x}}$. Where, τ depends on the probability of packet loss (p) and can be calculated by solving the following nonlinear equations [92],

$$p = 1 - P_{s_x} \cdot (1 - \tau \cdot P_{s_x})^{n-1} \quad (4.4)$$

$$\tau = \frac{2(1-2p)}{(1-2p)(CW_{min}+1)+pCW_{min}(1-(2p)^K)} \quad (4.5)$$

It is known that a typical node experiences three events. Packet success event occurs when no collision takes place with other nodes in the network and no fading occurs on direct or relay path. Packet failure event occurs when collision takes place with other

nodes, or when fading occurs on direct or relay path. In idle event, no transmission takes place. Then the saturation throughput for cooperative protocol x be expressed as [92],

$$S_{thr_x} = \frac{P_{tr_x} \cdot P_{trs_x} \cdot P_{s_x} \cdot (\text{payload bits})}{(1 - P_{tr_x})\sigma + P_{tr_x} \cdot (1 - P_{trs_x}) \cdot \bar{T}_c + P_{tr_x} \cdot P_{trs_x} \bar{T}_{s_x} + P_{tr_x} \cdot P_{trs_x} \bar{T}_{f_x}}, \quad (4.6)$$

where σ is the slot size; $\bar{T}_c = DIFS + Ebofff_x + RTS + SIFS$;

$Ebofff_x = \frac{\bar{K}_x \cdot (\sum_{j=0}^{\bar{K}_x} \mathbf{E}[CW_j])}{(\bar{K}_x + 1)}$ is the average back-off interval for failed

transmissions over uniformly distributed $\bar{K}_x + 1$ average transmissions (\mathbf{E} is

expectation); $P_{tr_x} \cdot P_{trs_x} \bar{T}_{s_x}$ is the average successful transmission time with no

collision and no fading and $P_{tr_x} \cdot P_{trs_x} \bar{T}_{f_x}$ is the average failure time due to fading but

no collision; $(1 - P_{tr_x})\sigma$ is the idle time and $P_{tr_x} \cdot (1 - P_{trs_x}) \cdot \bar{T}_c$ is the average

contention time due to collision. \bar{K}_x is the average number of retries up to a limit K and is

given by, $\bar{K}_x = \sum_{j=1}^K j P_{fx}^j = \frac{(1 - P_{fx}^K) \cdot P_{fx}}{(1 - P_{fx})^2} - \frac{K P_{fx}^{K+1}}{(1 - P_{fx})}$. P_{fx} is the probability of packet

transmission failure for the protocol x due to fading or collision and is given by, $P_{fx} =$

$1 - P_{s_x} \cdot (1 - \tau \cdot P_{s_x})^{n-1}$. Lastly, we define the constants (ignoring propagation delays)

and then calculate the average successful transmission time (\bar{T}_{s_x}) and average failure

time (\bar{T}_{f_x}) due to fading for each cooperative protocol in Appendix C. Plugging

calculated \bar{T}_{s_x} and \bar{T}_{f_x} into (4.6) will give the saturation throughput performance for

each protocol. The details of the calculations are provided in Appendix C.

4.1.5 Performance Evaluation

In this section, saturation throughput and delay performances of 2rcMAC, CoopMAC I

and UtdMAC protocols are discussed and compared under fast fading conditions. In the

context of this paper, saturation throughput is defined as the successfully transmitted payload bits per second given that a source node always has a packet to transmit in its buffer and delay is defined as the average time taken for successful transmission of a packet. To quantify performance, an event-based simulator is developed that precisely follows 802.11 MAC state transitions. For fair comparison, it is assumed that UtdMAC avoids possible contention between relay nodes by invoking one best relay node through RTS packet. On the other hand, CoopMAC I and 2rcMAC protocols are capable of handling such contentions.

4.1.5.1 Simulation Setup

The channel is assumed to have a flat Rayleigh fading which is constant during packet transmission, but changes from one packet to another. Each link also experiences i.i.d. fading. The received instantaneous signal-to-noise ratio ($snr(j, k)$) from node j to node k depends on transmitted power (P_T), processing gain (P_g), distance separation (d), propagation exponent ($2 \leq \beta \leq 6$), Rayleigh fading parameter (γ), slow lognormal fading (L), antenna gain product (G_p), antenna height effect (h_e), carrier wavelength (λ), noise power (N) and is given by [94],

$$snr(j, k) = \frac{P_T P_g G_p h_e \gamma^2 10^{\frac{L}{10}} \lambda^2}{16\pi^2 d^\beta N} \quad (4.7)$$

Where, $N = kTB N_f$, $k = 1.38e^{-23}$ is Boltzman's constant, $T = 300^\circ K$ is temperature, $B = 20 MHz$ is the bandwidth, and $N_f = 10$ is the receiver noise factor. As in [84-86], the corresponding approximate distance ranges (based on average signal-to-noise ratio) for 802.11b rates of 11 Mbps, 5.5 Mbps, 2 Mbps and 1 Mbps are 55 m, 70 m, 75 m, and

100 m, respectively. Table 4.1 shows simulation parameters adopted from IEEE 802.11b standard.

Table 4.1: Simulation Parameters

Parameter	Value	Parameter	Value
Frequency	2.4 GHz	CTS, ACK	112 bits
β	4	Slot time	20 μ s
$G_p, h_e, 10^{\left(\frac{L}{10}\right)}$	All set to 1	SIFS	10 μ s
λ	0.125 m	DIFS	50 μ s
P_T	0.1 W	Payload	1023 bytes
P_g	10	CW_{\min}	32
MAC Header	272 bits	CW_{\max}	1024
PHY Header	192 bits	Max. transmission attempts	6
RTS	160 bits	Rate for MAC and PHY headers, RTS, CTS, and ACK packets	1 Mbps

Simulation is carried out under saturation condition such that a source node always has a packet to transmit in its buffer. Enough relay nodes are placed randomly to guarantee relay(s) presence. We evaluate protocols (2rcMAC, UtdMAC and CoopMAC I) performance under two cases. In the first case, saturation throughput and delay performances are analyzed as a function of distance for a single source-destination pair. In the second case, saturation throughput performance is compared for increasing number of source nodes in the ad hoc network. All the nodes are randomly placed in a radius of 200 m. Concurrent transmissions always lead to collisions. Propagation delay is assumed negligible. The data collected is averaged over many runs. Each run uses a different seed value for random placement of nodes (relays and sources) and is executed for an extended period of time (about 1.5 million packets) to get stable results. Rayleigh fading parameters are generated using ITU-R outdoor vehicular multipath model [95] at the speed of 13 m/s.

4.1.5.2 Simulation Results and Discussion

Fig. 4.10 compares saturation throughput as a function of source-destination distance. For distance range of $d \leq 60 m$, the source-destination overlapping area is large and hence encompasses larger number of relay nodes for transmission. Relays in this range are most likely in close proximity of both source and the destination nodes and can offer transmission rates of 11 Mbps or 5.5 Mbps on source-to-relay and relay-to-destination links. However, in this range direct path transmission rates (of 11 Mbps and 5.5 Mbps) are always better than the combined rate through any relay path ($\frac{11 \times 11}{22} = 5.5$ Mbps). So, CoopMAC I initiates high rate direct transmission only. Whereas, 2rcMAC protocol initiates high rate direct transmission using high rate relay path as a backup path (in the same manner as the UtdMAC protocol). Thus, in case of packet failure, 2rcMAC and UtdMAC rely on high rate backup transmission, whereas, CoopMAC I starts a new transmission cycle for packet retransmission. Recall, that retransmission through a new transmission cycle requires more time due to DIFS sensing and back-off interval compared to the backup relay transmission time. Hence, CoopMAC I performs worse than UtdMAC and 2rcMAC due to lower transmission reliability (no backup path) and larger overhead (due to HTS packet and RTS packet extension). Further, recall that UtdMAC has no mechanism for storing relay information and invoking a specific relay for backup transmission. As such, it is assumed for fair comparison that UtdMAC can invoke a specific relay for help by adding address field in the RTS packet. Consequently, it is observed that 2rcMAC throughput performance is almost same as that of the UtdMAC protocol since both protocols operate with the backup relay path. Overall saturation throughput is high in this range for all the protocols.

For distance range of $60\text{ m} < d < 100\text{ m}$, it is observed that the source-destination overlapping reduces but still encompasses relays to allow for beneficial relay transmission. Interestingly, in this range relays offer better throughput improvement opportunities due to combined rates better than the direct transmission rates of 1-2 Mbps. These higher combined rates compensate for the overhead time in CoopMAC I. Thus, CoopMAC I performs better than UtdMAC (by 0.13 Mbps) at a distance of about 80 m due to improved throughput through the relay path. In this range, UtdMAC initiates direct transmission at the low rate of 1 Mbps. The backup relay also receives information from the source at this lower rate. In case of direct transmission failure, backup transmission entails larger transmission time compared to CoopMAC I. In this range, 2rcMAC really benefits from two relays, by using second relay (see conditions in Section 4.1.3.3) as a backup path for better reliability. 2rcMAC transmits to the first relay at high rate such that second relay is also able to receive at this rate. In case of failure through the first relay, the second backup relay transmission is also at higher rate. In essence, in 2rcMAC the total transmission time (including the transmission time through the second backup relay path) is less than the transmission time through the direct path. This improves 2rcMAC throughput significantly compared to the UtdMAC and CoopMAC I.

For the distance range of $d \geq 100\text{ m}$, it is observed that due to increased path loss and fast fading, direct transmission throughput is reduced below 1 Mbps. Furthermore, due to minimal overlapping and increased distances between relays, source and destination nodes, the average achievable rates on source-to-relay and relay-to-destination links are also reduced significantly. Thus, as expected the overall throughput is reduced for all protocols (see Fig. 4.10). Also note that the probability of success for source-destination

link is higher at the distance of 100 m compared to 120 m. UtdMAC transmission failure rate increases as the source to destination distance increases from 100 m to 120 m. Backup relay transmission is also at lower rate (due to increased distance between relay and destination node). Thus UtdMAC saturation throughput reduces from 0.81 Mbps to 5 kbps for distances of 100m and 120 m, respectively. CoopMAC I throughput remains lower than UtdMAC because for success through the relay path both source-to-relay and relay-to-destination links have to be in non-fading states at the transmitted rates. In contrast, 2rcMAC outperforms UtdMAC and CoopMAC I protocols because it makes use of two suitable relay paths that can provide higher throughput with higher reliability. The saturation throughput for 2rcMAC reduces from 0.86 Mbps to 0.13 Mbps for distances of 100 m and 120 m, respectively.

Figure 4.11 shows the delay comparison as a function of distance. Clearly, the delay of our protocol is lower than UtdMAC and CoopMAC I. At the distance of 100 m, the delay difference ($T_{utd,coop} - T_{2rcmac}$) is 0.55 ms and 2.28 ms with respect to UtdMAC and CoopMAC I, respectively. At the distance of 120 m, this time difference significantly increases to 1.57 s and 8.12 s with respect to UtdMAC and CoopMAC I, respectively. This is because of the two-relay approach that decreases the average transmission time and allows more packets to be transmitted within the given time duration. Note that the mean delay over the distance range of $20\text{ m} \leq d \leq 120\text{ m}$ is 0.28 s, 1.37 s and 0.01 s for UtdMAC, CoopMAC I and 2rcMAC, respectively.

Figure 4.12 compares the saturation throughput as a function of increasing number of transmitting nodes. The saturation throughput initially increases as the number of transmitting nodes increase. Then it remains almost flat up to 15 nodes and after that a

slight decline in throughput is observed. The reason for the decrease in throughput is because the collisions become dominant and it begins to offset the throughput improvement due to cooperation. However, it is worth mentioning that compared to non-cooperative protocols cooperative protocols will always scale well due to reduced transmission time and increased number of transmissions in a given time period. The mean throughput difference of 0.14 Mbps and 0.44 Mbps is observed with respect to UtdMAC and CoopMAC I, respectively.

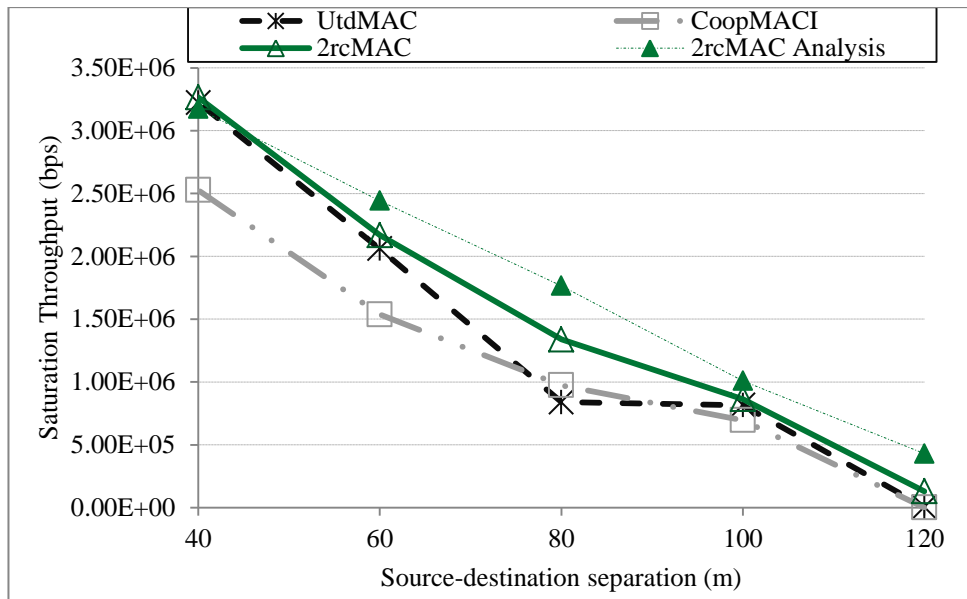


Figure 4.10: Saturation throughput comparison as a function of distance for 2rcMAC

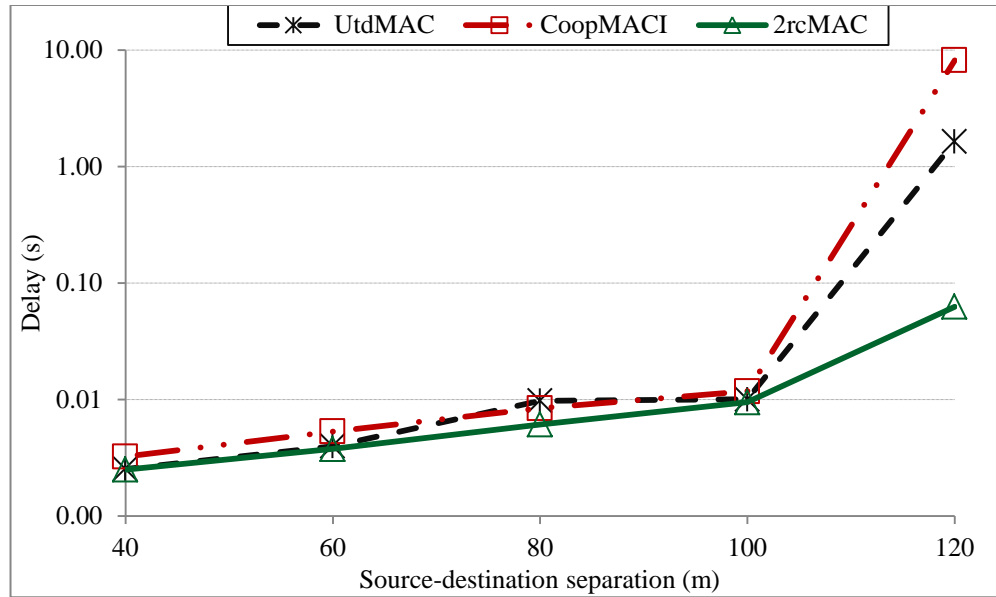


Figure 4.11: Average delay for successful packet transmission for 2rcMAC

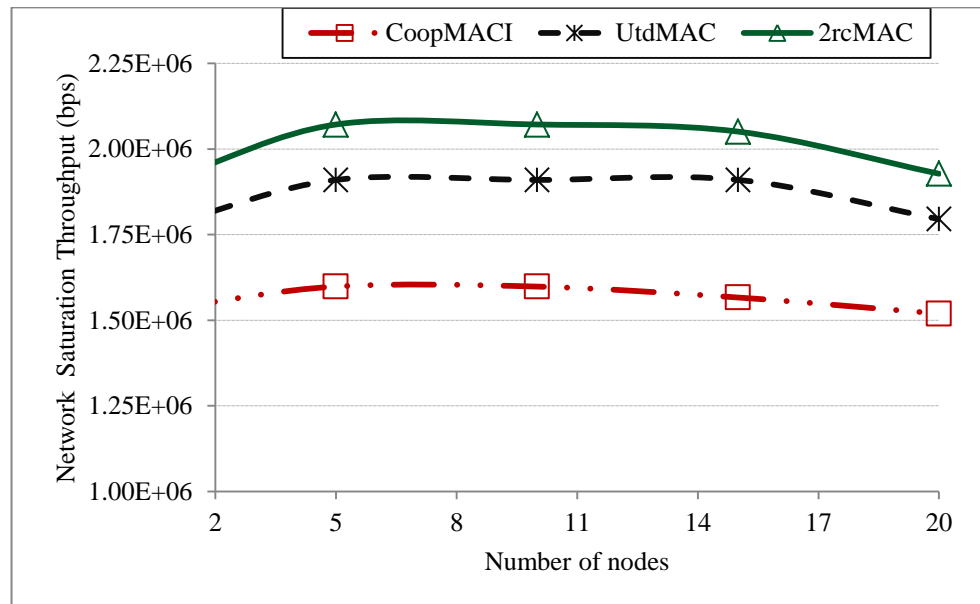


Figure 4.12: Network saturation throughput for 2rcMAC

4.2 Coherence Time Based Cooperative MAC Protocol

In this Section, we develop IrcMAC protocol that measures instantaneous signal-to-noise ratio (snr) on source-to-destination, source-to-relay and relay-to-destination links to evaluate packet transmission opportunities through direct and the candidate relay paths. A relay path becomes a candidate only when the channel coherence time is greater

than the total transmission time through the relay path. Once, IrcMAC selects the best candidate relay path, the packet is then transmitted through the path (direct or relay path) that incurs minimum transmission time. In case, no candidate relay path is available, the IrcMAC protocol transmits directly to the destination node at the rate estimated during the handshake procedure. Protocol details are provided in later sections.

4.2.1 Proposed IrcMAC Protocol

In this section, we explain the IrcMAC protocol, discuss the NAV adaptation and the framing used in the IrcMAC protocol, and lastly expound on the relay management feature of the protocol. The proposed protocol is mainly based on IEEE 802.11 DCF protocol.

4.2.1.1 IrcMAC Protocol Details

- 1) Idle nodes always passively monitor transmissions in the neighborhood. Nodes update the NAV tables for the duration of transmission. The data rate R is estimated using snr estimate at the receiver (source node uses CTS packet and relay nodes use RTS and CTS packets for snr estimation).
- 2) When the source node has a packet to transmit to the destination, it senses the channel for idleness. If the channel remains idle for the DIFS duration, the source then backs-off for a random duration as discussed in Section 4.1.3.1. Once the back-off counter reaches zero, the source then sends the RTS packet (at 1 Mbps) to the destination for channel reservation.
- 3) If the RTS packet is decoded correctly at the destination node, it responds with the CTS packet after SIFS duration. The source node uses CTS packet reception to estimate the instantaneous signal-to-noise ratio on source-to-destination link, i.e.,

snr_{sd} . The CTS packet is transmitted before relays respond so that source and relays can confirm the presence of the destination node under fast fading condition. Each available relay node uses the RTS and the CTS packet reception to estimate the snr on the source-to-relay and the relay-to-destination links, i.e., snr_{sr} and snr_{rd} , respectively. In IrcMAC protocol, relay path is picked only if the following two conditions are satisfied: 1) the sum of transmission time (i.e., the time taken by the data packet from the source node to reach the destination node through the relay path) through the relay node plus the time until the ACK is received by the source node is less than or equal to the channel coherence time; and 2) the total transmission time through the relay node is less than the direct path transmission time. In contrast to CoopMAC I, IrcMAC protocol uses instantaneous rates (based on estimated snr) for direct or indirect transmission and, more importantly, first condition also ensures reliable transmission through the relay path. Only the relay nodes that have their total transmission times less than the channel coherence time respond in the relay response (RR) frame with a single bit feedback (at 1Mbps) to inform the source node of their presence and the instantaneous rate capability. Generally, under heavy load and fast fading conditions relay nodes' dynamics necessitate relay information updates in real time. Furthermore, due to the presence of multiple relay nodes, collisions are also highly probable. As such, to manage relay contentions and retrieve rate information we introduce the RR frame as already explained in Section 4.1.3.3. A relay node that satisfies the total transmission time less than the channel coherence time chooses the appropriate instantaneous rate slot in RR frame and then sends a single bit feedback in a randomly picked bit interval location. Relays remain idle if they don't meet the

total transmission time requirement. We assume that the source node receives a single bit set to 1 when no collision takes place during a specific bit interval. Each relay node stores its bit interval location at which the response was sent to the source node (for example, a relay can send one bit feedback at the 54th bit interval location in the instantaneous rate category slot (11,11) and store this location).

- 4) Once the relay responses are received during the RR frame, the source node searches for the best relay starting from the (11,11) rate category. The best relay in the RR frame is the one that offers instantaneous combined rate ($R_C \equiv \frac{R_{sr} \cdot R_{rD}}{[R_{sr} + R_{rD}]}$) greater than the source-destination rate, i.e., $R_C > R_{SD}$.
- 5) If the best relay path is found, then the source sends data at the instantaneous rate of R_{sr} to the relay for eventual transmission at the instantaneous rate of R_{rD} to the destination node. Following successful data transmission completion by the relay, ACK is transmitted directly to the source (at 1 Mbps). If no ACK is heard from the destination node (due to increased interference on source-destination link), the source repeats the transmission cycle by retrying the failed data packet using exponential back-off process. The best-relay message sequence is shown in Fig. 4.13.
- 6) If no best relay is found with instantaneous combined rate better than the source-destination instantaneous rate, i.e., $\frac{R_{sr_i} \cdot R_{r_iD}}{(R_{sr_i} + R_{r_iD})} \leq R_{SD}$ for $\forall i$, then the source transmits the packet directly to the destination node at the instantaneous rate of R_{SD} (estimated during RTS/CTS handshake). The message sequence is similar to Fig. 4.5 shown earlier. Note that minimum R_{SD} is 1 Mbps, or else the source node repeats

the transmission cycle. In case of no ACK, the source repeats the transmission cycle by retrying the failed data packet using exponential back-off process.

- 7) In case, no relay feedback is received during the RR frame (due to collisions or due to absence of relays) then the source transmits directly to the destination in the same manner as in step (6).
- 8) In case, the relay path is chosen but the relay fails to receive the packet from the source (due to increased interference), the source then waits for the timeout (set to twice the SIFS duration) and then repeats the transmission cycle.

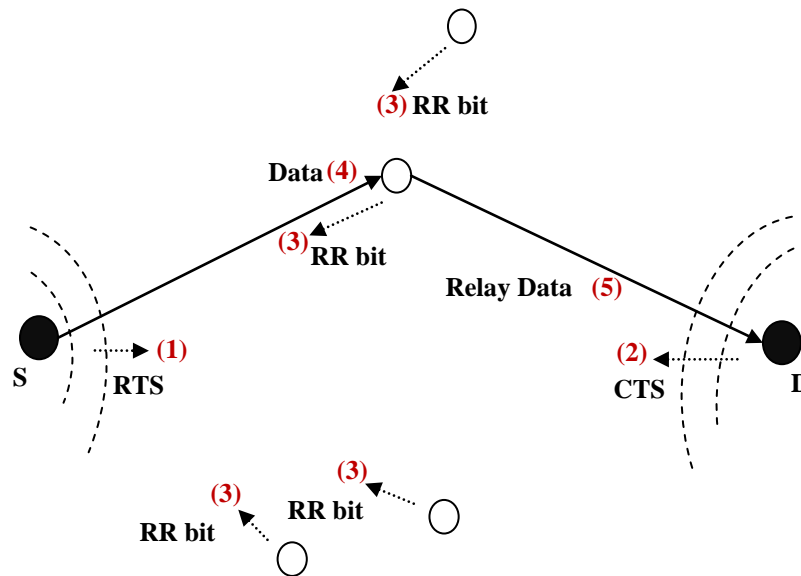


Figure 4.13: Message sequence for the best relay scenario for IrcMAC

4.2.1.2 NAV Adaptation in IrcMAC Protocol

In IrcMAC protocol, minimal signaling overhead is used to announce the transmission rates compared to CoopMAC I. The neighboring nodes in IrcMAC extract duration information from the RTS, CTS packets, and from MAC layer header which are transmitted at 1 Mbps. Thus nodes are assumed to be at least in mutual communication or

sensing range. Two points are worth mentioning when ad hoc network operates under heavy load and fast fading conditions. 1) A particular relay may not be reachable due to fading condition or out of coverage range and 2) multiple relays transmitting at the same time may result in contentions. The relay response (RR) frame with single-bit feedbacks provides relay rate information (R_{Sr} and R_{rD}) and also resolves collisions between the relays. From RR frame, the source may pick the available best relay for cooperation. Thus, only after RR frame the source and the neighbors can precisely know the data packet transmission duration. As such, this duration information is communicated through the duration field in the MAC header field.

In IrcMAC protocol, the source sets the duration field in the RTS to $2SIFS + CTS + RRF$ (ignore propagation delay for simplicity). The destination sets the CTS duration field to $2SIFS + RRF + Data_{rSD}$. Where, $Data_{rSD}$ is the duration of data transmission when source transmits payload data directly to the destination node at the rate of R_{SD} . The duration field in the MAC header is set to $payload\ time + 2SIFS$. In IrcMAC protocol, we assume that the neighboring nodes are aware that the duration in the CTS packet is an estimate and so they monitor and extract information from the MAC header. Although, neighboring nodes can also extract information from the signal and length fields in the physical header, but for IrcMAC we use duration field in the MAC header. We, henceforth, explain the NAV update mechanism for IrcMAC protocol for the best relay scenario.

When source sends data to the relay node then neighbors will update their NAVs to $Payload\ time_{Sr} + DATA_{rD} + 2SIFS + ACK$ by extracting duration information from the MAC header. The relay after receiving transmission from the source node will wait

for *SIFS* duration for eventual transmission to the destination node. The relay neighbors will, therefore, detect the transmission of data packet again from the relay to the destination node and will extract information from the MAC header to update their NAVs to $Payload\ time_{rD} + SIFS + ACK$. However, if no ACK is transmitted (due to interference) the NAV will expire and then the neighbors can continue carrier sensing for the DIFS duration for subsequent transmissions. Fig. 4.14 illustrates NAV update scheme in the case of the best relay scenario.

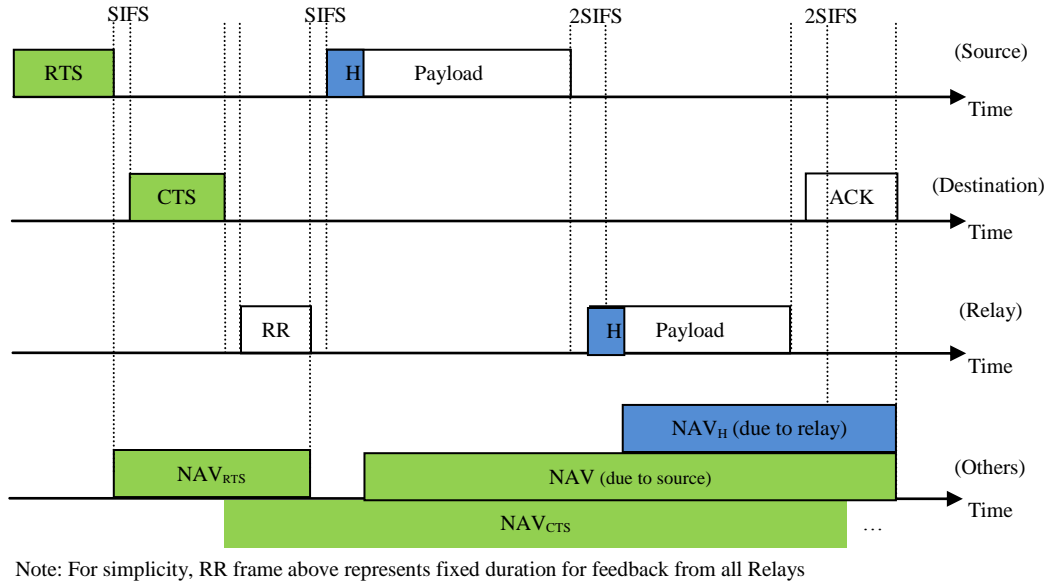


Figure 4.14: IrcMAC NAV update mechanism for best relay scenario

4.2.1.3 IrcMAC Framing and Logical Addressing

The IrcMAC protocol uses IEEE 802.11b physical and MAC layer frames for unicast transmission as in Fig. 4.7. Its major difference from 2rcMAC is that it invokes single relay only rather than two relays. To avoid this unnecessary overhead transmission we use logical addressing in IrcMAC protocol. We use frame control and Address 4 fields in the MAC header to invoke one best relay for help. If help from the available best relay is

needed the Subtype field in the frame control is set accordingly for data type (see [10]). For example, Subtype field could be set to 1000 for one best relay and 1111 for no relay help. Further, we use first octet of Address 4 to invoke specific relay. It identifies the best relay that is invoked for eventual transmission to the destination node. The best relay that is picked from the RR frame, have unique bit interval location in the RR frame. For example, suppose that the best relay that is picked transmitted one bit at the 52nd bit interval location. The source node changes the subtype field to 1000 and then inserts this unique bit location in the first octet of the Address 4 field. The contending relays always check the Subtype field and then the first octet of the Address 4 field. Relays then compare the Address 4 field with their stored bit interval locations. If the match is found then that relay transmits according to the IrcMAC protocol. When the best relay transmits the data packet to the destination node it sets the Subtype field to 1111 so that no other relays are invoked.

4.2.1.4 IrcMAC Relay Management

IrcMAC protocol fully exploits available relays and further resolves contention between relays under fast fading conditions in the same manner as the 2rcMAC protocol discussed earlier. Salient points are as follows: 1) All nodes passively monitor and estimate channel coherence time; 2) RTS and CTS messages are exchanged before relays can respond. This way only relays that can decode both RTS and CTS packets respond in the RR frame; 3) each relay with total transmission time less than the channel coherence time can only respond in RR frame; 4) each relay responds with a single bit at random bit interval location in an appropriate slot; and 5) source invokes relay with logical addressing by using Address 4 field in IEEE 802.11 MAC header.

4.2.2 Performance Evaluation

In this section, saturation throughput and delay performances of IrcMAC, CoopMAC I and UtdMAC protocols are compared and discussed under fast fading conditions. The channel is assumed to have flat Rayleigh fading for the duration of coherence time. When the channel coherence time is greater than the total packet transmission time along the path (direct, indirect/relay path), then the estimated snr is precisely known along that path (direct, indirect/relay path). Further, each payload transmission and each link also experience i.i.d. fading. At bit error rate of 10^{-5} or better, the rates of 11 Mbps, 5.5 Mbps, 2 Mbps and 1 Mbps correspond to signal-to-noise ratio ranges of $snr > 10$, $6.25 < snr \leq 10$, $5 < snr \leq 6.25$ and $0.62 \leq snr \leq 5$, respectively (adopted from [84,85]). For simulation parameter details see Section 4.1.5.1.

4.2.2.1 IrcMAC Simulation Results and Discussion

Figure 4.15 compares saturation throughput as a function of source-destination distance. For distance range of $d \leq 70 m$, the source-destination overlapping area is large and hence encompasses larger number of relay nodes for transmission. Relays in this range are most likely in close proximity of both source and the destination nodes and can offer transmission rates of 11 Mbps or 5.5 Mbps on source-to-relay and relay-to-destination links. However, in this range on average direct path transmission rates (of 11 Mbps and 5.5 Mbps) are always better than the average combined rate through any relay path ($\frac{11 \times 11}{22} = 5.5$ Mbps). So, CoopMAC I initiates high rate direct transmission only. Whereas, UtdMAC protocol initiates high rate direct transmission using high rate relay path as a backup path. Thus, in case of packet failure, UtdMAC rely on high rate backup transmission, whereas, CoopMAC I starts a new transmission cycle for packet

retransmission. Recall, that retransmission through a new transmission cycle requires more time due to DIFS sensing and back-off interval compared to the backup relay transmission time. Hence, CoopMAC I performs worse than UtdMAC due to lower transmission reliability (no backup path) and larger overhead (due to HTS packet and RTS packet extension). Our IrcMAC protocol relies on instantaneous rates available on relay and direct paths. IrcMAC protocol chooses relay only when it can offer reliable transmission path by comparing channel coherence time with the instantaneous combined rate through the relay. Thus, it is possible that although the direct path rate is better on the average, but at the transmission instant the direct path may encounter deep fade, whereas the relay path may offer relatively better combined instantaneous rate. In such case, IrcMAC protocol will then pick the relay path for reliable and fast transmission. As clear from Fig. 4.15, IrcMAC throughput is significantly better than both UtdMAC and CoopMAC I in this distance range. Overall saturation throughput is high in this range for all the protocols.

For distance range of $70\text{ m} < d < 100\text{ m}$, it is observed that the source-destination overlapping reduces but still encompasses relays to allow for beneficial relay transmission. Interestingly, in this range relays offer better throughput improvement opportunities due to combined rates better than the direct transmission rates of 1-2 Mbps. These higher combined rates compensate for the overhead time in CoopMAC I. Thus, CoopMAC I performs better than UtdMAC (by 0.13 Mbps) at a distance of about 80 m due to improved throughput through the relay path. In this range, UtdMAC initiates direct transmission at the low rate of 1 Mbps. The backup relay also receives information from the source at this lower rate. In case of direct transmission failure, backup transmission

entails larger transmission time compared to CoopMAC I. In this range, IrcMAC again performs considerably better than both the protocols due to reliable instantaneous rate transmission.

For the distance range of $d \geq 100$ m, it is observed that due to increased distance and fast fading, direct transmission throughput is reduced below 1 Mbps. Furthermore, due to minimal overlapping and increased distances between relays, source and destination nodes, the average achievable rates on source-to-relay and relay-to-destination links are also reduced significantly. Thus, as expected the overall throughput is reduced for all protocols (see Fig. 4.15). UtdMAC transmission failure rate increases as the source to destination distance increases from 100 m to 120 m. Backup relay transmission is also at lower rate (due to increased distance between relay and destination node). Thus UtdMAC saturation throughput reduces from 0.81 Mbps to 5 kbps for distances of 100m and 120 m, respectively. CoopMAC I throughput remains lower than UtdMAC because for success through the relay path both source-to-relay and relay-to-destination links have to be in non-fading states at the transmitted rates. In contrast, IrcMAC outperforms UtdMAC and CoopMAC I protocols because it makes use of instantaneous rates that can reliably provide higher throughput. The saturation throughput for IrcMAC reduces from 1.55 Mbps to 0.97 Mbps for distances of 100 m and 120 m, respectively.

Figure 4.16 shows the delay comparison as a function of distance. Clearly, the delay of our protocol is lower than UtdMAC and CoopMAC I. At the distance of 100 m, the delay difference ($T_{utd,coop} - T_{ircmac}$) is 4.71 ms and 6.44 ms with respect to UtdMAC and CoopMAC I, respectively. At the distance of 120 m, this time difference significantly increases to 1.63 s and 8.18 s with respect to UtdMAC and CoopMAC I, respectively.

This is because of the reliable transmission at higher instantaneous rate that decreases the average transmission time and allows more packets to be transmitted within the given time duration. Note that the mean delay over the distance range of $20\text{ m} \leq d \leq 120\text{ m}$ is 0.28s, 1.37s and 4.07 ms for UtdMAC, CoopMAC I and IrcMAC, respectively.

Figure 4.17 compares the saturation throughput as a function of increasing number of transmitting nodes. The saturation throughput initially increases as the number of transmitting nodes increase. Then it remains almost flat up to 15 nodes and after that a slight decline in throughput is observed. The reason for the decrease in throughput is because the collisions along with fast fading become dominant effects and begin to offset the throughput improvement due to cooperation. However, it is worth mentioning that compared to non-cooperative protocols cooperative protocols will always scale well with the number of nodes due to reduced transmission time and increased number of transmissions in a given time period. The mean throughput difference of 1.08 Mbps and 0.78 Mbps is observed with respect to CoopMAC I and UtdMAC, respectively.

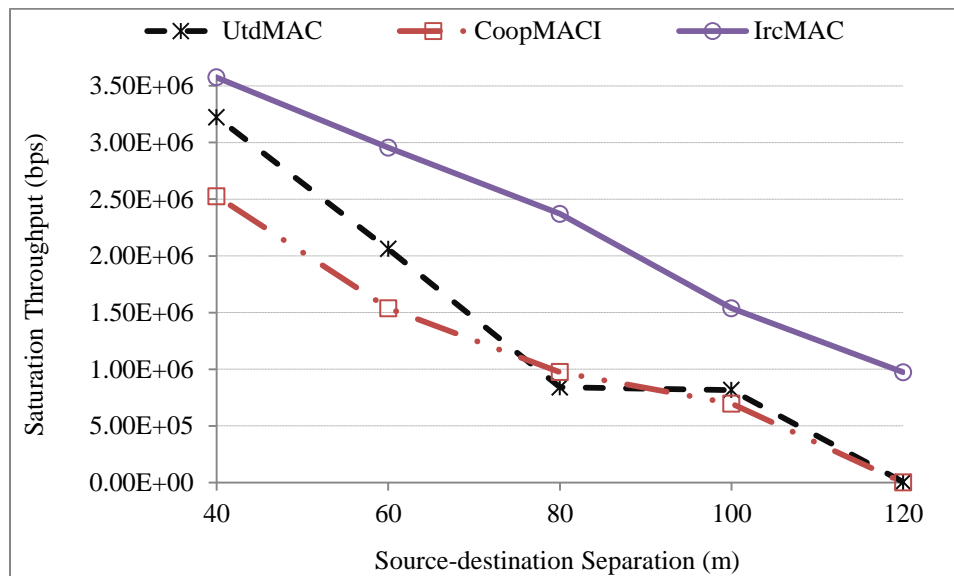


Figure 4.15: Saturation throughput comparison as a function of distance for IrcMAC

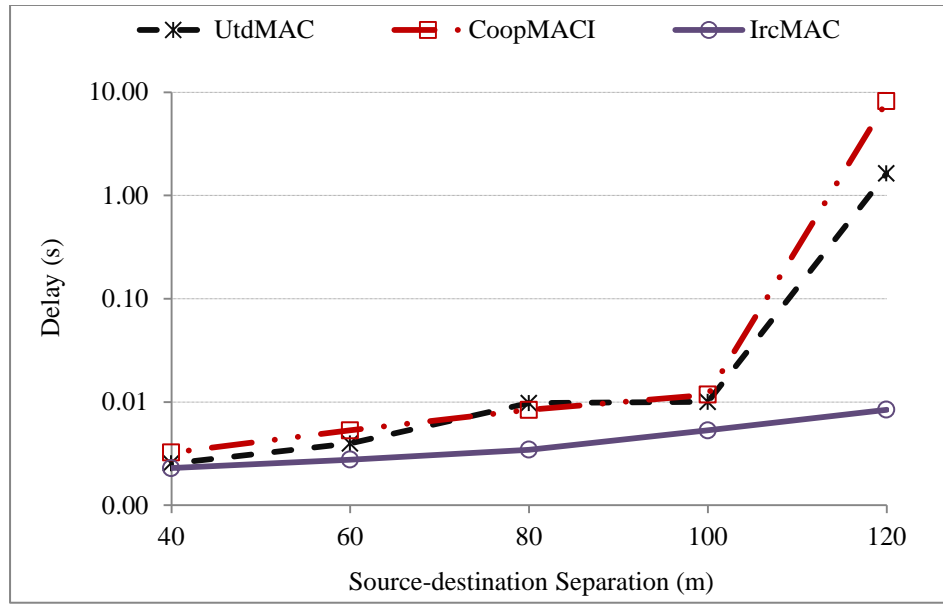


Figure 4.16: Average delay for successful packet transmission for IrcMAC

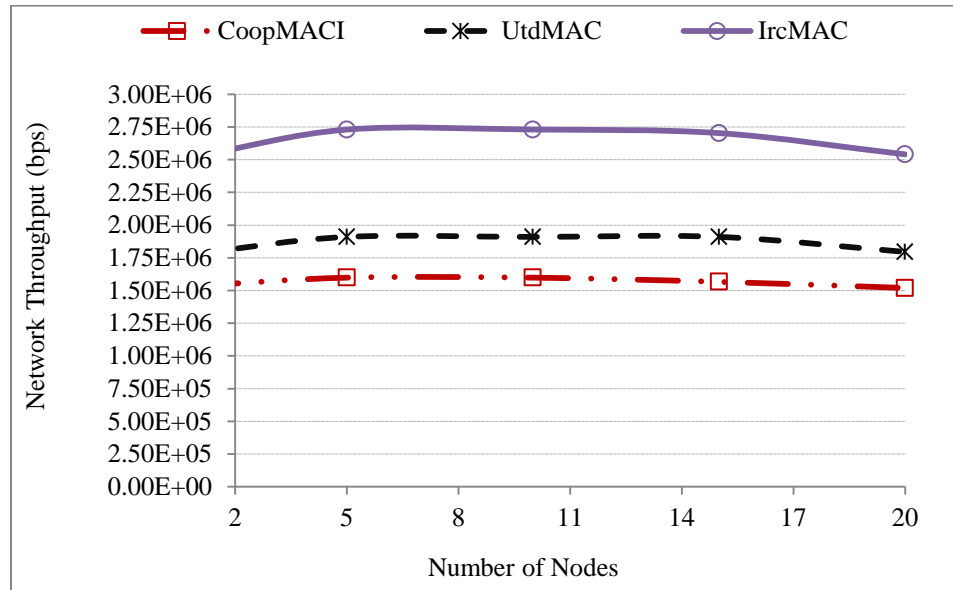


Figure 4.17: Network saturation throughput for IrcMAC

4.2.2.2 Impact of Coherence Time on Performance

In this section, we discuss the impact of increased mobility on the performance of IrcMAC protocol as a function of source-destination distance separation. We compare with the worst case speed of 27 m/s (corresponds to coherence time of ~ 2 ms) since we

don't foresee larger speed to be of any practical relevance at present. As mentioned before, only relays with total transmission times less than the channel coherence time transmit single bit feedbacks during the RR frame. Hence, a relay path is chosen only when it can offer reliable transmission path and incurs lesser transmission time compared to the direct transmission time. In case of increased mobility, quite intuitively the average channel coherence time is reduced and consequently we expect lesser number of relays to respond during the RR frame. Particularly, at increased source-destination distance separations, we expect the likelihood of relays responding during the RR frame to decrease. Further, at increased speeds, the estimated snr (and the corresponding estimated rate) during the RTS/CTS exchange may differ from the actual snr (the achievable rate) during payload transmission. Intuitively, we expect reduced throughput at the speed of 27 m/s due to reduced coherence time and the consequent difference between estimated snr and the actual snr during payload transmission. In Fig. 4.18, we observe that IrcMAC at 13 m/s and 27 m/s have lower throughput difference at distance ranges of $d < 60 m$ and $d > 100 m$. This is because for distance range of $d < 60 m$ direct path on average offers higher transmission rate compared to the combined rate through the relay path and the snr estimate is fairly accurate at both speeds. On the other hand, for distance range of $d > 100 m$, we observe a decrease in the number of relays (due to decreased source-destination overlap) and further the likelihood of transmission time through the relay being lesser than the coherence time is also reduced. Hence, again direct transmissions are frequent, but with increased inaccuracy of snr estimates (and corresponding rates) at both speeds. In the range of $60 m \leq d \leq 100 m$, IrcMAC at 13 m/s performs better than 27 m/s because of increased likelihood of relay paths with

transmission times better than the channel coherence time. Thus, in the range of $60 \text{ m} \leq d \leq 100 \text{ m}$, reliable relay path transmissions occur more often at 13 m/s. Note that the throughput gain for IrcMAC at 13 m/s is 41 % and 64 % with respect to UtdMAC and CoopMAC I, whereas at 27 m/s the gain reduces to 20 % and 39 %, respectively.

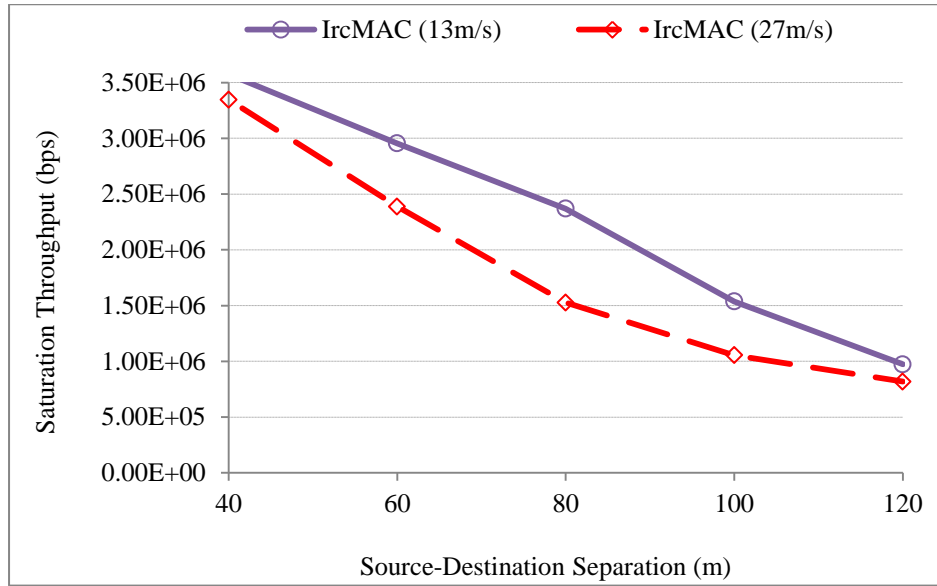


Figure 4.18: Impact of coherence time on saturation throughput for IrcMAC

4.3 Concluding Remarks

In this Chapter, we have proposed two novel relay-based cooperative MAC protocols, termed as 2rcMAC and IrcMAC, for ad hoc networks. 2rcMAC protocol makes use of two suitable relays for throughput and delay improvement. 2rcMAC adapts by switching between Utd mode and two-relay based approach that reduces transmission time with higher probability of success under fast fading conditions. Simulation results clearly show that 2rcMAC outperforms UtdMAC and CoopMAC I in terms of saturation throughput and delay as a function of distance and transmitting nodes.

IrcMAC protocol monitors instantaneous signal-to-noise ratio (snr) during handshake procedure and picks a relay path only when it incurs total transmission time (based on

snr) less than the channel coherence time and the direct path transmission time. Thus, the relay is tapped only when it can offer reliable transmission path, otherwise direct transmission takes place. Simulation results for IrcMAC show average throughput improvement of 41 % and 64 % and average delay improvement of 98.5 % and 99.7 % compared to UtdMAC and CoopMAC I protocols, respectively.

Furthermore, both protocols (2rcMAC and IrcMAC) introduce RR frame that resolves contentions among relay nodes and allows contending relays located in close proximity at the time to communicate rate information to the source node through single bit feedbacks. In the future, we will investigate improvement in 2rcMAC approach using spread spectrum and network coding techniques to resolve relay contentions and improve throughput and delay performances.

CHAPTER 5

DIRECTIONAL COMMUNICATION IN WIRELESS AD HOC NETWORKS

5.1 Introduction

Directional communication in a single-hop wireless ad hoc networks has been shown to reduce interference (thereby improves channel utilization) by effective spatial reuse in a given geographical area (see [24, 96, 97] and refs. therein). In this respect, multiple wireless nodes that desire to communicate with each other form separate directional beams that do not interfere with each other. By focusing energy in a specific direction, directional communication can improve spatial diversity and provide longer range for better connectivity. This consequently improves the average throughput and capacity in terms of node density of the entire wireless network. In directional communication, nodes communicate by using directional beams to maximize Signal-to-Interference ratio (SIR) for their respective sessions. However, implementing directional communication in single channel single hop ad hoc network poses many challenges which drastically affect throughput. Next section highlights some major problems associated with implementing directional communication in ad hoc networks.

5.2 Throughput Performance Issues in Directional Communication

As illustrated in Fig. 5.1, nodes A, B, C and D operating in omni-directional mode radiate energy in all directions and create severe interference. Node A wishing to transmit to node B sends request-to-send (RTS) packet in omni-directional mode to node B, which

responds with a clear-to-send (CTS) packet to node A. Once node A receives error-free CTS packet, it can start the transmission of data packet to node B. Node C is unaware of the session between nodes A and B due to lack of coverage overlap. Node C initiates transmission of RTS packet to node D. Since node D is within the coverage area of node A, it is aware of the ongoing transmission between nodes A and B. When node D receives RTS message from node C it is most likely going to be in error due to interference from node A's transmission. Further, since node D knows about ongoing transmission, it will never respond with the CTS message even if RTS message is received correctly. As such, node C receives no CTS response from node D. Node C may continue to retry RTS transmissions until retry timer limit is reached. This wastes precious bandwidth and aggravates throughput in the network. In contrast, when nodes use directional antennas with confined coverage (narrow beam width) to communicate with each other, concurrent sessions can easily co-exist as shown in Fig. 5.1. By using directional antennas nodes A and C can establish concurrent sessions with nodes B and D without creating significant interference. However, before sessions could be established, nodes A and C must know the directions where destination nodes B and D are located, respectively. In turn, to respond with directional CTS (DCTS) messages, nodes B and D must be able to estimate the directions using some kind of Angle-of-Arrival (AoA) estimation technique(s) [98]. However, to exploit full potential of directional communication compared to omni-directional communication, the directional beam needs to be controlled at each layer. Thus, to realize concurrent directional single-hop sessions in an efficient manner, following information and computations are indispensable:

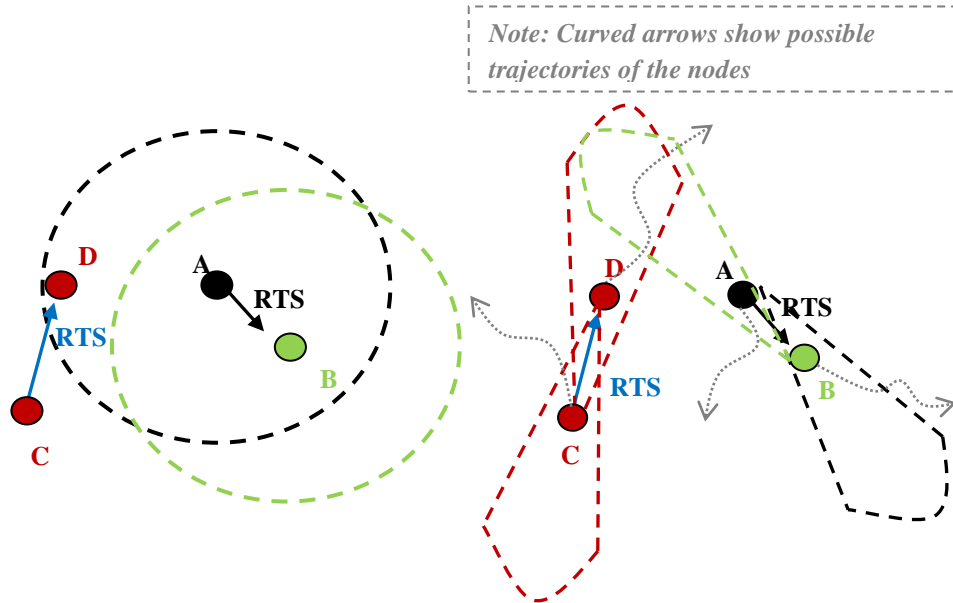


Figure 5.1 Illustration of directional versus omni-directional communications

- 1) Nodes A and C must be aware of the directions where nodes B and D are located, respectively.
- 2) Nodes B and D must be able to estimate the respective directions after receiving RTS messages from nodes A and C, respectively.
- 3) Nodes A, B, C, and D must be aware of the precise directions and time durations of any ongoing transmissions to avoid unnecessary interference with other sessions.

To efficiently utilize directional antennas, information gathering and computation described in the above requirements must be reliably done. As described in first requirement, a source node must be able to track its respective destination node before the session could be established. This information can be gathered by listening to ongoing transmissions and updating tables, or by initiating a neighbor discovery process. Performance of a particular neighbor discovery process depends on the underlying mechanism. Most of the proposed techniques rely on omni-directional transmission and

reception of control packets, GPS approach, and synchronous approach [99-103]. Further, all the neighbor discovery approaches require heavy signaling that degrades the throughput performance of directional communication in single-hop wireless ad hoc networks [102]. The extent of degradation in throughput depends on node density, mobility, beam-width, type of application (real time, non-real time, soft real time, hard real time), and the underlying neighbor discovery mechanism.

Another major factor that contributes to throughput degradation is described in the third requirement. We elaborate on the third requirement with a simple example. Suppose, now node A that was in session with node B finishes transmission and wants to establish session with node C, while nodes C and D are still engaged in a session. As node A is unaware of an ongoing session between C and D, it transmits RTS packet to node C and does not get CTS response from node C. This is because node C is unable to receive RTS packet due to half duplex operation. This problem is known as deafness problem in directional communication. Node A continues retransmitting RTS packets in this specific direction until retry limit expires. Then node A searches for node C by transmitting more RTS packets in a circular manner until it completes 360 ° span. This wastes huge amount of bandwidth and leads to a drastic throughput degradation [104]. If node A wanted to transmit to node D, it would create severe interference and might even lead to packet losses at node D. This creates an effect almost similar to the hidden terminal problem. In short, if node A has prior knowledge (acquired through signaling) of its neighbors' status, it would defer transmission and prevent unnecessary throughput degradation. Furthermore, there are many other problems that are created as a result of directional communication which degrades ad hoc network throughput [24, 105]. The proportion in

which failure factors can occur in directional communication are shown in Fig. 5.2 [104].

In general, directional communication problems can be categorized as [105]:

- 1) Neighbor discovery: Locating the exact direction of the destination node by circular polling, estimation, cooperation, or any other mechanism and caching the information in the table.
- 2) Deafness: A node cannot respond to RTS packet from another node as it is beam formed in a different direction.
- 3) Hidden terminal: A node transmits to another node in session due to unheard RTS/CTS packets.
- 4) RTS/CTS collision: The receiver or transmitter node cannot receive error-free control packets due to concurrent transmissions.
- 5) Location staleness: The cached location of the destination node is no longer valid.

To prevent throughput degradation due to neighbor discovery, deafness, hidden terminal and location staleness problems, myriad of techniques have been researched for single-hop directional communication (see [24, 27, 101-106] and refs. therein). For effective directional communication, all the proposed techniques for above-mentioned problems have to work together in an integrated manner. However, in case of heavy load, high density, mobility and narrow

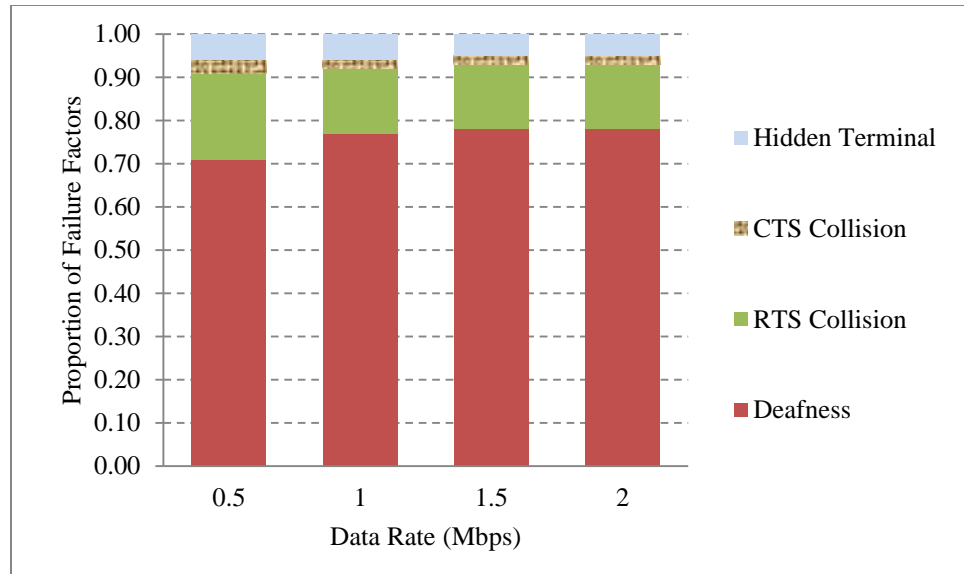


Figure 5.2 Percentage of failure factors in directional communication

beam-width, the signaling load drastically overshadows the throughput gain achieved by employing above-mentioned techniques [24, 101-103, 106].

Interestingly, all the proposed approaches implicitly try to reduce RTS/CTS collisions and interference generated due to excessive signaling. Schemes that explicitly mitigate RTS/CTS collisions and suppress interference are power controlled directional MAC protocols. Small amount of work is available with respect to power-controlled DMAC in single-channel single-hop wireless ad hoc networks [107-109]. The main difficulty in developing power control in single-channel single-hop ad hoc networks is estimating the required transmission power at the source node. RTS, CTS control packets are transmitted at maximum power to exchange power requirement at the receiver. This also requires receiver to estimate the random SIR and channel gain, and then convey the required power to the transmitter. Random fluctuations of SIR in ad hoc networks also make it extremely difficult to precisely control the transmit power. [109] proposed a theoretical interference model that is used to predict future interference in the network,

which is used to control transmitter power. [110] proposed a protocol that iteratively converges to an optimal common power subject to network connectivity constraint. However, in case of high mobility the overhead is overwhelming. Certain unrealistic assumptions inherent to most of the proposed power control schemes are summarized as follows:

- 1) CTS packet carries required power information besides other pre-defined control information;
- 2) Network SIR remains constant during data transfer [107, 109]; and
- 3) Interference margin and interference estimation using the SIR model is accurate.

The proposed solutions for the aforementioned problems in directional communication are developed under varying assumptions and further require heavy signaling which makes them difficult to use in reality, particularly, in case of heavy load applications, high density and mobility. A tradeoff between extent of signaling and network performance may depend on the particular application and scenario in ad hoc network. For example, in high density and heavy load situation, deafness and RTS collisions may become dominant factors contributing towards significant throughput degradation [104]. In such case, extra signaling required for power control may not be a viable option for throughput enhancement in real world ad hoc networks [24]. Thus, in this Chapter we focus on investigating the extent of throughput degradation when power control is not feasible in high density and heavy load scenario.

5.3 Description of DMAC Protocol

Most of the MAC protocols proposed for ad hoc networks are derived from the IEEE 802.11 distributed coordination function (DCF) protocol [111]. In the DCF scheme, the

sender sends a channel reservation request by sending an RTS control packet to the receiver. The intended receiver then responds by sending a CTS control packet to acknowledge the channel reservation. This handshake scheme takes care of two important issues:

- 1) Sender and receiver establish communication and initialize parameters.
- 2) The neighboring nodes that are in communication range of either the sender or the receiver avoid any transmission initiation during the ongoing session.

As mentioned, the RTS/CTS mechanism takes care of any possible collision due to neighboring nodes that are close to the sender or the receiver and wish to communicate at the same time. This resolves the well known “hidden node” problem. However, on the other hand, this RTS/CTS mechanism prohibits other neighboring nodes from establishing communication when their respective receivers are not in the communication range of the above sender. This problem is known as the “exposed node” problem. The RTS/CTS scheme used for omni-directional communication limits spatial reuse by creating a large number of exposed nodes in the network. This consequently leads to limited network utilization and lower average throughput. The directional communication using the DMAC (Directional Medium Access Control) protocol addresses the exposed node problem by using the directional RTS/CTS (DRTS/DCTS) and data packets transmissions. However, the hidden node problem due to asymmetric antenna gains and the deaf node problems also arise as a result of DMAC protocol which is comprehensively discussed in [96].

In basic DMAC protocol, each node communicates in a directional mode and so each node has to maintain a table which contains the direction of a communication sessions

active in the nodes' neighborhood as shown by DMAC state machine in Fig. 5.3. The nodes that are in idle mode sense the neighborhood using omni-directional antennas and update the table with direction information and the duration of the communication session. The direction information can be determined by means of GPS, or by selection diversity technique [99, 112]. The duration information is contained in the RTS/CTS packets for the nearby nodes to avoid possible interference. The corresponding region in the direction of the ongoing communication session is marked as busy for that duration. This information can later be looked up by the respective node if it wants to initiate transmission in a certain direction. Thus, it provides for what is known as the virtual sensing mechanism. The information gathered regarding the communication session direction and the duration is termed as Directional Network Allocation Vector (DNAV) which is similar in concept to the IEEE 802.11 Network Allocation vector (NAV) (see [92] and refs therein). The region that is marked as busy in the direction of communication session is defined by the DNAV angle.

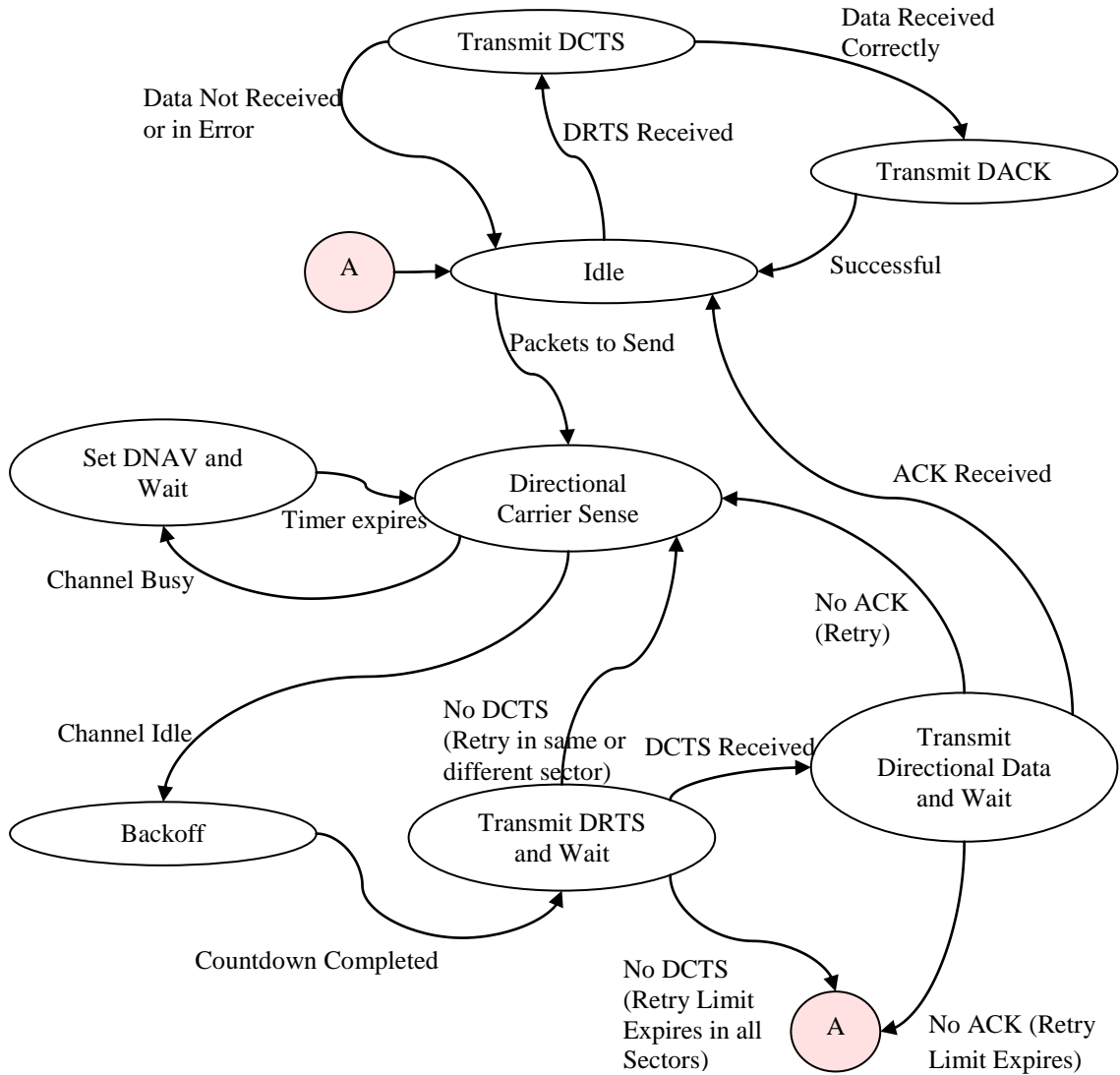


Figure 5.3 Finite state machine for DMAC

The sender node that wishes to transmit knows the direction of the intended receiver in addition to the DNAV information. The sender checks its DNAV table for any active session(s) in the intended direction. If DNAV table shows that the channel is busy then the sender defers its transmission. If DNAV table shows that the channel is idle in that specific direction, then the sender physically senses the channel in the direction of the intended receiver for the duration of distributed inter-frame space (DIFS). In case, the

channel is sensed busy the sender node delays the transmission based on the duration field in the packet, and updates its DNAV table. If there is no active session(s) in the intended direction then the sender backs-off by generating a uniform random number from 0 to w (where w is the contention window depending upon the transmission attempt) [24, 92].

If the channel remains idle during the back-off phase countdown, the directional RTS (DRTS) control packet is transmitted in the direction of the intended receiver. The receiver node operates in omni-directional mode when in idle state. When the intended receiver receives the DRTS packet; it determines the direction, checks its DNAV table for the intended direction, and senses the channel for the short inter-frame space (SIFS) in that direction. If the channel remains idle for the SIFS duration, the receiver node responds to the sender by sending the directional CTS (DCTS) packet. The DCTS packet is not transmitted when the receiver finds the channel busy due to communication activity in that direction. The sender node on the other hand waits for the DCTS packet and if the DRTS timer expires the sender prepares for retransmission of the DRTS packet. This completes the process of channel reservation. If reservation process is successful, the sender then transmits the data packet to the receiver in the given direction and the receiver sends the acknowledgement (ACK) for the correctly received data packet. If sender does not receive ACK packet, then it goes through the sensing and backoff phases again for retransmission. The timing sequence for the directional reservation mechanism is shown in Fig. 5.4.

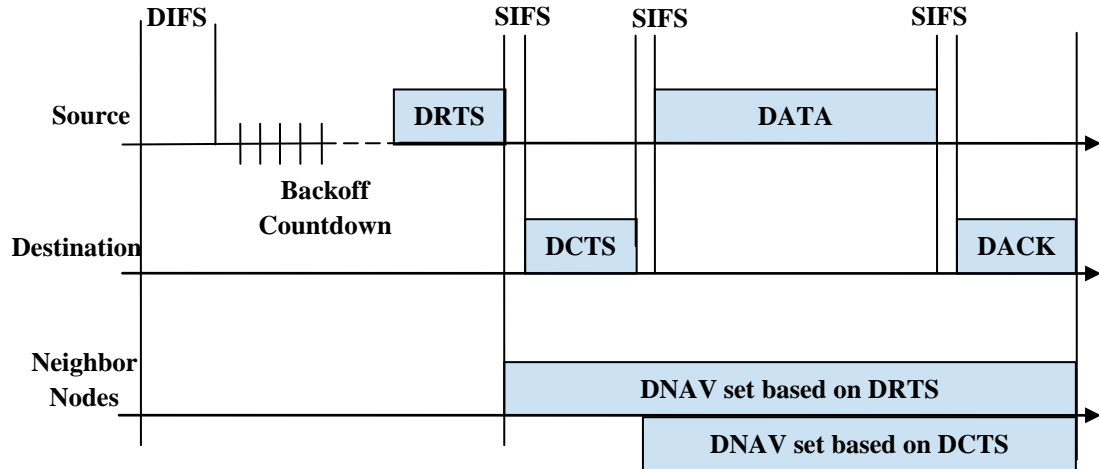


Figure 5.4 Directional channel reservation mechanism

5.4 Simulation Results and Discussion

Performance of directional communication depends on the network scenario and the MAC protocol that controls directional communication. We have used a simple DMAC protocol on top of steering beam antenna in *QualNet 4.0* simulator [113] to simulate the performance of directional communication versus the omni-directional and its limitations in a particular scenario.

5.4.1 Simulation Scenario

The geographical area is a flat terrain of dimension 100 m x 100 m. We have placed 10 nodes in pairs such that the pairs are uniformly distributed in the given area as shown in Fig. 5.5. Each pair consists of a source and a destination that are engaged in a communication session. The distance between the source and the destination belonging to the same pair (i.e., intra-pair) is less than the distance between the pairs (i.e., inter-pair). Pairs' orientations are random in every run. To effectively compare omni-directional and directional communication performance, nodes are stationary and the distances between the same pair source and the destination nodes is kept smaller than the inter-pair distance

separations, which forces only single hop sessions. Thus, we are only considering single-hop wireless ad hoc network simulation. To simulate high density and heavy load situation, the inter-pair distances are also kept short enough for severe interference and packets are continuously generated using CBR application. This creates a realistic scenario which can occur when a group of rescue personnel (nodes) are in close radio coverage proximity of each other as in a typical disaster relief situation.

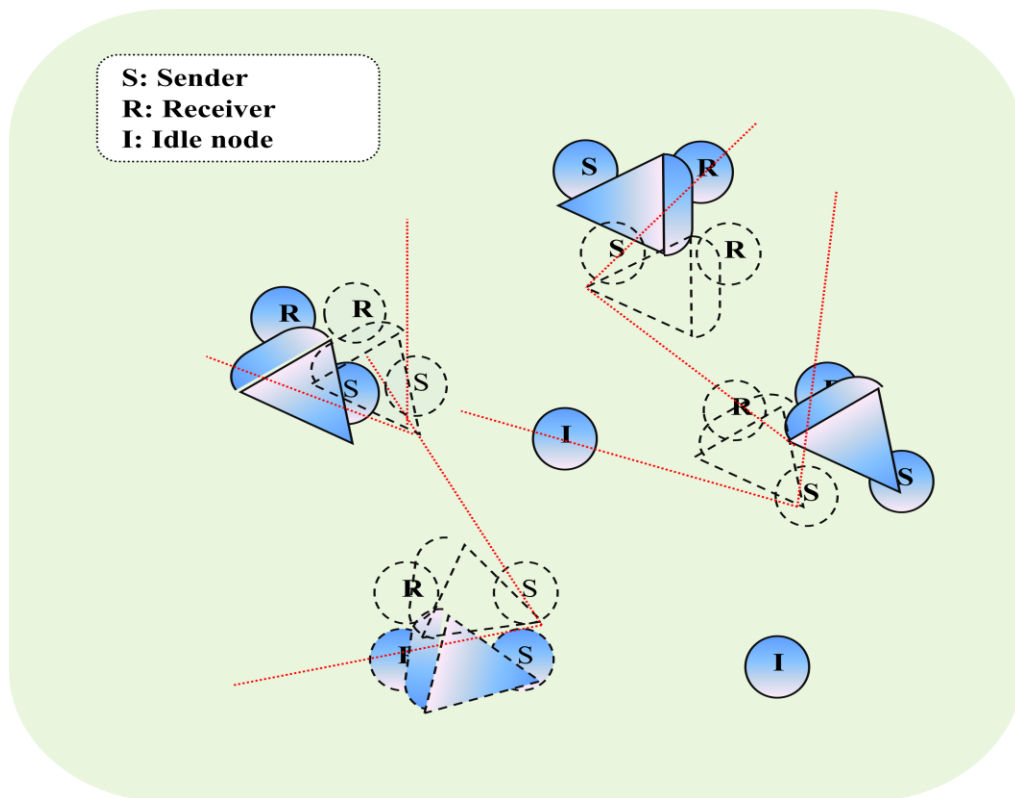


Figure 5.5 Simulation scenario snapshot

5.4.2 Simulation Parameters

To test the limits of directional communication we separate the simulation into two cases. In the first case, the sender-receiver pairs are approximately equidistant from each other and are stationary as shown in Fig. 5.5. In the second case, the same sender-receiver pairs are moved closer to each other (by about 30 m) such that the pairs remain

equidistant. The reason for moving them closer is to check the spatial reuse limitation of the directional communication. The intra-pair distance between the sender and the receiver nodes remains constant throughout the simulation cases. We compare omnidirectional versus directional communication using average node throughput as a metric.

Table 5.1 Simulation parameters

Parameter	Value
Area	100 m x 100 m
Total nodes	10
Mobility	No
Sender receiver orientations	Random
Total CBR packets sent per session	1000
CBR packet size	512 bytes
CBR packet inter-arrival time	2.1 ms to 0.1 s
Simulation time	300 s
Transmit power	15 dBm
Receiver sensitivity	-89 dBm
Power control	No
Path loss	2-ray model
Mean shadow loss	4 dB
DMAC NAV angle	45°
Antenna gain	15 dBi
Beamwidth	45°

The throughput measures the number of successfully received packets at the receiver. The throughput is evaluated as a function of the sender traffic rate increasing from 41 kbps to 1.95 Mbps for four simultaneous CBR sessions. Several runs are done separately for each traffic rate using different seed values for each run to get a good average estimate. The directional antenna used is the steerable beam-forming antenna in *QualNet 4.0* simulator with a peak-of-beam gain of 15 dBi and the approximate beam-width of 45 degrees. The details of physical, MAC and application layer parameters used in the simulation are listed in Table 5.1.

5.4.3 Simulation Results

We first give an intuitive account of omni-directional throughput curves and then expound on directional communication throughput as seen in the Figures 5.6 and 5.7. Since omni-directional pairs significantly interfere with each other, they rely on the IEEE 802.11 MAC sensing and back-off mechanism to avoid collision, and the RTS/CTS mechanism for channel reservation. In the event of simultaneous RTS/CTS packet transmissions, it is possible that a particular sender-receiver pair can still capture the RTS/CTS packet if the SIR is above the threshold value. In the low CBR traffic range from 41 kbps to 500 kbps, the channel access is not as high as the channel access in high CBR traffic rate range of 512 kbps to 1.95 Mbps. This implies frequent deferring or back-offs due to collisions in the high CBR traffic range compared to the low CBR traffic range. Since the lower CBR traffic range has lower channel access probability, the back-off window may remain nominal. On the other hand, in high CBR traffic rate region the channel access probability is tremendously high and this might increase the back-off window due to collisions.

Frequent back-offs (due to collisions) at the sender nodes lead to average throughput degradations at the respective receivers as seen in Figures 5.6 and 5.7. It is obvious that beyond 410 kbps the average throughput begins to decrease for omni-directional communication. In Figure 5.7, the pairs are moved closer to each other (about 30m) which increases the interference (lowers SIR), and decreases the probability of RTS/CTS packet capture. As a result, the average throughput of omni-directional communication is worse when sender-receiver pairs are moved closer.

In directional communication, the interference between the sender-receiver pairs actually depends on realistic antenna patterns, node density, relative distances, relative orientations and directional coverage range. Figure 5.6 clearly shows that the directional communication throughput is much higher than the omni-directional case. This is because the directional communication has directional coverage and the likelihood of interference is reduced due to inter-pair orientations and distances. Ideally, we would expect the directional communication throughput at the receiver to get close to 2 Mbps at the sender traffic rate of 2 Mbps. However, it is clear from Figure 5.6 that it does not happen because orientation of some pairs lead to significant interference and so the affected sender-receiver pairs rely on deferring or back-offs for packet transmission. The sender-receiver pairs that are oriented in non-overlapping manner generate higher throughputs, but are also limited by the inter-pair distances. In essence, the average throughput for directional communication in a given area is reduced due to some overlapping nodes performing worse than the non-overlapping nodes.

As CBR traffic rate is increased the average throughput decreases due to frequent back-offs. The reason why directional communication performs better than the omni-directional is because of the effective spatial reuse by some pairs that are oriented in a non-overlapping manner. In Figure 5.7, the directional communication throughput degrades significantly due to larger inter-pair overlap and high interference due to long range. In low CBR traffic rate range (41 kbps-500 kbps), the lower throughput is mainly due to infrequent channel access and strong interference. In the high CBR traffic range (512 kbps-1.95 Mbps), severe throughput degradation is observed due to significant

overlap and frequent back-offs. In high CBR traffic range, the throughput for directional communication reduces by approximately 40 %.

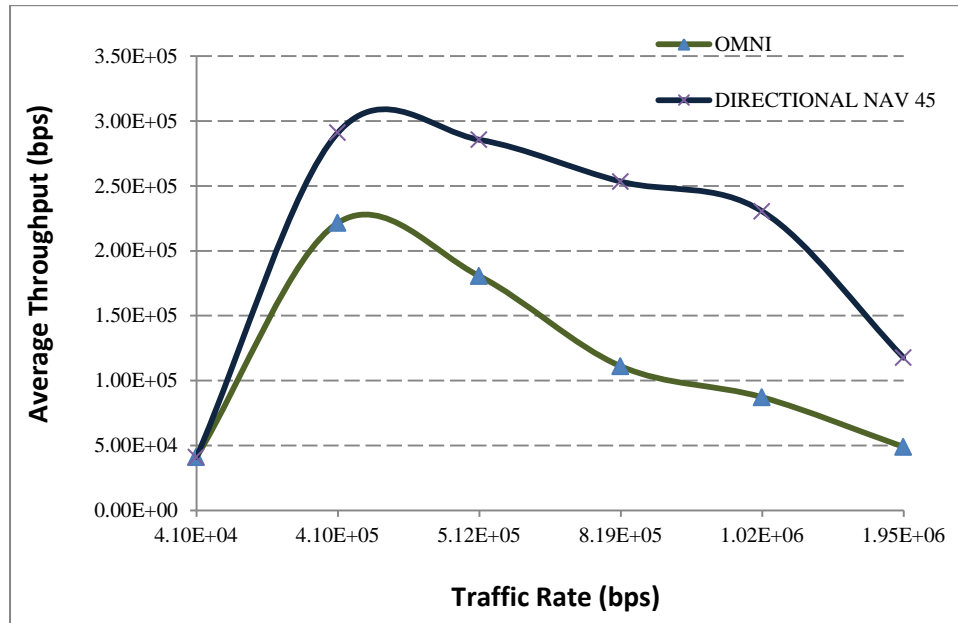


Figure 5.6 Throughput performance omni versus directional

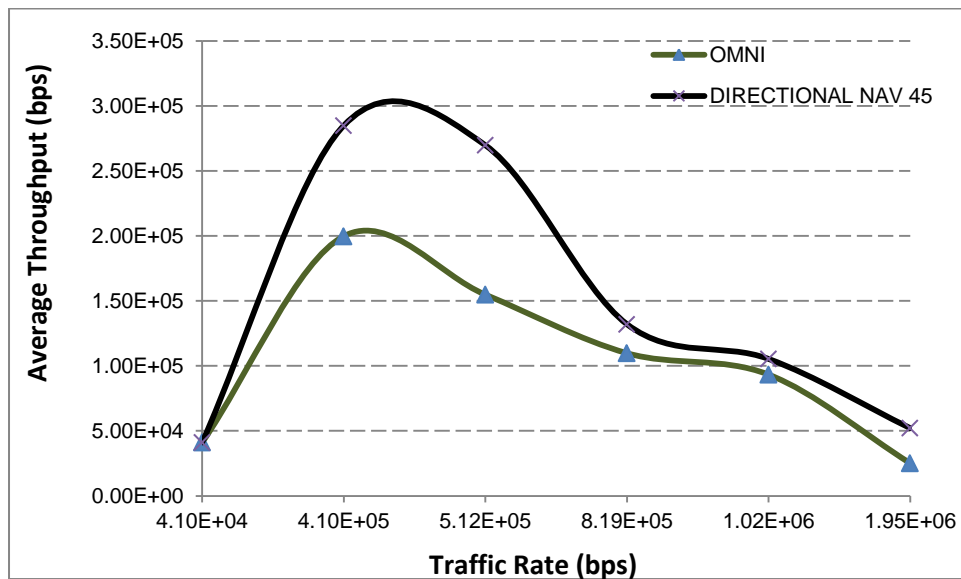


Figure 5.7 Throughput performance omni versus directional for reduced distance

5.5 Concluding Remarks

We have compared omni-directional and directional communication with respect to average node throughput performance metric. Simulation results show that directional

communication outperforms omni-directional in terms of throughput for low and high traffic rates. However, in high density situation when the distances between the sender-receiver pairs are reduced, the directional communication performance approaches the omni directional performance in high traffic rate region. The average directional throughput degrades by approximately 40 % in high CBR traffic range. We have also highlighted significant problems and performance issues when implementing directional communication in wireless ad hoc networks.

CHAPTER 6

ADAPTIVE DMAC PROTOCOL WITH INTEGRATED DESTINATION DISCOVERY FOR WIRELESS AD HOC NETWORKS

6.1 Introduction and Motivation

Extensive research has been carried out in the development of synchronous and asynchronous directional MAC protocols to establish directional communications which primarily relies on IEEE 802.11 DCF (Distributed Coordination Function) access scheme with RTS (Request-To-Send) and CTS (Clear-To-Send) handshake procedure, AoA (Angle of Arrival) estimation, and in many protocols on GPS (Global Positioning System) technology ([99, 100, 105] and refs. therein). Many of the proposed directional MAC (DMAC) protocols rely on some combinations of omni and directional modes, and use DNAV (Directional Network Allocation Vector) information by overhearing neighboring nodes, to establish connectivity with the desired destination. A critical challenge in directional ad hoc networks due to narrow beam-width and high mobility is to be able to locate and track the destination node. In cases of high mobility and narrow beam-width the dwell time of the prospective destination(s) within the beam-width coverage area becomes too short (depends on location, velocity, beam-width and distance between transmitter and receiver) and necessitates frequent table updates or control overhead [100]. The throughput performance gets worse as beam-width gets narrower [103]. Most of the research done in directional MAC with integrated neighbor discovery for ad hoc networks either does not consider high mobility or requires frequent updates or

polling mechanisms (see [103] and refs. therein). This frequent updates require heavy signaling particularly in high mobility, heavy density, heavy load and narrow beam-width situations. As already highlighted in chapter 5, directional communication deployment introduces lot of problems that entail heavy signaling requirement for resolution. Thus, for directional communication the proposed destination discovery approaches requiring heavy signaling, GPS information, and in many cases slot synchronization; may become impractical for realistic ad hoc deployments [24, 114]. This serves as a main motivation for our work. We propose an integrated neighbor discovery as part of the Directional MAC protocol (termed ADMAC) that estimates the probable region of destination based on the last sector, last known transmitter-receiver distance d , total elapsed time since last update $1/\mu$, average relative velocity v , and the beam-width α .

6.2 Literature Review

[99] proposes directional MAC with carrier sensing. In the proposed work, RTS and CTS are transmitted omni-directionally, whereas data packet is transmitted directionally. It is assumed that a node in omni-mode can find the direction of the reception by detecting the maximum power sector. However, no proper mechanism to locate or track nodes is mentioned in their work. Transmission in last sector is suggested for node location. [102] proposes synchronous approach known as polling based directional MAC protocol. Location information is achieved by scheduled polling of the nodes. However, protocol requires perfect synchronization, periodic signaling, and optimal frame duration estimation that are difficult to realize in a dense, narrow beam-width, and heavily loaded mobile ad hoc network. [103] proposes a fully distributed asynchronous directional-to-directional MAC protocol. It eliminates gain asymmetry and alleviates the effect of

deafness. However, it does not consider the mobility case and further does not provide any location tracking mechanism. In case of AoA cache timer expiration, random sector is chosen for transmission to a destination node. [112] proposes directional MAC protocol for static ad hoc networks. The proposed scheme uses omni-directional RTS/CTS exchange which cannot identify the precise direction of the destination node. It assumed that nodes' locations are precisely known by means of the GPS equipment. [115] proposes a directional MAC protocol where each node periodically transmits a beacon signal sequentially at 30 ° intervals until it covers 360 ° span. Receiving nodes determine the sector of maximum signal strength to form a table and then respond back with the information as a data packet with an RTS/CTS handshake. The control overhead of this protocol is overwhelming. In another version of this protocol, author proposed a receiver oriented approach to reduce control overhead. However, in this technique periodic beacons are transmitted at regular interval. Each beacon is preceded by a tone that also adds to the control overhead. [116] proposes directional MAC that relies on AoA (Angle-of-Arrival) cache for destination location. However, with mobility the destination location information quickly becomes stale. The protocol may resort to frequent omni-directional transmissions for node location discovery.

In essence, most of the work in directional MAC protocol for node tracking either entail heavy signaling that renders it infeasible in realistic ad hoc networks, or suggest transmission in the last or random sector for possible node location.

6.3 Proposed ADMAC Protocol

In this section, we describe the proposed directional MAC protocol with integrated destination discovery (termed ADMAC). Many proposed protocols make use of a

combination of omni and directional modes for location tracking [24]. However, for full exploitation of directional communication, transmitters and receivers must exchange RTS-CTS-DATA-ACK packets directionally so that high average throughput performance can be achieved [117]. For full directional communication many proposed protocols suggest transmission in random sector and last sector for destination tracking (see [103] and refs therein). Fig. 6.1 shows the detailed flow control of the transmitter node. The details of the proposed protocol are presented henceforth:

- 1) Idle Mode: In idle mode, a node listens to ongoing transmissions in omni-directional antenna configuration. When an idle node receives transmission, it uses selection diversity to select the sector (direction) with maximum signal strength in order to determine the direction of the source node [99]. In idle mode, node refreshes the AoA cache table with node ID, time of update, expiration time, estimated distance, and the sector where the maximum signal strength was received. The knowledge of transmission power, received power, and path loss model can be used to estimate the distance [99]. It is assumed that nodes have the capability to determine velocity which they can exchange with each other during packet transmission or reception. In idle mode node also keeps updating DNAV (directional network allocation vector) table as in other DMAC protocols.
- 2) Receive Mode: When a node receives a packet as a destination node, it goes into a reception mode from idle mode. In reception mode, a node determines the sector with maximum signal power, decodes the DRTS (directional RTS) packet and then transmits a DCTS (directional CTS) packet after SIFS duration to the source node. During the reception mode, a destination node also updates the AoA cache table

entries with source node information for later transmissions. The DRTS and DCTS packets are used for address and other control information exchange [24]. A node stays in receive mode to receive data packet(s) until the timer expires. After, receiving data packet(s) node transmits ACK (acknowledgement) packet if the data packet is error free, otherwise no ACK packet is transmitted. The node then goes into idle mode again.

- 3) Transmission Mode: When a node wishes to transmit a packet, it checks its AoA cache table for destination records (Fig. 6.1). If no records are found, the node starts transmission in a randomly selected sector. Before transmitting DRTS packet, the node performs virtual sensing by checking the DNAV table for that sector. If DNAV shows that the channel is busy then the transmission is deferred until the channel is free again. Once the channel is free for the DIFS duration, the node enters a standard backoff phase [92]. If during backoff phase the channel remains free the node then sends the DRTS packet and waits for the DCTS response. If no DCTS response is received within timer expiration limit, DRTS attempts are repeated in the sector. If DCTS packet is received successfully, then DATA can be transmitted to the destination node. If all DRTS retries fail in the sector, then the transmitter node goes to the next sector and repeats the transmission process as above. The transmissions are attempted in sectors in a clockwise direction until successful transmission or until the 360° span completes.

If destination node records exist and the AoA timer has not expired then the source node starts with the last known sector and continues in a clockwise direction until

successful transmission or until the 360° span completes. The transmission process details are the same as mentioned above.

However, if AoA timer has expired then the source node estimates a search span where the destination node is most likely going to be as illustrated in Fig. 6.2. Three cases are determined by the source node based on the last sector, estimated distance (d), elapsed time since last update ($1/\mu$), relative velocity (v), and the beam-width (α).

In Fig. 6.3, three possible cases arise when R (receiver) is assumed in the middle of the sector (under uniform distribution) and it moves uniformly at any point on the circle of radius r . Where, $r = v/\mu$ is the radius moved by the receiver at an average relative velocity v and in elapsed time $1/\mu$ (since last DNAV update). Case (a) occurs when the estimated distance between T and R is small, such that $d < r$. So, after the elapsed time R can move anywhere in zone I and zone II (360° search span around the transmitter). Case (b) occurs when R's distance satisfies $r \leq d \leq \{r/\sin(\alpha/2)\}$. Thus, in case (b), R can probably move anywhere within zone II depending on β (see later sections). Last case (c) occurs when $d > \{r/\sin(\alpha/2)\}$. In case (c), R will most certainly be inside the last sector in zone II after the elapsed time ($1/\mu$).

For cases (a) and (c), a different search pattern is specified. The source node starts from the last sector. If DRTS fails in the last sector then it searches the two adjacent sectors by sending DRTS packets. If DRTS retransmissions still fail then the source node searches remaining sectors in a clockwise direction until successful search is made or until the 360° span is completed in a failure. In case (c), it is highly probable that the destination node is going to be inside the beam-width of the source node. However, in case (a) destination node is very unlikely to be found inside the beam-width.

For case (b), the source node starts DRTS transmission from the last sector. If DRTS transmission fails in the last sector then the source node starts searching through the remaining sectors in the search span first. If all DRTS transmissions fail in the search span then the remaining sectors are searched for the destination node until transmission is successful or 360° span is completed. For case (b), source node computes β which is the angle subtended due to a tangent line from the T (transmitter) to a circle in case (b). Source node first computes $\beta = \sin^{-1}[v/(\mu \times d)]$ and then it estimates the number of sectors in the search span (including the last sector) as $1 + 2[\max(0, \beta - \alpha/2)/\alpha]$.

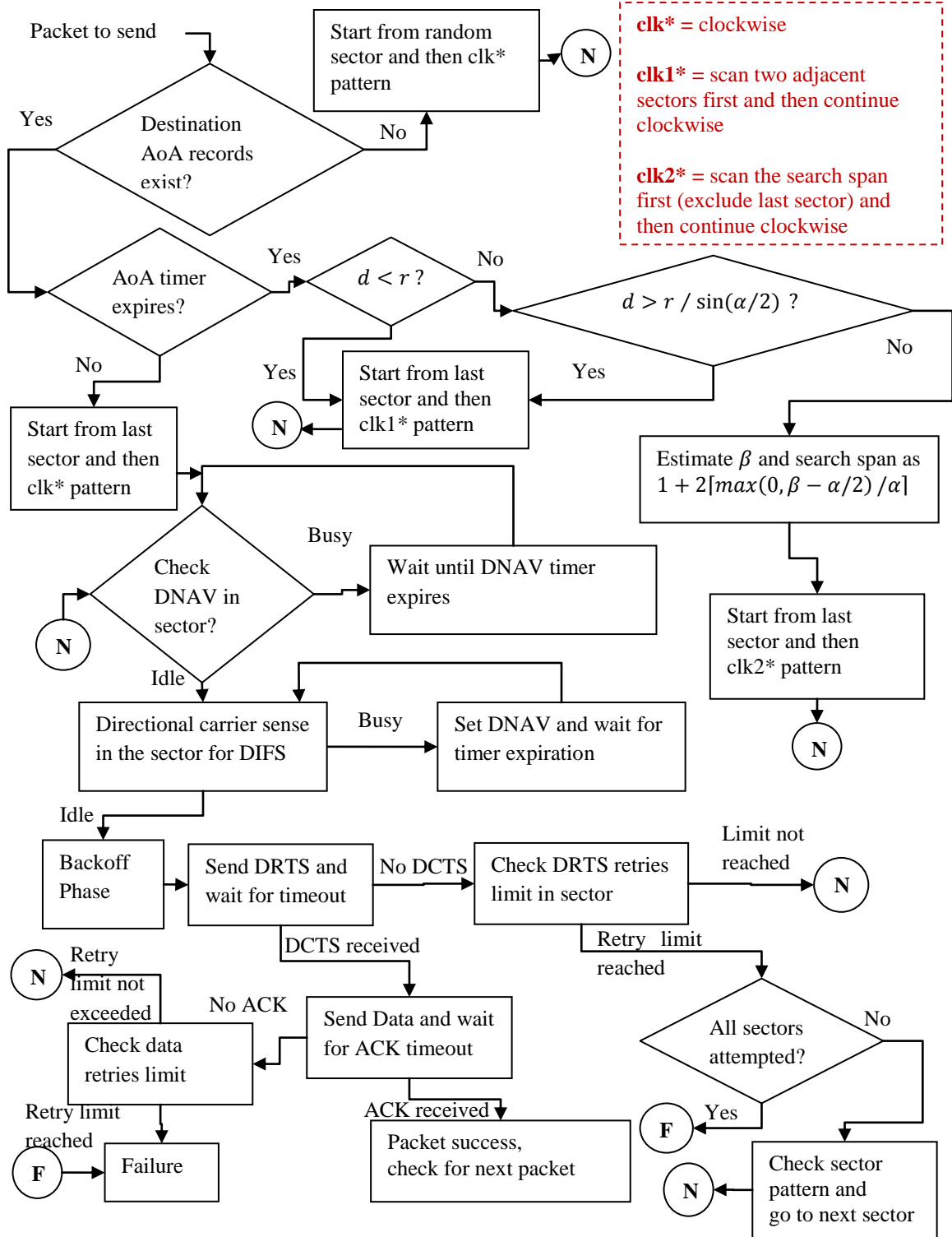


Figure 6.1 Source node flow control for ADMAC

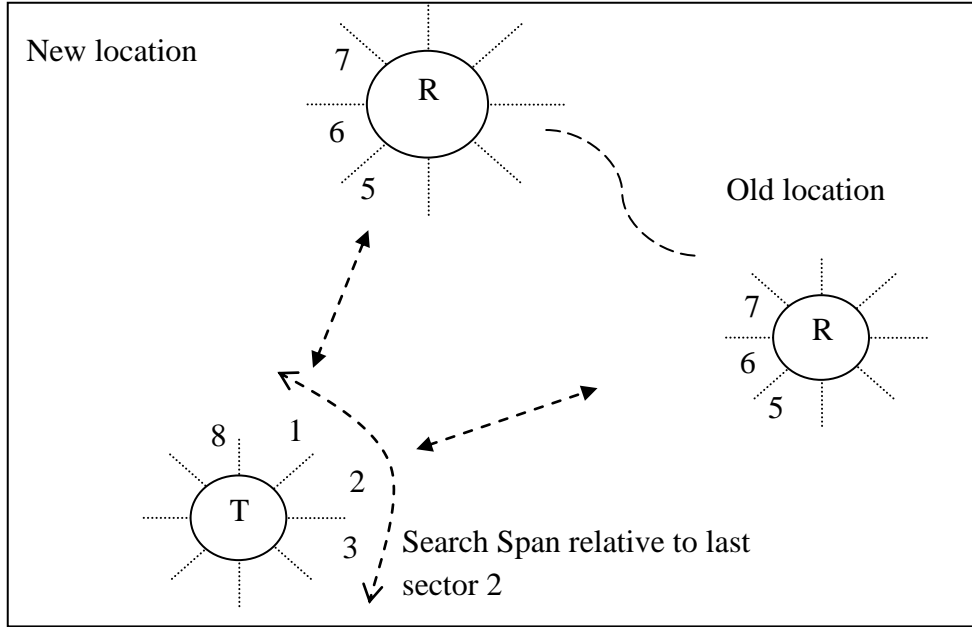


Figure 6.2 Transmitter (T) and Receiver (R) search span illustration

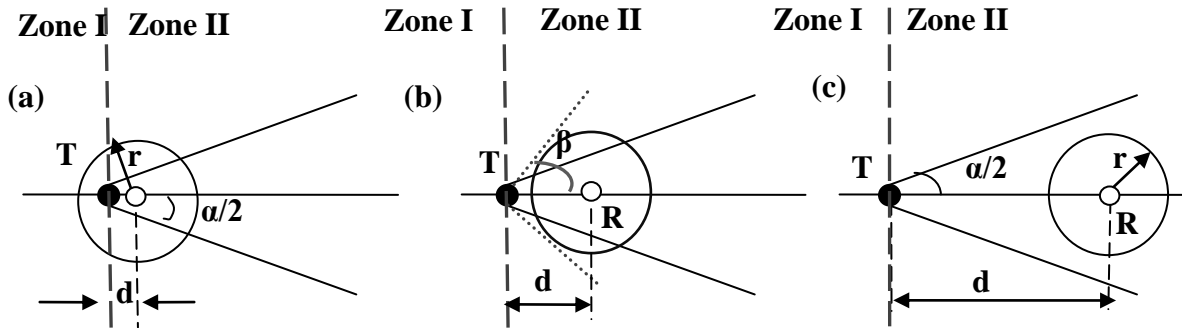


Figure 6.3 Illustration of cases for search span estimation

6.4 Analysis

We assume a homogeneous ad hoc network in steady state. Homogeneous in our case means that each node statistically experiences the same events as any other node. Further, each node always has packets in its buffer. A total of $N1$ transmitting nodes are uniformly distributed in a coverage area of a node. $N2$ are the number of nodes (sessions) that can concurrently coexist and establish sessions due to directional transmissions. Each node moves at an average relative velocity of v (m/s). A node is equipped with a switched beam antenna and employs AoA (Angle of Arrival) estimation for sector

finding when in omni mode. Each sector has a beam-width of α degrees (implies $360/\alpha$ sectors) and inter-sector switching time is negligible. Nodes only use sector location rather than specific location coordinates. When in idle mode, the receiver operates in omni-direction and continuously updates DNAV. However, RTS, CTS, Data and ACK (Acknowledgement) packets are transmitted in directional mode only. No periodic updates are sent by nodes.

The actual analytical formulation of $N2$ sessions depends on the beam width, SIR, topology, node density, traffic, mobility, etc. For mathematical convenience, we assume $N2$ to be a simple dual slope function (other aforementioned parameters are assumed constant) that decays with increasing value of α as,

$$N2 = \begin{cases} \frac{4}{50}(10 - \alpha) + 5 & \alpha \leq 60 \\ 1 & \alpha > 60. \end{cases} \quad (6.1)$$

It is well established that significant channel utilization is achieved per node for narrow beam-widths [102]. This is the reason for considering narrow beam-width range (i.e., $\alpha \leq 60$).

Let p_f be the average packet loss probability due to channel fading and τ be the probability of node transmission. The relationship between τ and the packet loss probability is already very well established in [92, 93], and so will not be pursued here. Suppose the distance separation r between the nodes follow the probability density function $f_r(r)$, and $p_f(r)$ is the loss probability due to fading at a given distance r . Then the average probability of packet loss due to fading is given as,

$$p_f = \int p_f(r) f_r(r) dr.$$

Now we define events that a typical node experiences as five states [93]: successful transmission (s); failed transmission (f); overhear successful transmission (os); overhear failed transmission (of); and idle states (i). In successful transmission event, the node succeeds in transmitting its data packet. In failed transmission event, the node transmission fails due to collision or fading. In over hear successful transmission event, the node hears successful transmission in its neighborhood. In overhear failed transmission event, the node hears collisions among the neighboring nodes. In idle event, the node does not transmit and finds the channel empty.

We define probability of success P_s as,

$$P_s =$$

Prob. {node transmits} \times Prob. {no packet loss due to fading} \times

Prob. {intended receiver is not transmitting} \times

Prob. {other nodes do not interfere} \times

Prob. {intended receiver is inside the sector}.

Thus, probabilities of all five states can be modified as [93]:

$$P_s = \tau (1 - \tau)(1 - p_f)\{1 - \tau(1 - p_f)\}^{N_1 - N_2 - 1} (\hat{P}). \quad (6.2)$$

Where, $\hat{P} = P_a \cdot \left(\frac{1}{m_a}\right) + P_b \cdot \left(\frac{1}{m_b}\right) + P_c$, $m_a = \frac{360}{\alpha}$ and $m_b = 1 + 2 \left\lceil \max\left(0, \beta - \frac{\alpha}{2}\right) / \alpha \right\rceil$.

$$P_f = \tau [1 - (1 - \tau)(1 - p_f)\{1 - \tau(1 - p_f)\}^{N_1 - N_2 - 1} \{\hat{P}\}]. \quad (6.3)$$

$$P_{os} = (1 - \tau) \left\{ \sum_{i=1}^{N_2} \binom{N_2}{i} [\tau \hat{P} (1 - \tau)(1 - p_f)]^i \right\} \{1 - \tau(1 - p_f)\}^{N_1 - N_2 - 1}. \quad (6.4)$$

$$P_{of} = (1 - \tau) \{1 - [1 - \tau(1 - p_f)]^{N_1 - 1}\} - P_{os}. \quad (6.5)$$

$$P_i = (1 - \tau) [1 - \tau(1 - p_f)]^{N_1 - 1}. \quad (6.6)$$

Note that \hat{P} is the probability of finding the destination in a sector which depends on the cases mentioned in Section 6.3. Furthermore, $\frac{1}{m_a}$ is the probability of finding the destination in a sector out of total sectors, and $\frac{1}{m_b}$ is the probability of finding the destination in a sector out of sectors in a search span.

The total average throughput of a typical node is given by,

$$\eta = \frac{N1 N2 P_s DATA}{P_s T_s + P_f T_f + P_{os} T_{os} + P_{of} T_{of} + P_i T_i}. \quad (6.7)$$

P_s, P_f, P_{os}, P_{of} , and P_i are probabilities of the five states characterized in (6.2) – (6.6). T_s, T_f, T_{os}, T_{of} , and T_i correspond to the average times a node spend in aforementioned five states. The average successful packet transmission time (T_s) and failure time (T_f) are dependent on uniform distribution over the total number of retries (R) and the uniformly distributed window size (CW). We compute the average times as follows with negligible propagation delays as:

$$T_s = DIFS + 3 * SIFS + DATA + RTS + CTS + ACK + PHY_{Header} + MAC_{Header} + Eboff_s;$$

$$T_f = Eboff_f;$$

$$T_{os} = T_s, T_{of} = T_f, \text{ and } T_i \text{ is the average idle time.}$$

Where, $Eboff_s = \frac{1}{R+1} [\sum_{j=1}^{R+1} E\{CW_j\}]$ and node transmits uniformly in window $CW_j = 2^j * CW_{min}$ at the j_{th} attempt such that $CW_j \in [CW_{min}, CW_{max}]$. Whereas, $Eboff_f = \frac{R}{R+1} [\sum_{j=1}^{R+1} E\{CW_j\}] + R \times [DIFS + SIFS + RTS]$. Readers are referred to [92] for definitions on some of the above parameters. Substituting all the above calculated parameters into (6.7) will give us the total average throughput in ad hoc network.

6.5 Results and Discussion

The total average throughput of ADMAC is compared with the RS and LS based DMAC protocols. Main parameters are listed in Table 6.1. From Figures 6.4 - 6.9, it is clear that total average throughput increases as α gets smaller due to increased spatial reuse.

Assume network behavior represented by cases (a), (b) and (c) in Fig. 6.3, have probabilities P_a , P_b and P_c . Precise characterization of P_a , P_b and P_c is difficult as it changes with the average distance (d), topology, mobility, elapsed time ($1/\mu$), beam-width (α), etc. However, intuitively we can expect the network to have a larger value of P_b as α gets narrower. We only consider $\alpha \leq 60^\circ$ (for increased spatial reuse) and so an appropriate choice of $P_b = 0.8$ was used in our simulations ($P_a = 0$, since in general $d \gg v/\mu$). In Fig. 6.4-6.9, average throughput of ADMAC is always better than RS approach for all α . ADMAC also performs better than LS approach, particularly as α

Table 6.1 Simulation Parameters

Parameter	Value	Parameter	Value
$N1$	10-50	$DIFS$	50 μ s
$N2$	1 - 5	$SIFS$	10 μ s
v	10 -70 m/s	RTS	352 μ s
$1/\mu$	0.2 s	ACK/CTS	304 μ s
α	$10^\circ - 60^\circ$	$Slot\ time$	20 μ s
P_a	0	PHY_{Header}	192 μ s
P_b	0.8	MAC_{Header}	224 μ s
P_c	0.2	CW_{min}	32
R	4	CW_{max}	1024
$Capacity$	1 Mbps	$DATA$	1 kbyte

gets smaller. This is due to the fact that as α gets smaller, the destination is more likely to move out of the sector for a given velocity and total elapsed time. For $\alpha = 60^\circ$, no average throughput improvement is seen when compared to the LS approach, because the

destination stays inside the sector for all velocities (10 - 70 m/s) in a given elapsed time. Thus, increasing α will not lead to any throughput improvement compared to LS approach. On the other hand, decreasing α will lead to throughput improvement even for smaller average velocity. For $\alpha = 30^\circ$, ADMAC is 40 % better than LS at $v = 70$ m/s. For $\alpha = 10^\circ$, ADMAC is 40 % and ~ 30 % better than LS for velocities of 30 and 70 m/s, respectively. Our results also show that ADMAC average throughput improvement is significant compared to RS approach (greater than 400 %) and in general increases for

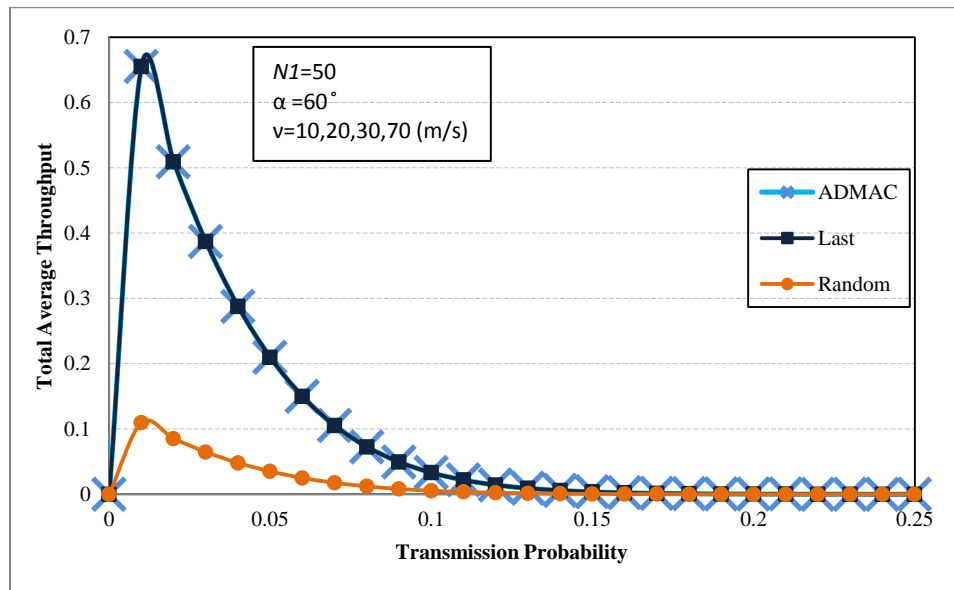


Figure 6.4 Total average throughput as a function of transmission probability for $\alpha = 60^\circ$ and $v = 10, 20, 30, 70$ (m/s)

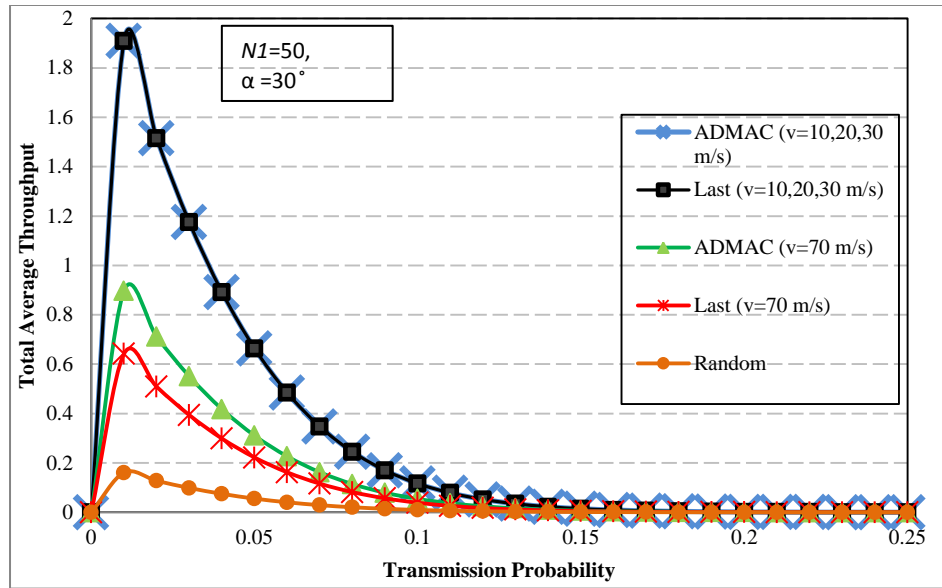


Figure 6.5 Total average throughput as a function of transmission probability for $\alpha = 30^\circ$ and $v = 10, 20, 30, 70$ (m/s)

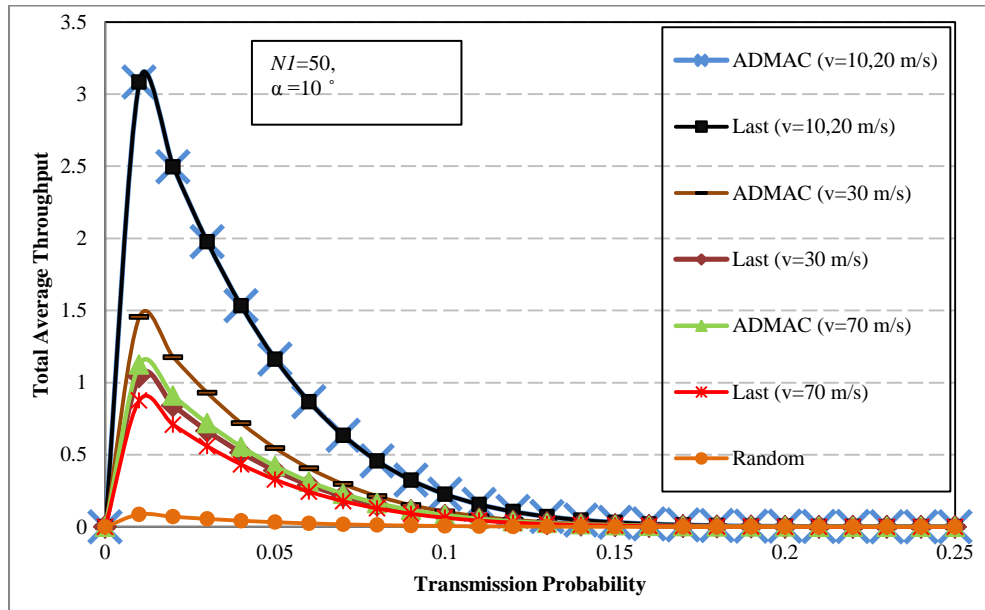


Figure 6.6 Total average throughput as a function of transmission probability for $\alpha = 10^\circ$ and $v = 10, 20, 30, 70$ (m/s)

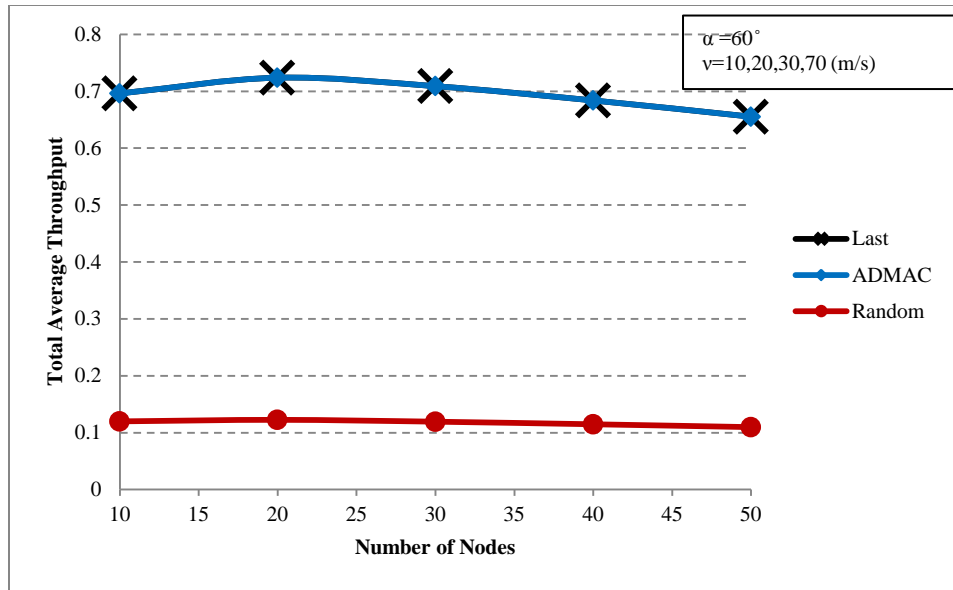


Figure 6.7 Total average throughput as a function of nodes for $\alpha = 60^\circ$ and $v = 10, 20, 30, 70$ (m/s)

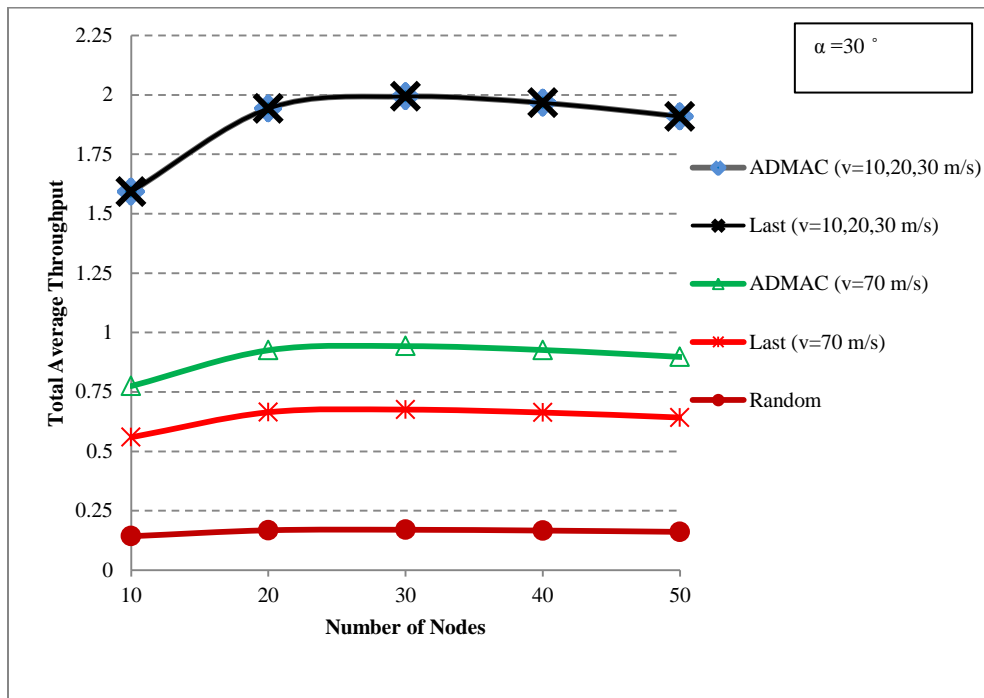


Figure 6.8 Total average throughput as a function of nodes for $\alpha = 30^\circ$ and $v = 10, 20, 30, 70$ (m/s)

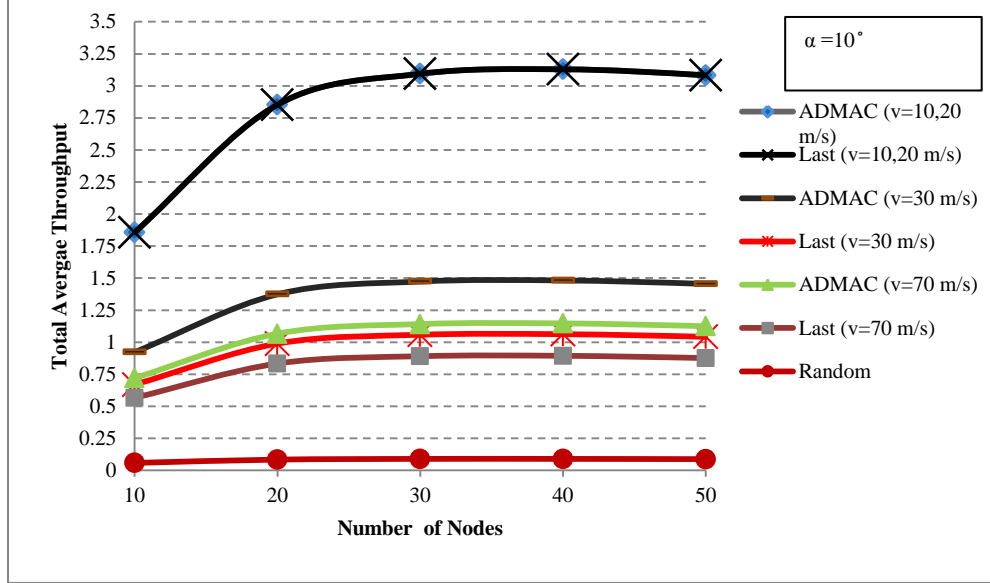


Figure 6.9 Total average throughput as a function of nodes for $\alpha = 10^\circ$ and $v = 10, 20, 30, 70$ (m/s)

smaller value of α (due to increase in the number of sectors). However, when we consider $P_a = 0$, $P_b = 0.2$, and $P_c = 0.8$ (represents larger beam-width network scenario), we observe no throughput improvement for $\alpha = 60^\circ$, and 4 % improvement for $\alpha = 30^\circ$ at $v = 70$ m/s compared to LS approach. Throughput improvement compared to RS approach remains greater than 400 % for $\alpha = 60^\circ$ and increases for smaller value of α .

For simulations, we place nodes in an area of 250 m x 250 m using parameters listed in Table 6.1. We use random direction mobility model for our simulations. Results depict that for $\alpha = 30^\circ$, ADMAC is roughly 27 % better than LS at $v = 70$ m/s. For $\alpha = 10^\circ$, ADMAC is 30 % and 23 % better than LS for velocities of 30 and 70 m/s. Further, compared to RS, average throughput improvement is also significantly large.

6.6 Concluding Remarks

A novel neighbor discovery ADMAC is proposed. Results confirm better average throughput performance over LS and RS based DMAC approaches particularly at lower

values of α (up to 40 % and greater than 400 % improvements over the LS based and the RS based DMAC protocols, respectively). Further, proposed ADMAC protocol is also highly scalable compared to LS and RS based DMAC protocols. Simulation results confirm better performance of the ADMAC protocol. Future work will entail investigation of average throughput and delay performances under optimal beam-width settings for search-span technique under mobility conditions.

CHAPTER 7

POLARIZATION BASED DMAC PROTOCOL FOR WIRELESS AD HOC NETWORKS

7.1 Introduction and Motivation

Performance enhancement in wireless ad hoc network poses unique challenges due to lack of central controller (distributed behavior), scarce channel resource, random interference characteristics, and dynamic topology [72] (see Chap. 1-6). The core medium access control (MAC) protocol in ad hoc network is primarily derived from the IEEE 802.11 distributed coordination function (DCF) protocol. The DCF heavily relies on physical and virtual carrier sensing, four-way handshaking and back-off mechanisms to minimize random channel contentions, reduce redundant signaling, and improve performance [92, 116]. Over the last decade, researchers have made significant strides in performance improvement by modification of the core DCF protocol to harness advances in physical layer techniques. For example, techniques such as, beam forming, multiple-input-multiple-output (MIMO), multiuser detection (MUD), multichannel configuration, and orthogonal frequency division multiplexing (OFDM) have been proposed with modifications to the DCF protocol for throughput improvement in wireless ad hoc networks [99, 106, 118-120].

One such seminal contribution towards ad hoc performance improvement has been the development of the directional MAC (DMAC) protocol that makes use of directional beam-forming to reduce co-channel interference, and allows multiple concurrent sessions

[96, 98, 99, 105, 112, 115, 117, 121]. However, directional beam-forming approach has also led to a set of problems, such as deafness, ready-to-send (RTS)/clear-to-send (CTS) collisions, hidden terminal due to unheard RTS/CTS, and destination discovery [96, 105]. All the aforementioned problems lead to increased interference and bandwidth wastage. Studies have confirmed that if the destination location is known then for the traditional DMAC protocol about 80 % of the failure rate is attributed to the deafness problem, whereas 15 % to 20 % is due to RTS/CTS collisions [96, 104, 105]. As such, recently there has been a considerable research focus on providing various solutions to deafness and destination discovery problems to improve network throughput performance [96, 102-104, 106].

Another common approach proposed for interference avoidance in ad hoc networks is the multichannel technique. Although, most multichannel schemes are primarily designed for omni-directional MAC, but they can be easily adapted for DMAC protocol [122-126].

Power control is also extensively explored as interference reduction technique in DMAC protocol. In [127], power control for DMAC was proposed which showed significant improvement in energy consumption and throughput performance. In [109] authors proposed a distributed power control scheme for DMAC based on temporal correlations and interference prediction that improved average throughput compared to DMAC by 48 %. In [107], power controlled DMAC was proposed. In this scheme the RTS and CTS packets are sent with maximum power, but the data packets are transmitted with power control to minimize interference to other nodes. It is worth mentioning that for effective power control adaptation many proposed algorithms require interference information from the neighboring nodes and signaling. For further reading on

multichannel, power control, and MIMO related techniques readers are referred to [119, 120, 128, 129], and references therein.

In essence, almost all the proposed modifications to DMAC protocols fall under the general categories of interference avoidance and interference mitigation. It was also mentioned in [127] (see refs. therein) that to achieve significant performance improvement, various above-mentioned techniques have to work together in an integrated manner.

In this chapter, we present polarization based single channel DMAC protocol that is fully distributed. In the proposed polarization based DMAC, a sender uses directional sensing to sense for both horizontal and vertical polarizations and chooses polarization channel that is available based on the power threshold. This geographically interleaves (or isolates) similar polarizations, which in turn minimizes cumulative co-channel interference in a given sender-receiver direction. Hence, this increases the probability of successful transmission which leads to increased average throughput in the network. Much of the work related to polarization diversity is done in the area of mobile cellular network that is managed by a central controller (base station). Interested readers are referred to literature available on the performance impact of polarization in cellular networks [130-133].

Work on distributed polarization diversity in outdoor ad hoc networks is almost non-existent. In the context of polarization diversity using DMAC, [134] is closest to our work, but is significantly different from our proposed PDMAC (Polarization based DMAC) protocol. In [134] authors proposed polarization diversity DMAC (termed as DMAC-PDX) for 60 GHz indoor short range wireless local area network. The DMAC-

PDX consists of two stages: testing and synchronization stage, and direction finding stage. In the testing and synchronization stage transmitter (source) and receiver (destination) identify the line-of-sight (LOS) or non-line-of-sight (NLOS) channel environment. Once the channel environment is identified, the DMAC switches to circular polarization for LOS path and to linear polarization for NLOS path, followed by data transmission. The DMAC-PDX only uses polarization diversity from the signal penetration point of view and, thus, it does not consider single channel distributed ad hoc interference (contention) environment. Further, signal strength characteristic is compared only with omni-directional MAC. In our work, we consider a typical outdoor (suburban/urban, predominantly NLOS) type of channel environment. Further, in multiuser interference limited ad hoc network, circular polarization (right hand or left hand) cannot be effectively used due to small cross polarization isolation between linear and circular polarizations.

Almost all of the research work done in polarization based interference cancellation is in centralized cellular systems, where nodes are not distributed and autonomous. In ad hoc networks, polarization based interference cancellation is almost non-existent mainly due to fully distributed nature of ad hoc network. This serves as the main motivation for our work in this chapter.

7.2 Outdoor Propagation and Preliminaries

DMAC protocols make use of directional antennas to suppress co-channel interference and improve network throughput. However, interference is not completely eliminated due to side lobes characteristic of a realistic antenna. Employing adaptive polarization diversity is a very effective way to suppress co-channel interference in directional

communication. Since PDMAC relies on polarization behavior, we provide a brief background related to polarization, propagation characteristics, and polarization diversity antenna in this section.

7.2.1 Polarization Background

The polarization of an electromagnetic wave is the orientation of the electric field vector that is always perpendicular to the direction of propagation. In ad hoc networks, antenna typically generates electromagnetic waves that are vertically polarized (vertical or horizontal polarization is termed as a linear polarization). The polarization of the wave changes as it propagates through the environment. Direct path between the transmitter and the receiver preserves the transmitted polarization (vertical or horizontal). Indirect paths that are the result of reflections and refractions induce change in the orientation of the polarization. This causes some of the energy to be transferred to the orthogonal polarization component with uncorrelated fading, which is also termed as cross coupling or depolarization [130, 132, 135, 136]. Moreover, it is important to mention that realistic antennas also generate cross coupling of about 30 - 40 dB in addition to the channel induced cross coupling or depolarization. The ratio of power in the desired polarization to the power transferred to orthogonal polarization is known as the cross polarization ratio (*CPR*).

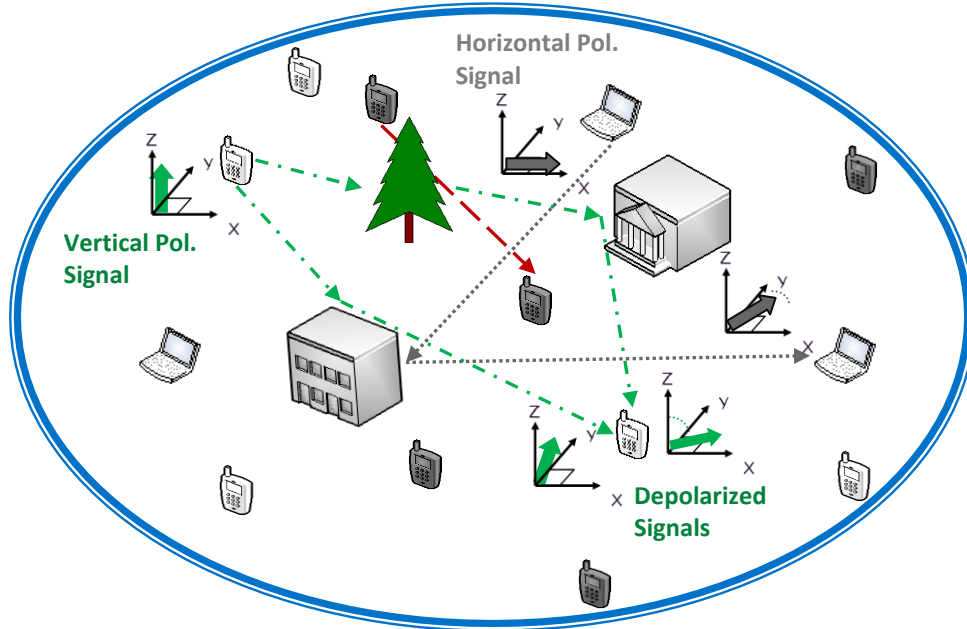


Figure 7.1 Depiction of depolarization in urban/suburban propagation environment

Thus, *CPR* quantifies the extent of depolarization or isolation between two orthogonal polarizations due to specific channel environment. The CPR for a vertically or horizontally polarized transmitted signal is given by,

$$CPR = \frac{P^{(c)}}{P^{(x)}}.$$

$P^{(c)}$ is the power in co-polar signal (desired polarization signal), and $P^{(x)}$ is the power transferred to cross polar component (orthogonal to radiated polarization) due to channel environment.

7.2.2 Outdoor Propagation Environment

We consider directional outdoor propagation in suburban/urban setting. In a typical suburban/urban wireless channel environment, a receiver node receives signal through

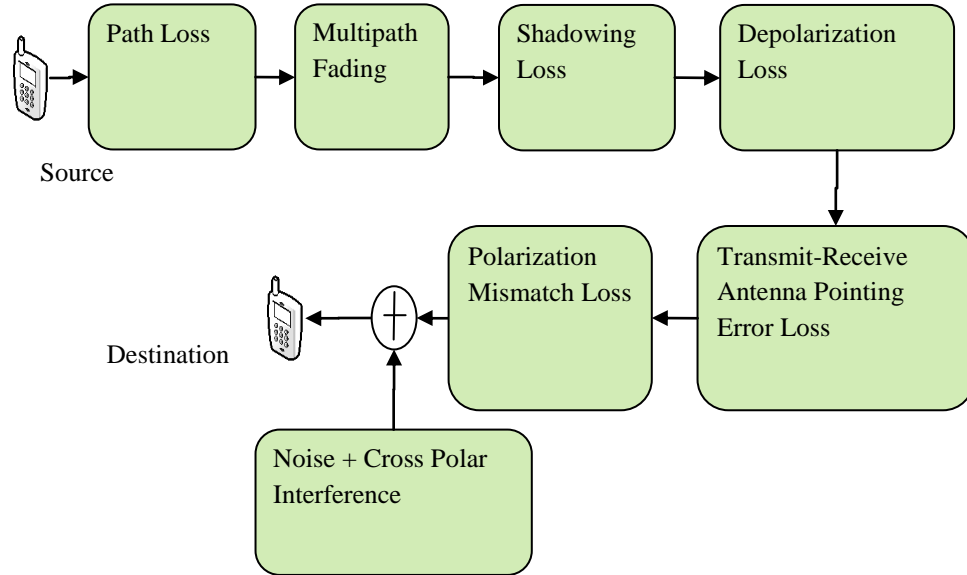


Figure 7.2 Signal losses and impairments through channel

direct path (LOS) and/or indirect paths (NLOS) which depends on the surrounding propagation environment (Fig. 7.1). The quality of signal received at the node is affected by path loss, loss due to signal blockage, transmitter-receiver antenna pointing error, transmitter-receiver polarization mismatch, depolarization, co-channel interference and multipath scattering as shown in Fig. 7.2. In a situation when transmitter and receiver are in NLOS environment, multipath reflections and scattering improves signal quality by mitigating losses due to signal blockage, polarization mismatch and antenna pointing errors [136]. However, it also adversely contributes to interference by propagating depolarized signals from concurrently transmitting distant nodes.

It is known that instantaneous *CPR* for outdoor environment is lognormally distributed and decreases as a function of distance [130, 137];

$$CPR = d^{-a} \chi. \quad (7.1)$$

d is the distance in meters, a is a constant such that $a \in \{R \mid 0 \leq a \leq 1\}$ and is typically much smaller than one; χ is lognormally distributed random variable with mean μ_c and standard deviation σ_c .

7.2.3 Polarization Diversity Antenna

In PDMAC transmitter-receiver nodes choose either horizontal or vertical polarization (HPol or VPol) for transmission based on the directional sensing of both types of polarizations. This requires each node to be equipped with a pair of linearly polarized antennas. Recent years have witnessed major research focus towards the development of small size microstrip dual polarized and dual frequency antennas [138, 139] for improved network performance. In this work, each node is assumed to be equipped with dual polarized antennas. Each antenna element consists of two orthogonal dipole antennas with a PIN diode circuit (see [139]). The pin-diode circuit selects either vertical or horizontal printed dipole based on the decision by the processing unit. The pin diode switching time is negligible and is on the order of a few nanoseconds. Further, the processing unit also adjusts the weights of each element for beam-forming in a specific direction.

As PDMAC requires sensing on both polarizations, by using dual polarized antennas each node can sample sufficient signal strength data in vertical and horizontal polarizations during the physical sensing phase.

7.3 Analysis

In this section, we formulate a *CPR*-based interference model to establish relationship between orthogonally polarized nodes that are uniformly distributed throughout a finite

area A . Further, we derive a lower bound for probability of success, and show how CPR affects the bound.

7.3.1 Directional System Model

Let ρ be the active node density given by N transmitting nodes uniformly distributed in a finite area A . The total node density is the sum of vertically and horizontally polarized node densities, such that $\rho = \rho_v + \rho_h$. Assume P is the transmitter power, G_t is the transmitter antenna gain, G_r is the receiver antenna gain, and α is the path loss exponent, $\mathbb{E}[L]$ is the average of lognormal fading component, h is a product of the square of transmitter and receiver antenna heights (assumed same for all node pairs), then the mean received power P_r at a given distance d is given by generic pathloss model [94],

$$P_r = \frac{P G_t G_r h \mathbb{E}[L]}{d^\alpha}. \quad (7.2)$$

For the purpose of analysis, we consider a flat-gain antenna model shown in Fig. 7.3. The reason for choosing this model is because of its mathematical simplicity. We consider an antenna of beam-width β with a flat mean gain of G_1 in the direction of transmission (i.e., main lobe). The mean side lobes gain is G_2 .

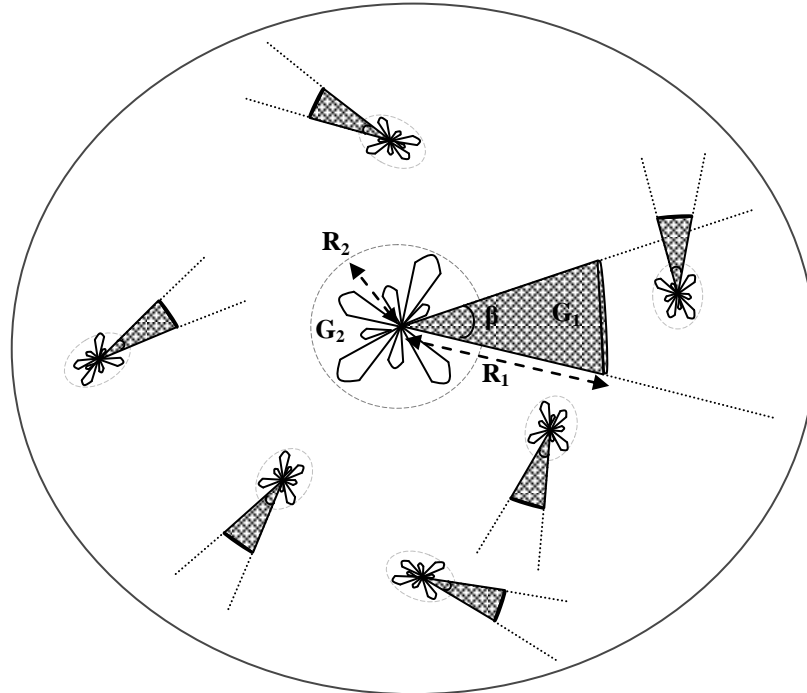


Figure 7.3 System model for interference analysis

In DMAC, each node virtually and physically senses in a specific direction (sector) before initiating transmission to the destination node (see [99, 116]). If the sensed power (interference) is above a pre-specified power threshold (P_{th}) then the transmission is delayed in that direction, until the on-going session (between other nodes) culminates. The cumulative interference power is received at the prospective transmitter-receiver pair through main and side lobes. Thus, concurrent transmissions of the prospective transmitter-receiver pair along with the other nodes can take place only when the interfering nodes' orientations and distances are such that cumulative interference is below the pre-specified power threshold. This consequently prohibits any close proximity nodes from transmitting simultaneously due to significant interference. Henceforth, we define forbidden region of a node as the area within which any other node(s) cannot concurrently transmit based on their orientations. To find R_1 and R_2 (see Fig. 7.3) of the forbidden region we take the approach in [140]. Since the interfering node(s) can have

random orientation, the average gain of the interferer(s) is given by $\hat{G} = \frac{G_1\beta}{2\pi} + \frac{G_2(2\pi-\beta)}{2\pi}$.

Then R_1 is the mean forbidden distance along the main lobe region at which the mean received interference power is equal to P_{th} and is given by, $R_1 = \left\{ \frac{P h G_1 \hat{G} \mathbb{E}[L]}{P_{th}} \right\}^{1/\alpha}$. R_2 is the mean forbidden distance along the side lobe region at which the mean received interference power is equal to P_{th} and is derived in terms of R_1 by, $R_2 = R_1 \left\{ \frac{G_2}{G_1} \right\}^{1/\alpha}$. In the next section we use R_1 and R_2 to perform average analysis.

7.3.2 Bound for \tilde{N}_v

There are quite a number of papers that have explored the capacity scaling laws of wireless ad hoc networks for omni-directional and directional antennas in static case [10, 140, 141]. However, in this section our objective is not to research scale law of network capacity, but rather to analytically show node throughput improvement as a function of *CPR* by using average analysis.

For the sake of analysis, we assume that a desired node that receives interference from uniformly distributed transmitting nodes is vertically polarized and oriented in a specific direction (see Fig. 7.3). All nodes transmit and receive directionally. The vertically polarized receiver under consideration receives average power as given by (7.2). Further, the desired transmitter-receiver pair antennas precisely point to each other with average main lobe gain G_1 . Assume that vertically and horizontally polarized interfering nodes are uniformly scattered in a finite area A . The interference at the receiver will be received through side lobes and the main lobe. Since, we have a finite number of randomly distributed nodes, therefore, cumulative interference is random. The bound on average

number of concurrently transmitting vertically and horizontally polarized nodes is established in the following lemma.

Lemma 7.1: In directional communication ad hoc network, the average number of concurrently transmitting vertically polarized nodes \tilde{N}_v is bounded by the difference between gain margin, and the product of average number of concurrently transmitting horizontally polarized nodes \tilde{N}_h and the polarization factor F ;

$$\tilde{N}_v \leq \frac{G_1^2}{\hat{G}\gamma d^\alpha} - \tilde{N}_h F.$$

Note that $\tilde{N}_v = N_{vm} G_1 R'_1 + N_{vs} G_2 R'_2$, $F = e^{\frac{\sigma_c^2}{2} - \mu_c}$,

$\tilde{N}_h = N_{hm} G_1 R'_{11} + N_{hs} G_2 R'_{22}$ and γ is the signal-to-interference (SIR) threshold.

Proof: Assume all nodes transmit equal power. Consider N_{vm} and N_{vs} to be the number of vertically polarized nodes that interfere with the vertically polarized receiver through main lobe and side lobes, respectively. Similarly, N_{hm} and N_{hs} are the horizontally polarized nodes that interfere through the main lobe and side lobes, respectively. The total random interference I at the vertically polarized receiver under consideration is given by,

$$I = \sum_{i=1}^{N_{vm}} \frac{P \hat{G} G_1 h L}{r_i^\alpha} + \sum_{j=1}^{N_{vs}} \frac{P \hat{G} G_2 h L}{r_j^\alpha} + \sum_{k=1}^{N_{hm}} \frac{P \hat{G} G_1 h L}{r_k^{\alpha-a} \chi} + \sum_{l=1}^{N_{hs}} \frac{P \hat{G} G_2 h L}{r_l^{\alpha-a} \chi}. \quad (7.3)$$

We assume that shadow fading (L), distances (r_i, r_j, r_k, r_l) and χ are independent random variables. Since all nodes have independent and identical distributions, the total average interference at the vertically polarized receiver is given by,

$$\mathbb{E}[I] =$$

$$P \hat{G} G_1 h \sum_{i=1}^{N_{vm}} \mathbb{E}[L] \mathbb{E} \left[\frac{1}{r_i^\alpha} \right] + P \hat{G} G_2 h \sum_{j=1}^{N_{vs}} \mathbb{E}[L] \mathbb{E} \left[\frac{1}{r_j^\alpha} \right] +$$

$$P \hat{G} G_1 h \sum_{k=1}^{N_{hm}} \mathbb{E}[L] \mathbb{E} \left[\frac{1}{r_k^{\alpha-a}} \right] \mathbb{E} \left[\frac{1}{\chi} \right] + P \hat{G} G_2 h \sum_{l=1}^{N_{hs}} \mathbb{E}[L] \mathbb{E} \left[\frac{1}{r_l^{\alpha-a}} \right] \mathbb{E} \left[\frac{1}{\chi} \right].$$

Derivations of mean values are fairly trivial and will not be shown here. L is zero mean lognormal random variable and its mean is evaluated to be $e^{\sigma_L^2/2}$. χ is also lognormal random variable with mean μ_c and standard deviation σ_c , and the mean of its inverse comes out to be $e^{\frac{\sigma_c^2}{2} - \mu_c}$. As mentioned in Section 7.3.1, for concurrent transmissions interfering nodes cannot be located within the range R_1 along the main lobe and R_2 along the side lobes of the receiver node. Since, the area is finite we assume there is a maximum range R_{max} up to which a receiver node can sense. So, we assume that all interfering nodes are uniformly distributed (independent of each other) from R_1 to R_{max} in the main lobe region and from R_2 to R_{max} in the side lobe region. The mean distances results are as follows:

$$R'_1 \equiv \mathbb{E} \left[\frac{1}{r_i^\alpha} \right] = \left\{ \frac{1}{R_1^{\alpha-1}} - \frac{1}{R_{max}^{\alpha-1}} \right\} \times \left\{ \frac{1}{(R_{max}-R_1) \cdot (\alpha-1)} \right\},$$

$$R'_2 \equiv \mathbb{E} \left[\frac{1}{r_j^\alpha} \right] = \left\{ \frac{1}{R_2^{\alpha-1}} - \frac{1}{R_{max}^{\alpha-1}} \right\} \times \left\{ \frac{1}{(R_{max}-R_2) \cdot (\alpha-1)} \right\},$$

$$R'_{11} \equiv \mathbb{E} \left[\frac{1}{r_k^{\alpha-a}} \right] = \left\{ \frac{1}{R_1^{\alpha-a-1}} - \frac{1}{R_{max}^{\alpha-a-1}} \right\} \times \left\{ \frac{1}{(R_{max}-R_1) \cdot (\alpha-a-1)} \right\},$$

$$R'_{22} \equiv \mathbb{E} \left[\frac{1}{r_l^{\alpha-a}} \right] = \left\{ \frac{1}{R_2^{\alpha-a-1}} - \frac{1}{R_{max}^{\alpha-a-1}} \right\} \times \left\{ \frac{1}{(R_{max}-R_2) \cdot (\alpha-a-1)} \right\}.$$

Now plugging and manipulating all evaluated mean values in $\mathbb{E}[I]$ gives us,

$$\mathbb{E}[I] = P \hat{G} h e^{\sigma_L^2/2} \{ N_{vm} G_1 R'_1 + N_{vs} G_2 R'_2 \} + P \hat{G} h e^{\sigma_L^2/2} e^{\frac{\sigma_c^2}{2} - \mu_c} \{ N_{hm} G_1 R'_{11} +$$

$$N_{hs} G_2 R'_{22} \}.$$

Now for successful transmission the signal-to-interference (SIR) ratio should be greater than or equal to the threshold γ as given by,

$$P \hat{G} h e^{\sigma_L^2/2} \{\tilde{N}_v\} + P \hat{G} h e^{\sigma_L^2/2} e^{\frac{\sigma_c^2}{2} - \mu_c} \{\tilde{N}_h\} \leq \frac{P G_1 G_1 h e^{\sigma_L^2/2}}{\gamma d^\alpha}. \text{ Hence a little manipulation of}$$

the above inequality proves lemma 1. Note that $\tilde{N}_v = N_{vm} G_1 R_1' + N_{vs} G_2 R_2'$, $\tilde{N}_h =$

$N_{hm} G_1 R_1' + N_{hs} G_2 R_2'$ and $F = e^{\frac{\sigma_c^2}{2} - \mu_c}$. Since all the terms are constant (mean values),

therefore, \tilde{N}_v and \tilde{N}_h represent the scaled number of vertically and horizontally polarized nodes. Where the numbers of horizontally and vertically polarized nodes are given by,

$$N_{vm} = \left\{ \frac{\rho_v}{2} \right\} \cdot \{R_{max}^2 - R_1^2\} \cdot \{\beta\};$$

$$N_{vs} = \left\{ \frac{\rho_v}{2} \right\} \cdot \{R_{max}^2 - R_2^2\} \cdot \{2\pi - \beta\};$$

$$N_{hm} = \left\{ \frac{\rho_h}{2} \right\} \cdot \{R_{max}^2 - R_1^2\} \cdot \{\beta\};$$

$$N_{hs} = \left\{ \frac{\rho_h}{2} \right\} \cdot \{R_{max}^2 - R_2^2\} \cdot \{2\pi - \beta\}.$$

7.3.3 Approximate Bound for P_s

Consider again a vertically polarized receiver that receives interference from uniformly distributed vertically and horizontally polarized nodes in a finite area (see Fig. 7.3). We again consider the settings in which the vertically polarized receiver is separated by a distance d from its desired transmitter. Since the cumulative interference exhibits more temporal variations than the transmitter-receiver pair under consideration, therefore, we consider the average value of the desired signal power. For finite number of interferers the actual cumulative distribution function of the interference is very complicated and, therefore, we make use of an approximate bound to show the throughput enhancement due to polarization diversity in directional wireless ad hoc networks.

We know that node throughput depends on the probability of successful transmission in a specific direction. Alternatively, the vertically polarized transmission in a specific direction would be unsuccessful when, random interference I (see (7.3)) satisfies the

Table 7.1 Parameter list

Parameter	Value
Beam-width	45°
Pathloss Exponent	4
Transmit Power	10 dBm
SIR Threshold	10 dB
Maximum Range	250 m
Cross Polar Exponent	0.1
Average Main Lobe Gain	1
Average Side Lobes Gain	0.01
Cross Polarization Standard Deviation	3 dB
Cross Polarization Mean	8,13 dB
Source-Destination Separation	80 m

condition, $I \geq \frac{P G_1 G_1 h e^{\sigma_L^2/2}}{\gamma' d^\alpha}$. We set $\gamma' = \gamma - \delta$ (where, $0 \leq \delta \ll 1$) for conformity with the inequality used in Section 7.3.2. The probability of unsuccessful transmission is difficult to evaluate, hence we make use of Markov inequality [142], which loosely bounds the unsuccessful probability as follows;

$$P\{I \geq \frac{P G_1 G_1 h e^{\frac{\sigma_L^2}{2}}}{\gamma' d^\alpha}\} \leq \frac{\gamma' d^\alpha \hat{G}\{[N_{vm} G_1 R_1' + N_{vs} G_2 R_2'] + e^{\frac{\sigma_c^2}{2} - \mu c} [N_{hm} G_1 R_{11}' + N_{hs} G_2 R_{22}']\}}{G_1^2}.$$

The lower bound for probability of successful transmission P_s is, therefore, given by

$$P_s \geq 1 - P\{I \geq \frac{P G_1 G_1 h e^{\frac{\sigma_L^2}{2}}}{\gamma' d^\alpha}\}.$$

The derived bound clearly depends on the polarization factor $F = e^{\frac{\sigma_c^2}{2} - \mu c}$.

For a given node density of vertically and horizontally polarized nodes, we notice that smaller the polarization factor the larger is the mean value of the *CPR* (Section 7.2), and thus higher is the probability of success.

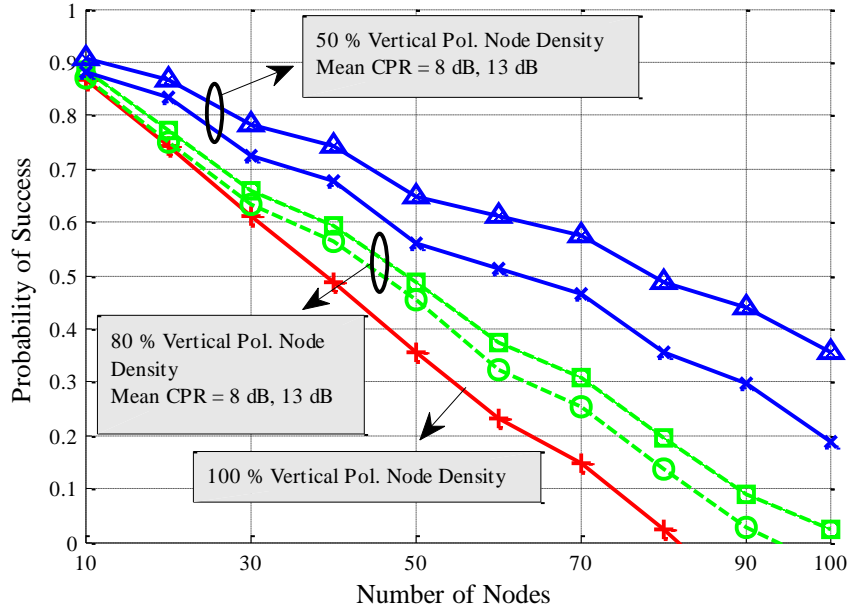


Figure 7.4 Lower bound for probability of success in directional antenna case

In Fig. 7.4, we plot the probability of success lower bound for different values of mean *CPR* and different values of vertically polarized node density. The parameters used are listed in Table 7.1. Typical mean (μ_c) and standard deviation (σ_c) values of *CPR* are taken from outdoor measurements reported in [137]. Fig. 7.4 show that probability of success improves when the vertically polarized node density reduces in the network. When vertically polarized node density is 50 % of the total node density, we observe an improvement of 28 % and 300 % compared to no polarization (means 100 % nodes are vertically polarized) for a total of 30 and 70 nodes, respectively. We also notice that the difference between the probability of success bounds for 50 % and 100 % vertically polarized nodes (out of total nodes) gets wider as total node density increases. This is due

to increase in the number of uniformly distributed horizontally polarized nodes. Note that we only consider up to 50 % vertically polarized nodes because if we decrease below 50 % then the interference at the horizontally polarized receiver will increase. So, 50 % establishes an optimal balance in interference experienced by the vertical and horizontal nodes, and thereby achieves maximum polarization diversity gain.

7.4 Proposed Polarization Based DMAC Protocol

In this section, we expound on the PDMAC protocol. The basic idea is that each polarization (vertical or horizontal) is used as a separate channel (polarization diversity). Due to depolarization effect the two channels are not completely orthogonal, but exhibit interference based on distance separation (between the interferer node and the desired receiver node) and the propagation environment.

Generally for smaller distances (typically ~ 50 to 200 m for ad hoc network) and LOS in urban/suburban settings the channel orthogonality is preserved, but for NLOS situation due to multipath characteristic the polarization orthogonality is reduced (mean *CPR* is typically 8-15 dB) [137]. Reduced orthogonality essentially translates to increased distance separation requirement between the desired receiver and the dominant interfering node. On the other hand, if polarization is not used to provide channel orthogonality then the distance separation requirement further increases which leads to reduced capacity in the network.

To employ polarization in a distributed manner in an ad hoc network, each node senses and picks a polarization channel that is free in a sector and later transmits on it. Picking a polarization channel that is free guarantees that the dominant interfering node uses orthogonal polarization channel and also satisfies the distance separation requirement

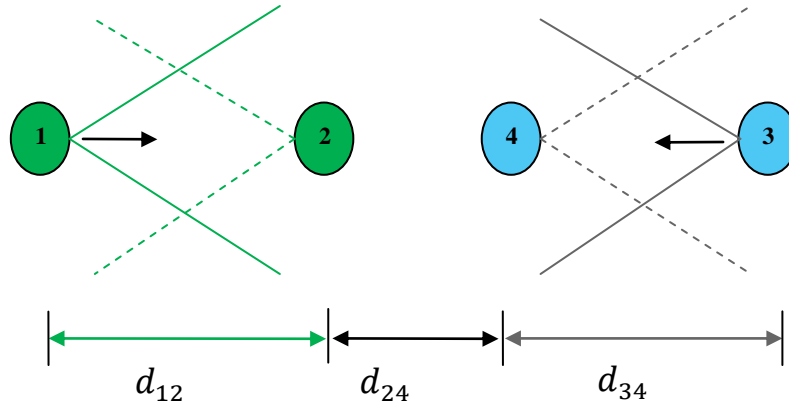


Figure 7.5 Interference example

based on the *CPR*. This leads to alternate polarization channels between adjacent nodes. We illustrate this with an example as shown in Fig. 7.5. Suppose node 1 transmits to node 2 directionally in a sector. Node 3 wants to transmit to node 4, but is located inside the sector in which node 1 transmits. In case of single polarization, if node 1 and node 3 start DRTS (directional ready-to-send) transmission at the same time then collision can occur depending on the distance separation. However, if node 1 transmits first then based on distance separation node 3 may set its DNAV (directional network allocation vector) and defer transmission until node 1 session is over. However, for concurrent successful DRTS/DCTS (directional clear-to-send) handshake and data transmission between nodes 3 and 4, the received interference (from node 1) at node 3 and node 4 should satisfy (using simple pathloss model), $I_{r3} = \frac{PG_1^2}{d_{13}^\alpha} < P_{th}$, and $I_{r4} = \frac{PG_1G_2}{d_{14}^\alpha} < P_{th}$. Where, P is transmitted power, G_1 is the mean sector gain, G_2 is the mean side lobe gain, d_{13} is separation between node 1 and 3, d_{14} is the separation between node 1 and 4, α is the propagation exponent, and P_{th} is the receiver power threshold.

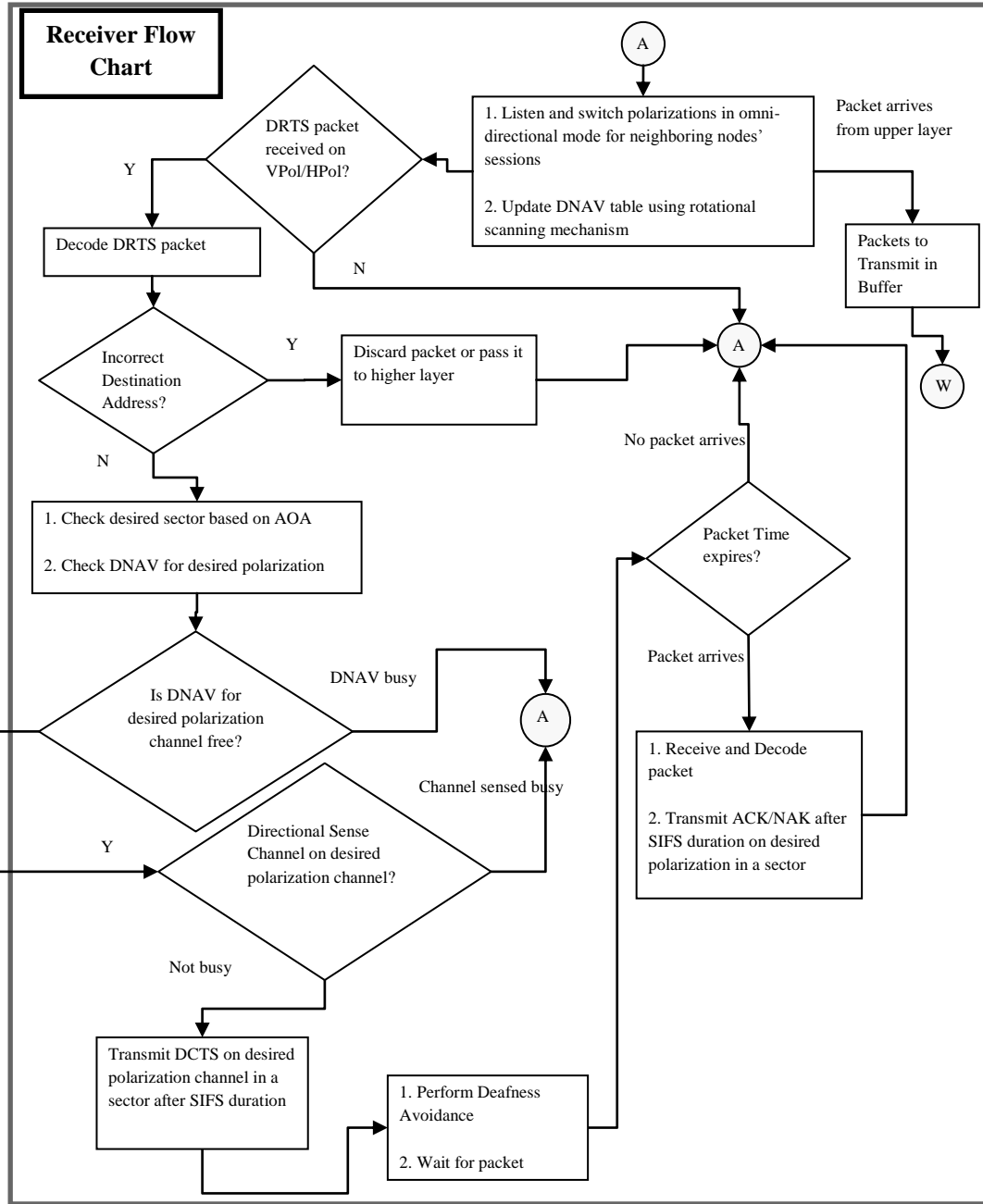


Figure 7.6 Receiver flow chart

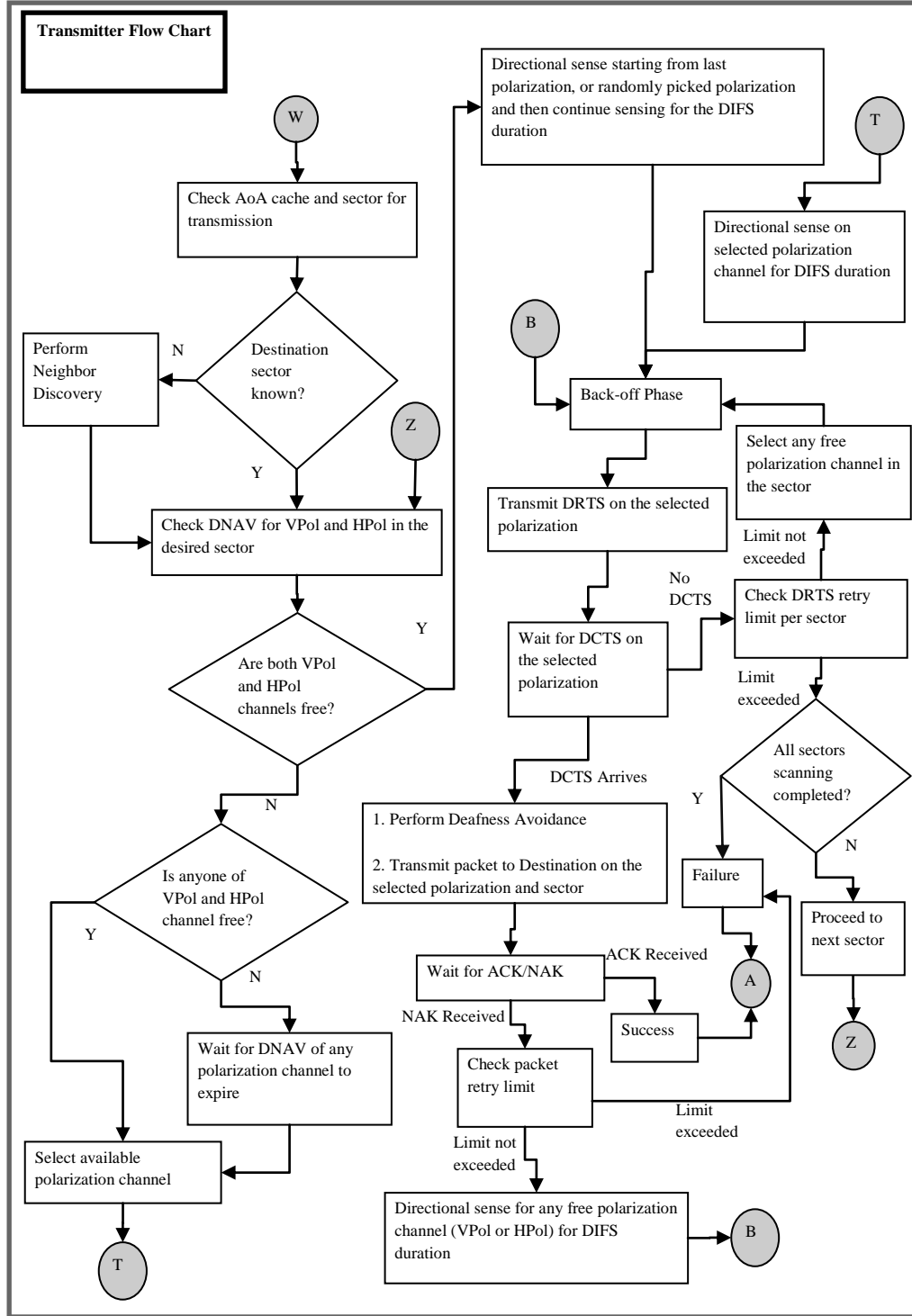


Figure 7.7 Transmitter flow chart

Thus, node 3 and node 4 will start concurrent transmission (DRTS/DCTS exchange)

when distance separations satisfy $d_{13} > \left\{ \frac{PG_1^2}{P_{th}} \right\}^{1/\alpha}$ and $d_{14} > \left\{ \frac{PG_1G_2}{P_{th}} \right\}^{1/\alpha}$, respectively.

Similarly, the signal-to-interference (SIR) ratios at all the receiving nodes should be above the threshold γ for successful completion of data transmissions. With little manipulation this translates to distance separations for the nodes 2 and 4 (receivers) which should satisfy, $d_{23} > d_{12} \left\{ \frac{G_2 \gamma}{G_1} \right\}^{1/\alpha}$ and $d_{14} > d_{34} \left\{ \frac{G_2 \gamma}{G_1} \right\}^{1/\alpha}$, respectively. Thus, all the above distance separations requirements for single polarization case must be met for concurrent transmissions to take place successfully.

Now, let us assume that nodes 1 and 2 communicate using vertical polarization. Then to start successful DRTS/DCTS exchange between nodes 3 and 4, the above distance separations should satisfy $d_{13} > \left\{ \frac{PG_1^2}{\bar{\chi} P_{th}} \right\}^{1/\alpha - a}$ and $d_{14} > \left\{ \frac{PG_1 G_2}{\bar{\chi} P_{th}} \right\}^{1/\alpha - a}$ (using (7.1)).

Where, $\bar{\chi}$ is the mean CPR and $\frac{a}{\alpha} \ll 1$ (see [130]). Based on the SIR threshold requirement and $\frac{a}{\alpha} \ll 1$, the distance separations for the nodes 2 and 4 (receivers) should

also satisfy, $d_{23} > d_{12} \left\{ \frac{G_2 \gamma}{\bar{\chi} G_1} \right\}^{1/\alpha}$ and $d_{14} > d_{34} \left\{ \frac{G_2 \gamma}{\bar{\chi} G_1} \right\}^{1/\alpha}$, respectively. Note that distance

requirements are reduced by a factor of $\left(\frac{1}{\bar{\chi}} \right)^{1/\alpha}$ for opposite polarization channels when

compared with the single polarization. For typical values of $\alpha = 2.5$ and $\bar{\chi} = 15.84$ (12 dB), note that the required distances are reduced by one-third [137]. It is probable that

when nodes 3 and 4 sense directionally using vertical polarization they may not meet the distance requirement due to interfering signal strength above threshold (P_{th}). However, if

nodes 3 and 4 sense using horizontal polarization it is likely that they may meet the reduced distance requirement (1/3 or 1/4 depending upon α and $\bar{\chi}$). As such, by adapting

to opposite polarization, nodes 3 and 4 would communicate concurrently along with

nodes 1 and 2 and, therefore, double the capacity. Thus, nodes can adapt polarizations in their respective sectors to minimize interference in a distributed asynchronous manner. This mainly forms the basis of our PDMAC protocol.

The PDMAC protocol follows 4-way handshake process by directionally transmitting DRTS-DCTS-DATA-DACK packets on a specific polarization. It is assumed that a node is capable of operating in directional and omni-directional modes. Further, each node is equipped with one transceiver only, so it can listen to only one type of polarization channel at a time. The PDMAC can also easily integrate with the existing protocols for deafness avoidance [104, 106] and neighbor discovery [27, 98, 143] as shown in flowcharts in Figures 7.6 and 7.7. The proposed PDMAC is a fully distributed, asynchronous, and compatible polarization diversity protocol. Henceforth, we explain node polarization adaptation during idle, reception, and transmission modes of the PDMAC algorithm.

7.4.1 Idle Mode

In idle mode a node has no packet to transmit, and so it listens to ongoing transmissions in omni-directional mode as in IEEE 802.11 [92]. The node continuously switches polarization (can be set to 25 μ s) to monitor the ongoing transmissions. The switching time between horizontal and vertical polarization is assumed negligible (see Section 7.2.3). If a node observes ongoing transmission between neighboring nodes on either polarization, it estimates the AoA (Angle of Arrival) and sets the DNAVs accordingly for the busy polarization channel. Hence, in each sector a node is aware of the neighbor nodes signal strengths in vertical and horizontal polarizations.

7.4.2 Reception Mode

In idle mode if a node receives a DRTS packet on a specific polarization, it estimates the AoA to find the sector (direction of the source) and then checks the DNAV for the received polarization. If DNAV for the received polarization is free then the node physically senses the channel on the same received polarization in a specific sector. If the polarization channel is free for SIFS (short inter-frame space) duration then DCTS is transmitted using the same polarization. If for the received polarization, DNAV is not free or the polarization channel is sensed busy then node goes in to idle mode as depicted by receiver flowchart in Fig. 7.6.

7.4.3 Transmission Mode

As shown in Fig. 7.7, when a packet arrives from upper layer, the node determines the sector in which the receiver (destination) is located. If the sector is not known, location discovery is performed using techniques in [27, 98, 143]. If the receiver sector is known and the AoA timer is not expired, then DNAVs for both polarizations are checked in that sector. If both DNAVs are free then both polarization channels are initially sensed with priority given to last used polarization channel. For the polarization channel that is found free, sensing continues for the DIFS (Distributed inter-frame space) duration as in standard IEEE 802.11 protocol [92]. If only one DNAV polarization is free then sensing is done for that polarization for the DIFS duration. After DIFS duration if the channel remains free on the sensed polarization, DRTS is transmitted on the same polarization and then the source waits for the DCTS on the same polarization (no polarization switching is performed). If no DCTS is received retries are attempted in the same sector following the back-off using the same sensing process as above. If all retries fail, the

same transmission process is repeated in other sectors until 360° span completes. In case channel is sensed busy, transmission of DRTS on the selected polarization channel is deferred until channel becomes available. During back-off phase, the PDMAC continues sensing on the selected polarization channel only.

7.5 Simulation Results and Discussion

As discussed in Section 7.3, polarization diversity improves average throughput per node in an ad hoc network. In this section, we simulate PDMAC protocol using QualNet 5.0 environment [113]. We compare average throughput per node of our protocol with basic DMAC protocol in almost static case (pedestrian speed).

To create severe interference limited environment, nodes are uniformly placed in a geographical area of dimension 100 m x 100 m. The source-destination pairs are kept fixed during the entire simulation duration of 300s. Hundred separate runs are done using different seed values for good average estimates. The average throughput is evaluated as a function of the sender constant bit rate (CBR) ranging from 41 kbps to 1.95 Mbps. To test scalability we compare average throughput performance under varying node density against the basic

Table 7.2 Simulation Parameters

Parameters	Value
Area	100 m x 100 m
Total Nodes	8, 16, 24, 32
Mobility	Random Walk
Total Packets to Send	1000
Packet Size	512 Bytes
Data Rate	41 kbps – 1.95 Mbps
Transmit Power	10 dBm
Power Control	No
Pathloss	2-Ray Model
Channel Capacity	2 Mbps
Mean Orientation and Shadow Loss	4 dB
Directional Antenna Gain	15 dBi
DNAV Angle	37°
Directional Antenna Beam-width	45°
Mean CPR	12 dB
Receiver Threshold	-81 dBm
Receiver Sensitivity	-91 dBm
Threshold Signal-to-Noise Ratio	10 dB

DMAC protocol. Further, realistic mean value of *CPR* (12 dB) for urban propagation environment is used for all nodes [137]. The details of physical, MAC and application layer parameters used in the simulation are listed in Table 7.2.

Nodes generate significant interference through their main beam. However, nodes oriented in different directions create interference through side lobes that is also significant enough to prevent concurrent transmissions within a certain distance separation as discussed in Sections 7.3 and 7.4.

As node density increases, interference through side lobes further becomes significant. Nodes rely on IEEE 802.11 sensing and back-off mechanism to avoid collisions, and the DRTS/DCTS mechanism for channel reservation. In the event of simultaneous

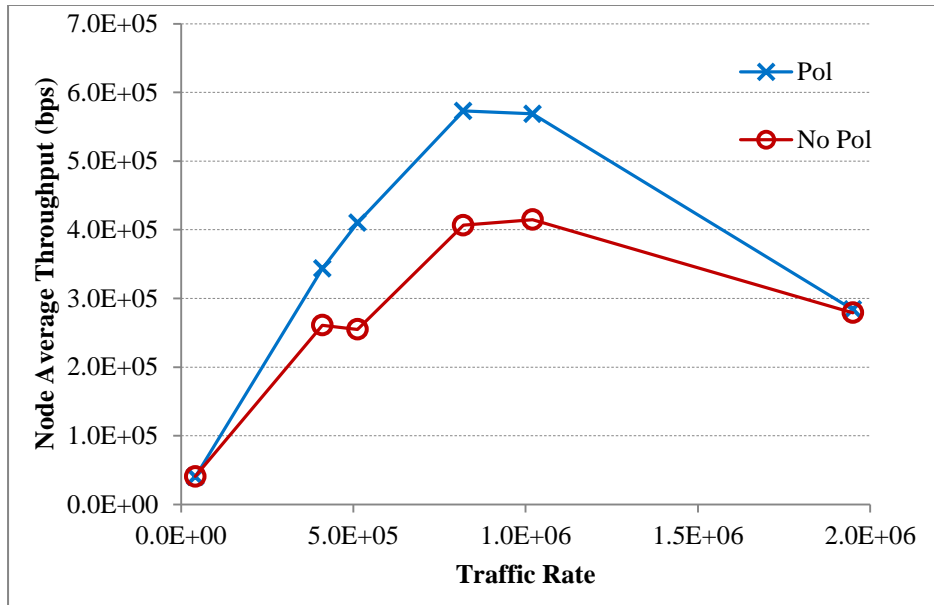


Figure 7.8 Node average throughput performance for 8 nodes

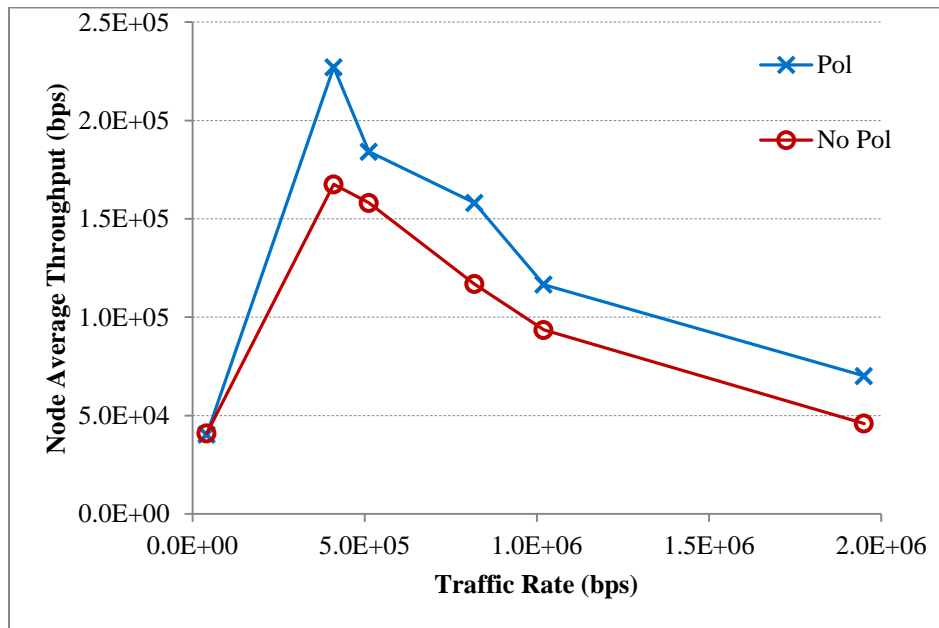


Figure 7.9 Node average throughput performance for 16 nodes

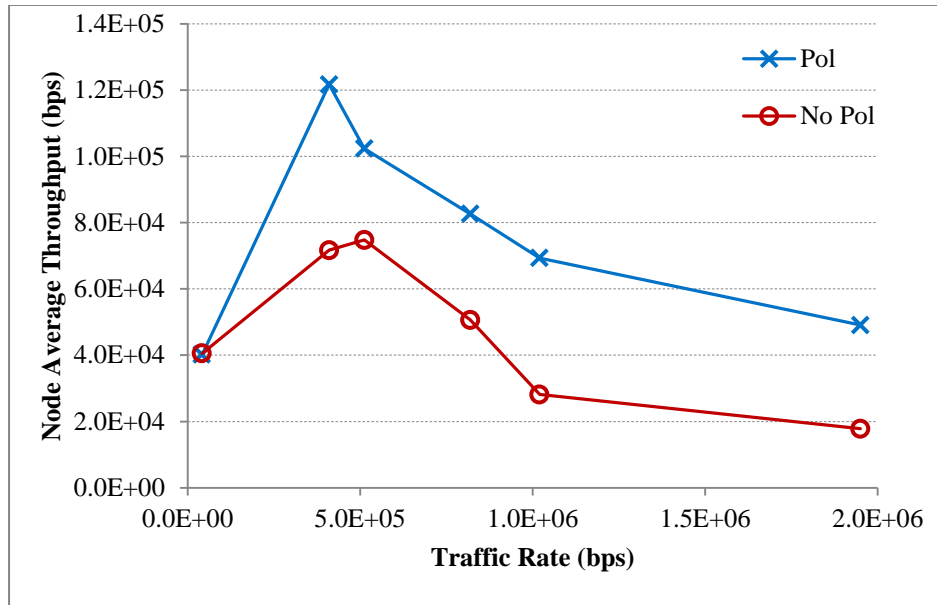


Figure 7.10 Node average throughput performance for 24 nodes

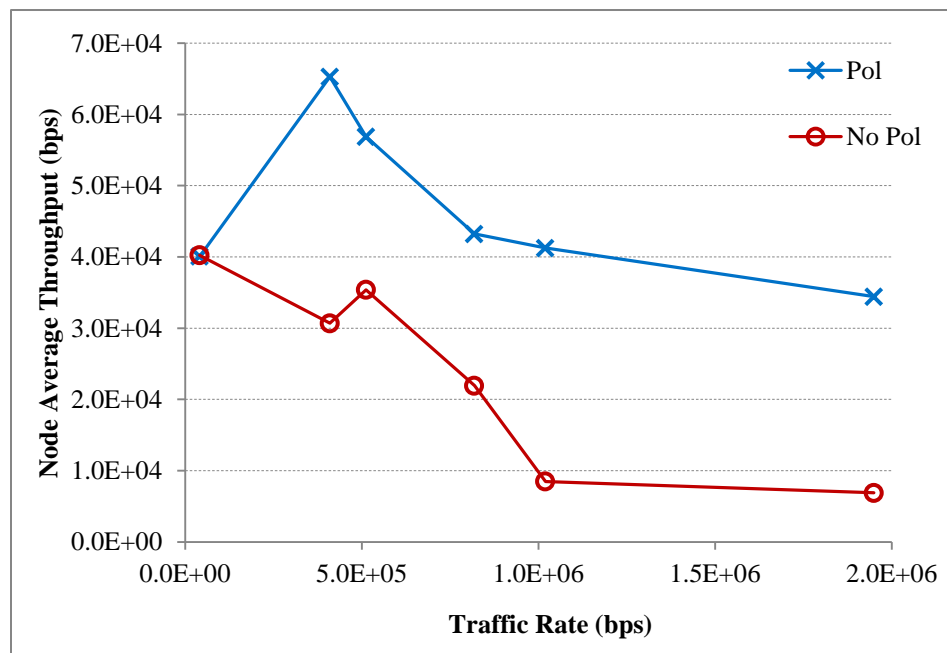


Figure 7.11 Node average throughput performance for 32 nodes

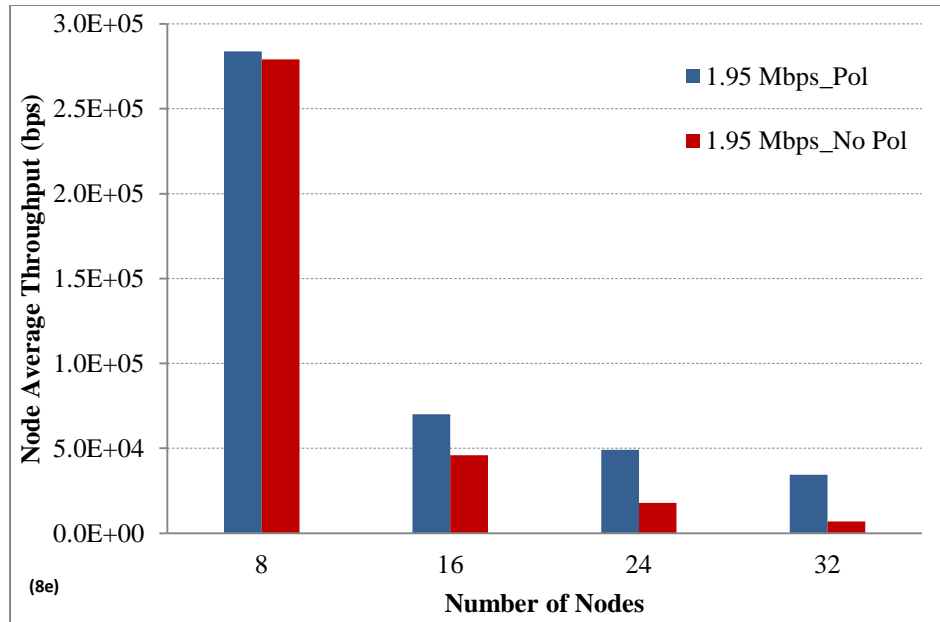


Figure 7.12 Node average throughput for 8, 16, 24, and 32 nodes at 1.95 Mbps

DRTS/DCTS transmissions, it is possible that the source-destination pair can still capture the DRTS/DCTS packets if the SIR is above the threshold value. Generally, at low traffic rate the channel access probability is low and so back-off window mechanism works well to prevent interference and packet collisions. As traffic rate increases, the channel access probability increases and so does the interference and packet collisions. Thus, nodes frequently back-off to prevent packet collisions which consequently reduces average throughput. Thus, in a network of finite area, randomly oriented source-destination pairs that experience minimal interference through main lobe and side lobes contribute the most to the average node throughput. On the other hand, nodes that experience significant interference through main lobe and side lobes frequently back-off and reduce average node throughput in the network.

Figures 7.8-7.11 depict average node throughput as a function of traffic rates for different node densities. As shown in Fig. 7.8, basic DMAC protocol average throughput is same as the PDMAC at the traffic rate of 41 kbps. This is because at low traffic rates

not much interference is created, and so performance is same. As traffic rate is increased to 1 Mbps we observe that average throughput difference increases to 0.1 Mbps due to reduced interference and collisions in case of PDMAC.

However, at higher traffic rate of 1.95 Mbps, average throughput difference reduces to 5 kbps. This reduced difference is due to increased interference and smaller polarization diversity gain (due to 4 source-destination pairs) as discussed in Sections 7.3 and 7.4. As obvious from Fig. 7.8-7.11, average throughput decreases as the number of nodes increase in the network. However, for larger number of nodes polarization diversity gain is also larger. As shown in Fig. 7.11, for 32 nodes in the network, average throughput of basic DMAC protocol is reduced appreciably due to increased interference. Specifically, average throughput at the traffic rate of 1.95 Mbps (and 32 nodes) for basic DMAC is 6.8 kbps. On the other hand, PDMAC reduces interference by creating polarization diversity which in turn leads to a graceful degradation of average throughput. This consequently increases the capture probability. Hence, for traffic rate of 1.95 Mbps (and 32 nodes) PDMAC average throughput reduces to 34.4 kbps as shown in Fig. 7.11. Fig. 7.12 compares average throughput between basic DMAC and PDMAC for the worst case traffic rate of 1.95 Mbps for 8, 16, 24 and 32 nodes. Note that for the worst case of 1.95 Mbps, the average throughput improvement due to PDMAC is about 176 % and 400 % for 24 and 32 nodes, respectively. This is a significant improvement when the network operates at a maximum traffic rate of 1.95 Mbps. Increase in average throughput improvement for larger number of nodes at the maximum traffic rate of 1.95 Mbps also validates that PDMAC is highly scalable compared to basic DMAC protocol. PDMAC exploits polarization diversity that allows for more simultaneous communications, which

in turn leads to lesser average delay as shown in Figures 7.13-7.15. For 8 and 16 nodes, the mean delay difference over all traffic rates is 340 ms (milliseconds) between PDMAC and DMAC, however, for 24 nodes the mean delay difference over all rates reduces to 40 ms.

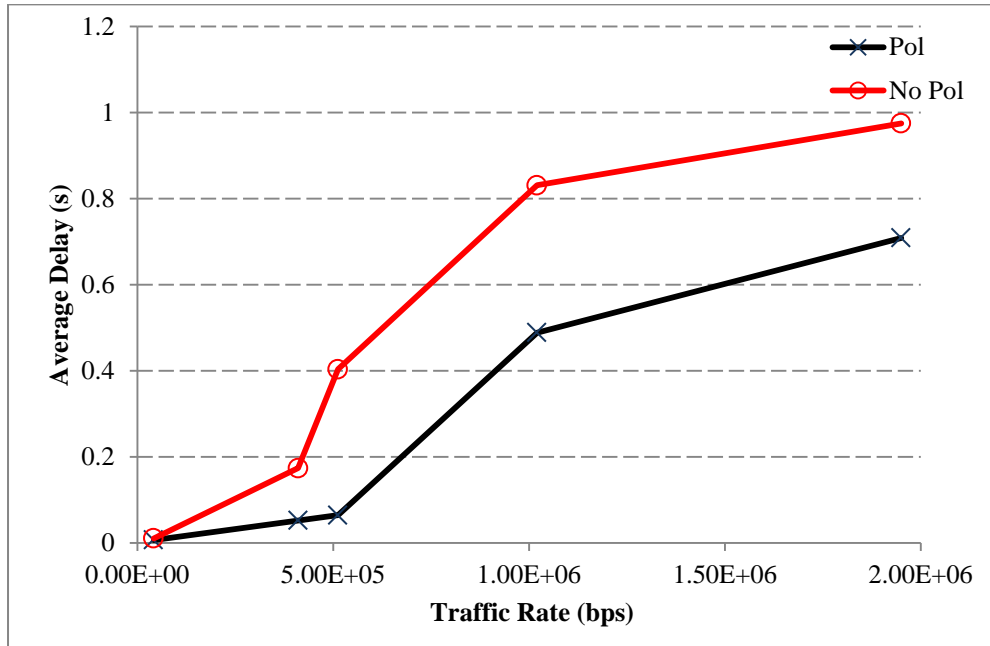


Figure 7.13 Comparison of average delay for 8 nodes

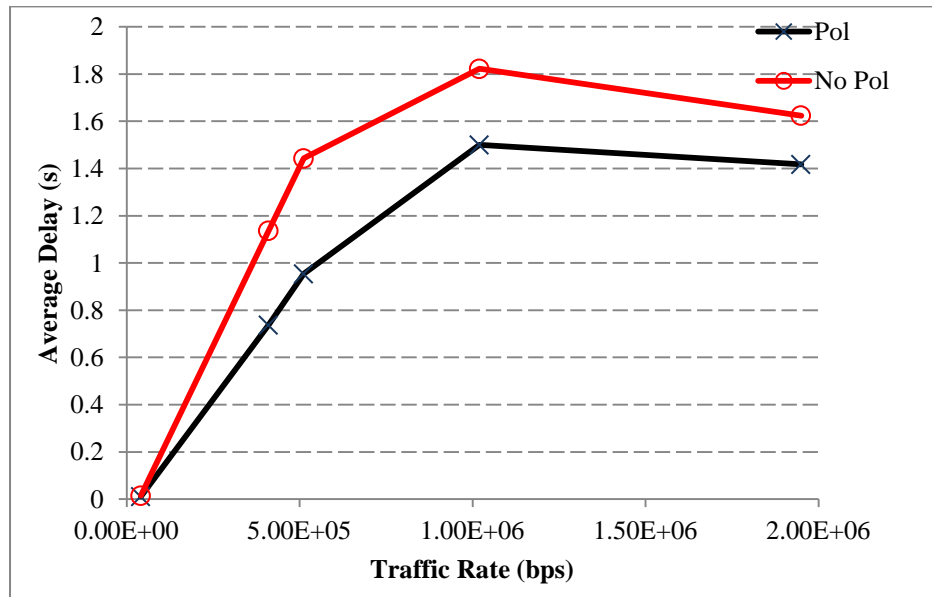


Figure 7.14 Comparison of average delay for 16 nodes

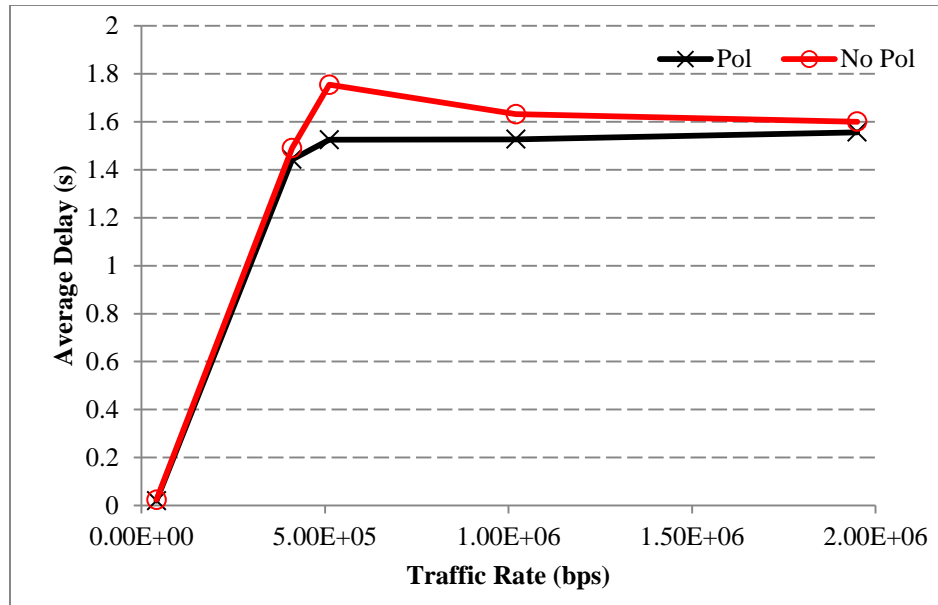


Figure 7.15 Comparison of average delay for 24 nodes

7.6 Concluding Remarks

A novel polarization diversity DMAC protocol (termed PDMAC) is proposed that is fully distributed, asynchronous, and compatible with the existing DMAC protocols. Each node senses directionally on both vertical and horizontal polarizations and dynamically adapts polarization to transmit to its respective destination which minimizes overall interference in the network and improves capacity. Based on generic pathloss model, we have established a bound on the average number of concurrently transmitting vertically and horizontally polarized nodes as a function of cross polarization ratio (*CPR*). Clearly, smaller value of polarization factor and smaller average source-destination distance separations allow for larger number of concurrently transmitting orthogonally polarized nodes. Further, we have also derived an approximate lower bound for the probability of successful transmission as a function of mean *CPR*. Derived lower bound depicts that ad hoc network capacity improves with higher polarization diversity and larger mean *CPR*. Simulations results show that PDMAC improves average node throughput compared to

basic DMAC protocol, particularly for a larger number of nodes in the network. For the worst case of 1.95 Mbps, the average throughput improvement due to PDMAC is about 2 % and 400 % for 8 and 32 nodes, respectively. Increase in average node throughput improvement for a larger number of nodes also validates that PDMAC is scalable compared to basic DMAC protocol. PDMAC average delay performance is also considerably better than DMAC protocol.

CHAPTER 8

CONCLUSION AND FUTURE DIRECTIONS

Wireless ad hoc network is expected to become an integral part of our everyday life. However, ad hoc network introduce many intrinsic challenges and constraints that require specialized cross layer solutions [17]. A conceptual cross layer framework based on vertical layer architecture with a detailed account of functional blocks and parameters for local and global performance optimization was presented [19]. Remainder of the dissertation focused on joint MAC and physical layer design for single-hop ad hoc networks, using cross layer information coupling and design coupling approaches. Specifically, we considered enhancement of throughput, delay, fairness, and scalability performance parameters. Significant and original contributions in this dissertation are listed below:

8.1 Main Contributions

- 1) *Finite Horizon Scheduling for Performance Improvement in Wireless Ad hoc Networks*

A simple multi-window adaptation approach for throughput maximization with fairness in a finite horizon is presented for wireless ad hoc network. In the proposed SR scheme thresholds are myopically adapted for performance improvement in each window. The attractive feature of the SR scheme is its simplicity because it only requires knowledge of the total backlog of all the users in a window. Simulation results clearly show that compared to non-cooperative random access scheme, SR scheme achieves stable

throughput performance, behaves fairly even under asymmetric channel conditions (fairness index remains 99 %), and is highly scalable [20].

Further, it is shown that throughput performance of SR scheme degrades in asymmetric channel condition. The proposed GR scheme (enhancement to SR scheme) dynamically adapts between fairness and throughput maximization depending upon channel conditions and the backlogs. It clearly outperforms the SR scheme in case of asymmetric channels. In the last part, we have derived a general sufficient condition for throughput guarantee using the GR scheduling scheme, which depends on the number of users, users' backlogs and channel states, and total sum of backlog-channel states product [21].

2) *Cooperative Relay Based MAC Protocols for Performance Enhancement in Wireless Ad hoc Networks*

Two novel relay-based cooperative MAC protocols, termed as 2rcMAC and IrcMAC, for ad hoc networks are proposed. 2rcMAC protocol makes use of two suitable relays for throughput and delay improvement. 2rcMAC adapts by switching between Utd mode and two-relay based approach that reduces transmission time with higher probability of success under fast fading conditions. Simulation results clearly show that 2rcMAC outperforms UtdMAC and CoopMAC I in terms of saturation throughput and delay as a function of distance and transmitting nodes [22].

IrcMAC protocol monitors instantaneous signal-to-noise ratio (snr) during handshake procedure and picks a relay path only when it incurs total transmission time (based on snr) less than the channel coherence time and the direct path transmission time. Thus, the relay is tapped only when it can offer reliable transmission path, otherwise direct transmission takes place. Simulation results for IrcMAC show average throughput

improvement of 41 % and 64 % and average delay improvement of 98.5 % and 99.7 % compared to UtdMAC and CoopMAC I protocols, respectively [23].

Furthermore, both protocols (2rcMAC and IrcMAC) introduce RR frame that resolves contentions among relay nodes and allows contending relays located in close proximity at the time to communicate rate information to the source node through single bit feedbacks.

3) *Adaptive DMAC Protocol with Integrated Destination Discovery for Performance Enhancement in Wireless Ad hoc Networks*

A novel neighbor discovery protocol is proposed as part of the directional MAC protocol (termed ADMAC) that estimates the probable region of destination based on the last sector, last known transmitter-receiver distance d , total elapsed time since last update $1/\mu$, average relative velocity v , and the beam-width α . Under high density, mobility and heavy load conditions, results confirm improved average throughput performance over LS and RS based DMAC approaches particularly at lower values of α (up to 40 % and greater than 400 % improvements over the LS based and the RS based DMAC protocols, respectively). Further, proposed ADMAC protocol is also scalable compared to LS and RS based DMAC protocols. Simulation results confirm enhanced performance of the ADMAC protocol [27].

4) *Polarization based DMAC Protocol for Performance Improvement in Wireless Ad hoc Networks*

A novel polarization diversity DMAC protocol (termed PDMAC) is proposed that is fully distributed, asynchronous, and compatible with the existing DMAC protocols. Each node senses directionally on both vertical and horizontal polarizations and dynamically adapts polarization to transmit to its respective destination which minimizes overall interference

in the network and improves capacity. Based on generic pathloss model, we have established a bound on the average number of concurrently transmitting vertically and horizontally polarized nodes as a function of cross polarization ratio (*CPR*). We have also derived a lower bound for the probability of successful transmission as a function of mean *CPR*. Derived lower bound depicts that ad hoc network capacity improves with higher polarization diversity and larger mean *CPR*. Simulations results show that PDMAC significantly improves average node throughput compared to basic DMAC protocol, particularly for a larger number of nodes in the network. For the worst case of 1.95 Mbps, the average throughput improvement due to PDMAC is about 2 % and 400 % for 8 and 32 nodes, respectively. Increase in average node throughput improvement for a larger number of nodes also validates that PDMAC is highly scalable compared to basic DMAC protocol. PDMAC average delay performance is also considerably better than DMAC protocol [28].

8.2 Future Directions

There are topics that remain unexplored and are closely related to our work. We envision the following extensions to the studies done in this dissertation:

- 1) Implementing the proposed vertical layer based cross layer framework under different applications scenarios would be an interesting future task.
- 2) Finite horizon scheduling considers homogeneous users with same priority. It would be interesting to see throughput and scalability limitations under heterogeneous users.
- 3) It would be interesting to investigate improvement in 2rcMAC protocol using network coding and spread spectrum techniques to resolve simultaneous relay contentions and improve throughput and delay performance.

- 4) It would be interesting to study the proposed ADMAC algorithm under different mobility models and optimal beam-width setting.

REFERENCES

- [1] S. Toumpis and D. Toumpakaris, "Wireless Ad hoc Networks and Related Topologies: Applications and Research Challenges," *Elektrotechnik and Informationstechnik*, Springer Wein, Vol. 123, No. 6, Oct. 2006.
- [2] S. Basagni, M. Conti, S. Giordano, I. Stojmenovic (Eds.), "Mobile Ad hoc Networking," IEEE Press and Wiley, 2004.
- [3] M. Conti and S. Giordano, "Multihop Ad hoc Networking: The Theory," *IEEE Communication Magazine*, pp. 78-86, April 2007.
- [4] M. Conti and S. Giordano, "Multihop Ad hoc Networking: The Reality," *IEEE Communication Magazine*, pp. 88-95, April 2007.
- [5] T. Calçada and M. Ricardo, "Extending the Coverage of a 4G Telecom Network Using Hybrid Ad-hoc Networks: A Case Study," *Challenges in Ad hoc Networking*, Springer Boston, Vol. 197, pp. 367-376, 2006.
- [6] A. Boukerche (Ed.), "Algorithms and Protocols for Wireless Sensor Networks," John Wiley and Sons, 2009.
- [7] I. Akyildiz, X. Wang and W. Wang, "Wireless Mesh Networks: A Survey," *Computer Networks Journal*, Elsevier, Vol. 47, Issue 4, pp. 445-487, Mar. 2005.
- [8] FleetNet Project: <http://www.et2.tu-harburg.de/fleetnet/index>.
- [9] Networks on Wheels Project: <http://www.network-on-wheels.de>.
- [10] P. Gupta and P.R. Kumar, "The Capacity of Wireless Networks," *IEEE Transaction on Information Theory*, Vol. 46, pp. 388-404, March 2000.
- [11] P. Gupta, R. Gray and P.R. Kumar, "An Experimental Scaling Law for Ad hoc Networks," http://black1.csl.uiuc.edu/~prkumar/html_files/postscript_files.html, 2001.
- [12] C. Tschudin, P. Gunningberg, H. Lundgren and E. Nordstrom, "Lessons from Experimental MANET Research," *Ad Hoc Networks Journal*, Special Issue on Ad Hoc Networking for Pervasive Systems, Elsevier, Vol. 3, No. 2, pp. 221-233, Mar. 2005.

- [13] H. Zhai and Y. Fang, "Distributed flow control and medium access in multihop ad hoc networks," *IEEE Trans. on Mobile Computing*, Vol. 5, No. 11, pp. 1503-1514, Nov. 2006.
- [14] M. Grossglauser and D. N. C. Tse, "Mobility Increases the Capacity of Ad-Hoc Wireless Networks," *IEEE/ACM Trans. on Networking*, Vol. 10, No. 4, pp. 477-486, Aug. 2002.
- [15] F. Foukalas, V. Gazis and N. Alonistioti, "Cross-Layer Design Proposals for Wireless Mobile Networks: A Survey and Taxonomy" *IEEE Communication Surveys*, Vol. 10, No. 1, pp. 70-85, 1st Quarter 2008.
- [16] V. Srivastava, M. Motani, "Cross-Layer Design: A Survey and the Road Ahead," *IEEE Communication Magazine*, Vol. 43, Issue 12, pp. 112-119, 2005.
- [17] R. Jurdak, "Wireless Ad hoc and Sensor Networks: A Cross Layer Design Perspective," Springer Science, 2007.
- [18] R. Jurdak, "Modeling and Optimization of Ad Hoc and Sensor Networks," Bren School of Information and Computer Science, University of California Irvine, Ph.D. Dissertation, Sept. 2005.
- [19] M. Khalid, R. Sankar and I. Ra, "Towards Cross Layer Framework for Ad hoc Wireless Networks," *IEEE Symposium on Computers and Communications (ISCC)*, Sousse, Tunisia, pp. 159-164, July 5-8, Tunisia, 2009.
- [20] M. Khalid, X. Le, I. Ra and R. Sankar, "Finite Horizon Scheduling in Wireless Ad hoc Networks," *IEEE Globecom Workshop*, Dec. 6-10, Florida, USA, 2010.
- [21] —, "Distributed Adaptive Scheduling for Finite Horizon in Wireless Ad hoc Networks," Submitted to *Journal of Communications*, 2010.
- [22] M. Khalid, Y. Wang, I. Ra, R. Sankar, "Two-Relay based Cooperative MAC Protocol for Wireless Ad hoc Networks," Submitted to *IEEE Transactions on Vehicular Technology*, VT-2010-01401 (under revision).
- [23] M. Khalid, Y. Wang, I. Butun, I. Ra, R. Sankar, "Coherence time Based Cooperative MAC Protocol for Wireless Ad hoc Networks," Submitted to *EURASIP Journal on Wireless Communications and Networking*, JWCN/850605 (under revision).
- [24] S. Bandyopadhyay, S. Roy and T. Ueda, "Enhancing Performance of Ad hoc Wireless Networks with Smart Antennas," Auerbach Publications, 2006.

- [25] M. Khalid, I-h Ra, Y. Joo and R. Sankar, "A Scenario-based Directional Communication Performance in Wireless Ad Hoc Networks," IEEE/IFIP Embedded and Ubiquitous Computing, pp. 266-271, Dec. 17-20, Shanghai, China, 2008.
- [26] —, "Directional Communication in Wireless Ad Hoc Networks- A Scenario," International Conference on Soft Computing and Intelligent Systems and International Symposium on Advanced Intelligent Systems (SCIS and ISIS), pp. 656-663, Sept. 17-21, Nagoya, Japan, 2008.
- [27] M. Khalid, X. Le, I. Ra and R. Sankar, "Adaptive Directional MAC with Integrated Destination Discovery for Ad Hoc Networks," IEEE Communication Letters, Vol. 14, No. 8, pp. 1-3, Aug. 2010.
- [28] —, "Polarization based Directional MAC Protocol for Ad Hoc Networks," accepted for publication in Ad hoc Networks Journal, Elsevier, 2011.
- [29] V. Kawadia and P.R. Kumar, "A Cautionary Perspective On Cross-Layer Design," IEEE Wireless Communications Magazine, pp. 3-11, February 2005.
- [30] T. Melodia, M.C. Vuran, and D. Pompili, "The state of the art in cross layer design for Wireless Sensor Networks," in Wireless Systems and Network Architectures in Next Generation Internet, Vol. 3883, pp. 78–92, Springer-Verlag, Berlin Heidelberg, 2006.
- [31] G. Dimic, N. D. Sidiropoulos, and R. Zhang, "Medium Access Control — Physical Cross-Layer Design," IEEE Signal Processing, Vol. 21, No. 5, pp. 40-50, Sept. 2004.
- [32] J. Mirkovic, G. Orfanos, H. Reumerman, and D. Denteneer, "A MAC Protocol for MIMO Based IEEE 802.11 Wireless Local Area Networks," IEEE WCNC, pp. 2133-2138, 2007.
- [33] T. Elbatt and T. Andersen, "Cross-layer Interference-aware Routing for Wireless Multi-hop Networks," IWCMC 2006.
- [34] D. Chafekar, V. Kumar, M. Marathe, S. Parthasarathy, and A. Srinivasan, "Cross-Layer Latency Minimization in Wireless Networks with SINR Constraints," ACM. Mobihoc, pp. 110-119, 2007.
- [35] G. Kulkarni, V. Raghunathan, and M. Srivastava, "Joint End-to-End Scheduling, Power Control and Rate Control in Multi-hop Wireless Networks," IEEE GLOBECOM , pp. 3357-3362, Dec. 2004.
- [36] L. Chen, S. Low, M. Chiang, and J. Doyle, "Cross-layer Congestion Control, Routing and Scheduling Design in Ad Hoc Wireless Networks," in Proceedings of INFOCOM, 2006.

- [37] T. Girici and A. Ephremides, "Joint Routing and Scheduling Metrics in Wireless Ad Hoc Networks," Proc. 36th Asilomar Conference on Signals Systems and Computers, Nov. 2002.
- [38] R. Cruz and A. Santhanam, "Optimal routing, link scheduling and power control in multi-hop wireless networks," in Proceedings of INFOCOM, pp. 702–711, San Francisco, USA, March 2003.
- [39] K. Chen, S.H. Shah and K. Nahrstedt, "Cross-layer Design for Data Accessibility in Mobile Ad Hoc Networks," Kluwer Wireless Personal Communications, 21:4976, 2002.
- [40] M. Tiado, R. Dhaou and A. Beylot, "A New Method for Cross-Layer Network Modeling and Simulation," June 2005, <http://whitepapers.techrepublic.com/abstract.aspx?docid=307826>.
- [41] V. Zaborovsky, A. Gorodetsky, and A. Lapin, "Network Complexity: Cross Layer Models and Characteristics," Advanced International Conference on Telecommunications, May 2007.
- [42] C. Barrett, M. Drozda, A. Marathe, and M.V. Marathe, "Characterizing the Interaction Between Routing and MAC Protocols in Ad-hoc Networks," ACM Mobihoc, pp. 92-103, June 2002.
- [43] M. Conti, G. Maselli, G. Turi, and S. Giordano, "Cross-Layering in Mobile Ad Hoc Network Design," IEEE Computer Society, Vol. 37, Issue 2, pp. 48-51, Feb. 2004.
- [44] H. Celebi and H. Arslan, "Enabling Location and Environment Awareness in Cognitive Radios," Elsevier Computer Communications-Special Issue on Advanced Location-Based Services, Vol. 31, Issue 6, pp. 1114-1125, Apr. 2008.
- [45] X. Liu, E. Chong, and N. Shroff, "Optimal opportunistic scheduling in wireless networks," in Proceedings of Vehicular Technology Conference 2003-Fall, Vol. 3, pp. 1417-1421, Oct. 2003.
- [46] D. Zheng, W. Ge, and J. Zhang, "Distributed opportunistic scheduling for ad-hoc networks with random access: An optimal stopping approach," IEEE Trans. on Information Theory, Jan 2009.
- [47] S. Chakrabarti and A. Mishra, "QoS issues in ad hoc wireless networks," IEEE Communications Magazine, Vol. 39, Issue 2, pp. 142-148, Feb. 2001.
- [48] R. Ramanathan and Martha Steenstrup, "Hierarchically-organized multihop mobile wireless networks for quality-of-service," Special Issue: Mobile multimedia communications, ACM, Vol. 3, Issue 1, pp. 101-119, June 1998.

- [49] S. Kulkarni and C. Rosenberg, "Opportunistic scheduling: Generalizations to include multiple constraints, multiple interfaces, and short term fairness," *Wireless Networks*, Vol. 11, Issue 5, pp. 557-569, Sept. 2005.
- [50] Q. Zhang, Q. Chen, F. Yang, X. Shen, Z. Niu, "Cooperative and opportunistic transmission for wireless ad hoc networks," *IEEE Networks*, Vol. 21, Issue 1, pp. 14-20, Feb. 2007.
- [51] Y. Cao and V. Li, "Scheduling algorithms in broadband wireless networks," *IEEE Proceedings*, Vol. 89, Issue. 1, pp. 76-87, Jan. 2001.
- [52] R. Knopp and P. Humblet, "Information capacity and power control in single cell multiuser communications," in *Proceedings of IEEE International Conference on Communications*, Seattle, USA, pp. 331-335, June 1995.
- [53] L. Yang and M. Alouini, "Performance analysis of multiuser selection diversity," in *Proceedings of IEEE International Conference on Communications*, Paris, France, pp. 3066-3070, June 2004.
- [54] E. Chaponniere, P. Black, J. Holtzman, D. Tse, "Transmitter directed code division multiple access system using path diversity to equitably maximize throughput," U.S. Patent # 6449490, Sept. 2002.
- [55] J. Holtzman, "Asymptotic analysis of proportional fair algorithm," in *Proceedings of IEEE Symposium on Personal, Indoor and Mobile Radio Communications*, Vol. 2, San Diego, USA, pp. 33-37, Sept. 2001.
- [56] M. Anderws, K. Kumaran, K. Ramanan, A. Stoylar, P. Whiting, and R. Vijaykumar, "Providing quality of service over a shared wireless link," *IEEE Communication Magazine*, Vol. 39, Issue 2, pp. 150-153, Feb. 2001.
- [57] M. Anderws, S. Borst, F. Dominique, P. Jelenkovic, K. Kumaran, K. Ramahrishnan, and P. Whiting, "Dynamic bandwidth allocation algorithms for high-speed data wireless networks," *Bell Labs Technical Report* 2000.
- [58] S. Shakkottai and A. Stoylar, "Scheduling algorithms for mixture of real-time and non real-time data in HDR," *Bell Labs Technical Report* 2000.
- [59] T. Bonald, "A score-based opportunistic scheduler for fading channels," in *Proceedings of European Wireless*, 2004.
- [60] X. Liu, E. Chong, N. Shroff, "A framework for opportunistic scheduling in wireless networks," *Computer Networks*, Elsevier, Vol. 41, Issue 4, pp. 451-474, Mar. 2003.

- [61] S. Borst and P. Whiting, "Dynamic rate control algorithms for HDR throughput optimization," in Proceedings of IEEE INFOCOM, Vol. 2, Alaska, USA, pp. 976-985, 2001.
- [62] S. Kulkarni and C. Rosenberg, "Opportunistic scheduling policies for wireless systems with short term fairness constraints," in Proceedings of IEEE Globecom, Vol. 1, pp. 533-537, Dec. 2003.
- [63] H. Bang, T. Ekman D. Gesbert, "A channel predictive proportional fair scheduling algorithm," in Proceedings of IEEE Workshop on Signal Processing Advances in Wireless Communications, New York, USA, pp. 620-624, June 2005.
- [64] R. Berry and R. Gallager, "Communications over fading channels with delay constraints," IEEE Trans. on Information Theory, Vol. 48, pp. 1135-1149, May 2002.
- [65] K. Jagannathan, S. Borst, P. Whiting and E. Modiano, "Efficient scheduling of multiuser multi-antenna systems," in Intl. Symposium on Modeling and Optimization in Mobile Ad Hoc and Wireless Networks, Boston, USA, pp. 1-8, Apr. 2006.
- [66] J. Hossain, M. Alouini and V. Bhargava, "Real-time multiresolution data transmission over correlated fading channels using hierarchical constellations," in Proceedings of IEEE Vehicular Technology Conference, Spring 2006.
- [67] M. Hu and J. Zhang, "Traffic Aided opportunistic scheduling for downlink transmissions: Algorithms and performance bounds," in Proceedings of IEEE INFOCOM, 2004.
- [68] M. Neely, E. Modiano and C. Li, "Fairness and optimal stochastic control for heterogeneous networks," IEEE/ACM Trans. on Networking, Vol. 16, Issue 2, pp. 396-409, Apr. 2008.
- [69] M. Ngo and V. Krishnamurthy, "On optimality of monotone channel-aware transmission policies: A constrained Markov decision process approach," in Proceedings of IEEE International Conference on Acoustic, Speech and Signal Processing, Vol. 3, pp. 621-624, Apr. 2007.
- [70] E. Altman and S. Stidham, "Optimality of monotonic policies for two-action Markovian decision processes, with applications to control of queues with delayed information," Queueing Systems, Springer, Vol. 21, Issue 3-4, pp. 267-291, Sept. 1995.
- [71] H. Hassanein and A. Safwat, "Virtual base stations for wireless mobile ad hoc communications: an Infrastructure for infrastructure-less," International Journal of Communications, 14:763, 2001.

- [72] A. Boukerche, "Handbook of Algorithms for Wireless Networking and Mobile Computing," Chapman and Hall, 2006.
- [73] P. Sadeghi, R. Kennedy, P. Rapajic and R. Shams, "Finite-State Markov Modeling of fading channels," IEEE Signal processing Magazine, Vol. 25. Issue 5, pp. 57-80, Sept. 2008.
- [74] P. Chaporkar, K. Kar, X. Luo, S. Sarkar, "Throughput and fairness guarantees through maximal scheduling in wireless networks," IEEE Trans. on Information Theory, Vol. 54, Issue 2, pp. 572-594, Feb. 2008.
- [75] L. Johnston and V. Krishnamurthy, "Opportunistic file transfer over a fading channel: A POMDP search theory formulation with optimal threshold policies," IEEE Trans. on Wireless Communications, Vol. 5, Issue 2, Feb. 2006.
- [76] M. Puterman, "Markov Decision Processes: Discrete Stochastic Dynamic Programming," Wiley-Interscience, 1st Edition, Apr. 1994.
- [77] R. K. Jain, D. W. Chiu, and W. R. Hawe, "A quantitative measure of fairness and discrimination for resource allocation and shared computer system," Technical Report DEC-TR-301, Digital Equipment Corporation, 1984.
- [78] NIST/SEMATECH e-Handbook of Statistical Methods, <http://www.itl.nist.gov/div898/handbook/>
- [79] V. Hassel, G. Oien and D. Gesbert, "Throughput guarantees for wireless networks with opportunistic scheduling: a comparative study," IEEE Transaction on Wireless Communications, Vol. 6, Issue 12, pp. 4215-4220, Dec. 2007.
- [80] http://en.wikipedia.org/wiki/Hoeffding%27s_inequality
- [81] J. Laneman, G. Wornell and D. Tse, "An Efficient Protocol for Realizing Cooperative Diversity in Wireless Networks," in Proc. IEEE ISIT, USA, pp. 294, June 2001.
- [82] A. Sendonaris, E. Erkip and B. Aazhang, "User Cooperation Diversity Part I: System Description," IEEE Trans. Communication, Vol. 51, No.11, pp. 1927-1938, 2003
- [83] T. Ho and D. S. Lun, "Network Coding: An Introduction," Cambridge University Press, Cambridge, U.K., April 2008.
- [84] P. Liu, Z. Tao and S. Panwar, "A Co-operative MAC Protocol for Wireless Local Area Networks," Proc. IEEE International Conference on Communications (ICC), Seoul, Korea, pp. 2962-2968, May 2005.
- [85] P. Liu, Z. Tao, S. Narayanan, T. Korakis and S. Panwar, "CoopMAC: A Cooperative MAC for Wireless LANs, IEEE JSAC, Vol. 25, No. 2, Feb. 2007.

- [86] T. Korakis, Z. Tao, Y. Slutskiy and S. Panwar, "A Cooperative MAC Protocol for Ad hoc Networks," IEEE Pervasive Computing and Communications Workshop (PerComW), USA, Mar. 2007.
- [87] N. Agarwal, D. Channe Gowda, L. Kannan, M. Tacca and A. Fumagalli, "IEEE 802.11b Cooperative Protocols: A Performance Study," LNCS, Vol. 4479/2007, pp. 415-426, 2007.
- [88] H. Zhu and G. Cao, "rDCF: A Relay-Enabled Medium Access Control Protocol for Wireless Ad Hoc Networks," IEEE Transaction on Mobile Computing, Vol. 5, No. 9, pp 1201-1214, Sept. 2006.
- [89] H. Zhu and G. Cao, "On Improving the Performance of IEEE 802.11 with Relay-Enabled PCF," ACM/Kluwer Mobile Networking and Applications (MONET), Vol. 9, pp. 423-434, 2004.
- [90] "IEEE Std. 802.11b-1999, Part 11: Wireless LAN Medium Access Control (MAC) and Physical Layer (PHY) Specifications: High-Speed Physical Layer Extension in the 2.4 GHz Band," 1999.
- [91] Andrea Goldsmith, "Wireless Communications," Cambridge University Press, 2006
- [92] G. Bianchi, "Performance Analysis of the IEEE 802.11 Distributed Coordination Function," IEEE Journal Selected Areas Communication, Vol. 18, No. 3, pp. 535-547, Mar. 2000.
- [93] K. Fakih, J. Diouris and G. Andrieux, "Beamforming in Ad Hoc Networks: MAC Design and Performance Modeling," EURASIP Journal on Wireless Communications and Networking, Vol. 2009, ID839421, pp. 1-15, 2009.
- [94] T. Rappaport, "Wireless Communications Principles and Practices," Prentice Hall Communications, 2nd Ed., 2002.
- [95] Recommendation ITU-R M.1225, <http://www.itu.int/oth/R0A0E00000C/en>, Feb. 2009.
- [96] R. Choudhury, X. Yang, R. Ramanathan and N. Vaidya, "On Designing MAC Protocols for Wireless Networks Using Directional Antennas," IEEE Transaction on Mobile Computing, Vol. 5, No. 5, May 2006.
- [97] R. Ramanathan, "On the Performance of Ad Hoc Networks with Beamforming Antennas," in Proc. MobiHoc, Long Beach, USA, June 2001.
- [98] T. Ueda, S. Bandyopadhyay and K. Hasuike, "An adaptive Media Access Control Protocol and System Performance of Wireless Ad Hoc Network using Smart antenna," Electronics and Communications In Japan, Part I, Vol. 87, No. 3, pp. 50-58, Wiley Periodicals, 2004.

- [99] A. Nasipuri, S. Ye, J. You and R. Hiromoto, "A MAC Protocol for Mobile Ad Hoc Networks using Directional Antennas," IEEE WCNC, pp. 1214-1219, Chicago, IL, Sept. 2000.
- [100] S. Bandyopadhyay, M. Pal, D. Saha, T. Ueda, K. Hasuike and R. Pal, "Improving System Performance of Ad Hoc Wireless Network with Directional Antenna," IEEE Conference on Communications, Alaska, Vol. 2, pp. 1146-1150, May 2003.
- [101] S. Bandyopadhyay, "An Adaptive MAC Protocol for Ad-Hoc Networks with Directional Antennas", IEICE Trans. Comm., Vol. E84-B, No.11, Nov. 2001.
- [102] G. Jakllari, W. Luo and S. Krishnamurthy, "An integrated Neighbor Discovery and MAC Protocol for Ad Hoc Networks Using Directional Antennas," IEEE Transaction on Wireless Communications, Vol. 6, No. 3, pp. 1114-1124, Mar. 2007.
- [103] E. Shihab, L. Cai and J. Pan, "A Distributed, Asynchronous Directional-to-Directional MAC Protocol for Wireless Ad Hoc Networks," IEEE Trans. Vehicular Technology, Apr. 2009.
- [104] M. Takata, M. Bandai and T. Watanabe, "Performance Evaluation of Directional MAC Protocols for Deafness Problem in Ad hoc Networks," IPSJ Digital Courier, Vol. 3, pp. 468-479, July 2007.
- [105] R. Choudhury, X. Yang, R. Ramanathan and N. Vaidya, "Using Directional Antennas for Medium Access Control in Ad Hoc Networks", in Proc. ACM Mobicom, Atlanta, Georgia, Sept. 2002.
- [106] A. Munari, F. Rossetto and M. Zorzi, "A New Cooperative Strategy for Deafness Prevention in Directional Ad Hoc Networks," Internation Conference on communications (ICC), pp. 3154-3160, 2007.
- [107] A. Nasipuri, K. Li and U. Sappidi, "Power Consumption and Throughput in Mobile Ad Hoc Networks Using Directional Antennas," IEEE International Conference on Computer Communications and Networks, Oct. 14-16, Miami, Florida, 2002.
- [108] R. Ramanathan, "On the Performance of Ad Hoc Networks with Beamforming Antennas," ACM Mobihoc, Oct. 2001.
- [109] B. Alawieh, C. Assi, "Distributed Correlative Power Control Schemes for Mobile Ad Hoc Networks Using Directional Antennas," IEEE Transactions On Vehicular Technology, Vol. 57, No. 3, May 2008.
- [110] S. Narayanaswamy, V. Kawadia, R. Sreenivas and P. Kumar, "Power Control in Ad hoc Networks: Theory, Architecture, Algorithm and Implementation of the COMPOW Protocol," European Wireless Conference, Florence, Italy 2002.

- [111] IEEE Standard for Wireless LAN Medium Access Control and Physical layer Specifications, Nov. 1997, P802.11.
- [112] Y. Ko, V. Shankarkumar and N. Vaidya, "Medium Access Control Protocols Using Directional Antennas In Ad Hoc Networks," IEEE INFOCOM, Mar. 2000.
- [113] "QualNet simulator," Scalable Network Technologies. [www.scalable-networks.com.]
- [114] R. Choudhury and N. Vaidya, "Impact of Directional Antennas on Ad Hoc Routing," Personal Wireless Communications, Vol. 2775, pp. 590-600, Springer Berlin/Heidelberg, 2003.
- [115] S. Bandyopadhyay, K. Hasuike, S. Horisawa and S. Tawara, "An Adaptive MAC Protocol for Wireless Ad Hoc Community Network (WACNet) Using Electronically Steerable Passive Array Radiator Antenna," IEEE Globecom, pp. 25-29, San Antonio, Texas, Nov. 2001.
- [116] M. Takai, J. Martin, A. Ren and R. Bagrodia, "Directional Virtual Carrier Sensing for Directional Antennas in Mobile Ad Hoc Networks," ACM Mobihoc, June 2002.
- [117] Y. Wang and J. Garcia-Luna-Aceves, "Spatial Reuse and Collision Avoidance in Ad Hoc Networks with Directional Antennas," IEEE Globecom, Vol. 1, pp. 112-116, Nov. 2002.
- [118] T. Tang, M. Park, R. Heath and S. Nettles, "A Joint MIMO-OFDM Transceiver and MAC Design for Mobile Ad Hoc Networking," International Workshop on Wireless Ad Hoc Networking, pp. 315-319, May 31 - June 3, Oulu, Finland, 2004.
- [119] M. Siam and M. Krunz, "Channel Access Scheme for MIMO Enabled Ad Hoc Networks with Adaptive Diversity/Multiplexing Gains," Journal of Mobile Networks and Applications, Springer, Vol. 14, No. 4, pp. 433-450, Aug. 2009.
- [120] B. Chen and M.J. Gans, "MIMO Communications in Ad Hoc Networks," IEEE Transaction on Signal Processing, Vol. 54, pp. 2773-2783, July 2006.
- [121] J. Zander, "Slotted Aloha Multihop Packet Radio Networks with Directional Antennas, IET Electronic Letters, Vol. 26, No. 25, 1990.
- [122] A. Nasipuri, J. Zhuang, S.R. Das, "A Multichannel CSMA MAC Protocol for Multihop Wireless Networks," in Proc. of the IEEE Wireless Communications and Networking Conference (WCNC), pp. 1402-1406, Sept. 1999.

- [123] J. So and N.H. Vaidya, "Multi-Channel MAC for Ad Hoc Networks: Handling Multi-Channel Hidden Terminals Using A Single Transceiver," ACM MOBIHOC, May 24–26, 2004.
- [124] J. Deng, Z.J. Haas, "Dual Busy Tone Multiple Access (DBTMA): A Medium Access Control for Multihop Networks," in Proc. IEEE Wireless Communications and Networking Conference, New Orleans, Louisiana, September 1999.
- [125] N. Jain, S.R. Das, A. Nasipuri, "A Multichannel MAC Protocol with Receiver based Channel Selection for Multihop Wireless Networks," in Proc. of the 10th International Conference on Computer Communications and Networks (ICCCN), pp. 432-439, 2001.
- [126] S.L. Wu, Y.C. Tseng, C.Y. Lin and J.P. Sheu, "A Multi-Channel MAC Protocol with Power Control for Multi-hop Mobile Ad hoc Networks," The Computer Journal, Vol. 45, No. 1, pp. 101-110, 2002.
- [127] R. Ramanathan, J. Redi, C. Santivanez, D. Wiggins and S. Polit, "Ad Hoc Networking with Directional Antennas: A Complete Solution," IEEE Journal on Selected Areas in Communications, Vol. 23, No. 3, pp. 496-506, Mar. 2005.
- [128] A. Muqattash, M. Krunz, "POWMAC: A Single-Channel Power-Control Protocol for Throughput Enhancement in Wireless Ad Hoc Networks," IEEE Journal on Selected Areas in Communications, Vol. 23, No. 5, pp. 1067-1084, May 2005.
- [129] Z. Xiaodong, L. Jiandong and Z. Dongfang, "A Novel Power Control Multiple Access Protocol for Ad Hoc Networks with Directional Antennas," in Proc. International Conference on Advanced Information Networking and Applications (AINA), 2006.
- [130] V. Erceg, P. Soma, D.S. Baum and S. Catreux, "Multiple-Input Multiple-Output Fixed Wireless Radio Channel Measurements and Modeling Using Dual-Polarized Antennas at 2.5 GHz," IEEE Trans. on Wireless Communications, Vol. 3, No. 6, pp. 2288-2298, Nov. 2004.
- [131] H. Xiao, S. Ouyang, Z. Nie, "The Cross Polarization Discrimination of MIMO Antennas at Mobile Station," International Conference on Communication, Circuits and Systems (ICCCAS), pp. 203-206, 2008.
- [132] P. Soma, D.S. Baum, V. Erceg, R. Krishnamurthy, A.J. Paulraj, "Analysis and Modeling of Multiple-input multiple-output (MIMO) Radio Channel based on Outdoor Measurements Conducted at 2.5 GHz for Fixed BWA Applications," IEEE International Conference on Communications (ICC), Vol. 1, pp. 272-276, 2002.

- [133] R. Valentin, H. Giloi and K. Metzger, "Performance of Digital Radio Systems in Co-Channel Cross-Polarized Operation," IEEE GLOBECOM, Vol. 3, pp. 1791-1795, 1991.
- [134] T. Yildirim and L. Huaping, "Directional MAC for 60 GHz Using Polarization Diversity Extension (DMAC-PDX)," IEEE GLOBECOM, pp. 4697-4701, 2007.
- [135] H. Laitinen, K. Kalliola, and P. Vainikainen, "Angular Signal Distribution and Cross-Polarization Power Ratio Seen by a Mobile Receiver at 2.15 GHz," in Proc. Millennium Conference on Antennas and Propagation (AP), Davos, Switzerland, April 2000.
- [136] D. Cox, R. Murray, H. Arnold, A. Norris and M. Wazowicz, "Cross-Polarization Coupling Measured for 800 MHz Radio Transmission in and around Houses and Large Buildings," IEEE Trans. On Antennas and Propagation, Vol. 34, No. 1, pp. 83-87, 1986.
- [137] K. Kalliola, H. Laitinen, K. Sulonen, L. Vuokko and P. Vainikainen, "Directional Radio Channel Measurements at Mobile Station in Different Radio Environments at 2.15 GHz," European Personal Mobile Communications Conference (EPMCC), Vienna, Feb. 2001.
- [138] M. Murli, S.K. Behera and P.K. Sahul, "Design of Single Feed Dual Polarized and Dual Frequency Rectangular Patch Antenna," 5th International Conference on Microwave, Antenna, Propagation and Remote Sensing, Dec. 2009.
- [139] H. Chuang, L. Kuo, C. Lin and W. Chen, "A 2.4 GHz Polarization-Diversity Planar Printed Antenna for WLAN and Wireless Communication Systems," IEEE International Symposium on Antennas and Propagation, Vol. 4, pp. 76-79, 2002.
- [140] A. Spyropoulos and C.S. Raghavendra, "Asymptotic Capacity Bounds for Ad hoc Networks revisited: The Directional and Smart Antennas Cases," IEEE GLOBECOM, Vol. 3, pp. 1216-1220, 2003.
- [141] S. Yi, Y. Pei and S. Kalyanaraman, "On the Capacity Improvement of Ad Hoc Wireless Networks Using Directional Antennas," MOBIHOC, USA, June 2003.
- [142] A. Papoulis and S.U. Pillai, "Probability, Random Variables and Stochastic Processes," McGraw Hill, 4th Ed. 2002.
- [143] A. Nasipuri, and K. Li, "A Directionality-based Location Discovery Scheme for Wireless Sensor Networks," in Proc. 1st ACM International Workshop on Wireless Sensor Networks and Applications, Atlanta, Georgia, Sept. 2002.

APPENDICES

Appendix A

AWARENESS PARAMETERS	INTERFACE	AWARENESS DESCRIPTORS	SUMMARY
Energy	System and User Interface	System Awareness	Represents energy state of the node (local view)
System Interrupt	System and User Interface	System Awareness	Represents system bugs, loops, failures and interrupts (local view)
Meteorological State	Protocol Stack Interface (source: PHY Layer)	Meteorological Awareness	Represents weather state for adaptation (local view)
Topographical State	Protocol Stack Interface (source: PHY Layer)	Topographical Awareness	Represents detailed terrain, vegetation, buildings, Google map information for adaptation (local view)
Modulation and Coding	Protocol Stack Interface (source: PHY and MAC Layers)	Protocol Stack Awareness	Represents modulation and coding used for transmission (local view)
Antenna Mode	Protocol Stack Interface (source: PHY and MAC Layers)	RF Awareness	Represents multi-antenna multiplexing, diversity or beam-forming modes (local view)
Protocol Suite	Protocol Stack Interface (source: All Layers)	Protocol Stack Awareness	Represents protocol combinations used through all the layers (local view)
RF State	Protocol Stack Interface (source: PHY Layer)	RF Awareness	Represents RF parameters: Angular Spread, Delay Spread, Doppler Spread, Signal-to-Noise Plus Interference, BER, Signal Strength, Power, Frequency Band (local view)
MAC State	Protocol Stack Interface (source: MAC Layer)	Protocol Stack Awareness, Network Awareness	Represents MAC layer parameters: No. of stations, No. of retransmissions, Messages to/from PHY layer, No. of ACKs, ARQ techniques, Back-off techniques, Average Back-off window size (local view)

Appendix A (Continued)

AWARENESS PARAMETERS	INTERFACE	AWARENESS DESCRIPTORS	SUMMARY
NET State	Protocol Stack Interface (source: NET Layer)	Protocol Stack Awareness, Network Awareness	Represents Network layer parameters: ICMP control parameters (if enabled), No. of Route Requests, No. of Route Updates, No. of Route Errors, Average data and control queue length, Average data and control queue delay, No. of fragments to MAC layer, No. of fragment retransmissions, No. of hops, TTL, Queue policy, Scheduling policy (global and local view)
TRAN State	Protocol Stack Interface (source: TRAN Layer)	Protocol Stack Awareness, Network Awareness	Represents Transport layer parameters: Control messages, RTT, No. of DuPACK, No. of ACKs, Window Size, No. of packets exchanged with adjacent layers, No. of packets retransmitted, MTU size, Control messages (global and local view)
User Time and Location	System and User Interface	User Awareness	Represents user behavior in time and space using GPS based Location Awareness (local view)
User Interrupt	System and User Interface	User Awareness	Represents user command (local view)
Network Type	Protocol Stack Interface (source: All Layers)	Network Awareness	Represents network service type, security policy, network mode, (global view)
Application Type	Protocol Layer Interface (source: App Layer)	Application Awareness	Represents real time, non real time performance constraints, security and encryption constraints

Appendix B

The probability of success for any i_{th} user is given as,

$$P_{S_t}^{(i)} = \tau_t^{(i)} * P_{g_t}^{(i)} * \left\{ \prod_{\substack{j=1 \\ j \neq i}}^n (1 - \tau_t^{(j)} P_{g_t}^{(j)}) \right\} \quad (\text{B.1})$$

For simple ratio (SR) based scheme the adaptive probability of transmission in a slot is

given by, $\tau_t^{*(i)} = \frac{\eta_t^i}{\sum_{k=1}^n \eta_t^k}$. Plugging $\tau_t^{*(i)}$ into (B.1) gives us,

$$P_{S_t}^{(i)} = \frac{\eta_t^{(i)}}{\sum_{k=1}^n \eta_t^{(k)}} * P_{g_t}^{(i)} * \left\{ \prod_{\substack{j=1 \\ j \neq i}}^n \left(1 - \frac{\eta_t^{(j)}}{\sum_{k=1}^n \eta_t^{(k)}} P_{g_t}^{(j)} \right) \right\}. \quad (\text{B.2})$$

Taking $\sum_{k=1}^n \eta_t^{(k)}$ as common and simplifying leads to,

$$P_{S_t}^{(i)} = \frac{\eta_t^{(i)}}{\left\{ \sum_{k=1}^n \eta_t^{(k)} \right\}^n} * P_{g_t}^{(i)} * \left\{ \prod_{\substack{j=1 \\ j \neq i}}^n \left(\sum_{k=1}^n \eta_t^{(k)} - \eta_t^{(j)} P_{g_t}^{(j)} \right) \right\}. \quad (\text{B.3})$$

Appendix C

We first define the following constants (ignoring propagation delays): $T_c = DIFS + RTS + SIFS + CTS + SIFS$; $\hat{T}_c = T_c + headers + payload_{SD} + SIFS$; $T_{2c} = T_c + RRF + SIFS$; and $T_{cp} = T_c + HTS + SIFS$, then we calculate the average successful transmission time ($\bar{T}_{s,x}$) and average failure time ($\bar{T}_{f,x}$) as in (C.1)-(C.6), where, $payload_{r2D}$ above represents payload transmission time from relay 2 (backup relay) to the destination which depends on their distance separation. Further, HTS packet is sent by the helper to the source, RTSE represents RTS extension field used in CoopMAC I

$$\text{and } Eboff_{sx} = \frac{(\sum_{j=0}^{\bar{K}_x} E[CW_j])}{(\bar{K}_x + 1)}.$$

$$\bar{T}_{s_utd} = P_{SD} \cdot (\hat{T}_c + Eboff_{sutd} + ACK) + (1 - P_{SD}) \cdot P_{Sr1} \cdot P_{r1D} \cdot (\hat{T}_c + Eboff_{sutd} + SIFS + headers + payload_{r1D} + 2SIFS + 2ACK); \quad (C.1)$$

$$\bar{T}_{f_utd} = (1 - P_{SD}) \cdot \{(1 - P_{Sr1}) \cdot P_{r1D} \cdot (\hat{T}_c + Eboff_{futd} + SIFS) + P_{Sr1} \cdot (1 - P_{r1D}) \cdot (\hat{T}_c + Eboff_{futd} + SIFS + headers + payload_{r1D} + 2SIFS) + (1 - P_{Sr1}) \cdot (1 - P_{r1D}) \cdot (\hat{T}_c + Eboff_{futd} + SIFS)\}; \quad (C.2)$$

$$\bar{T}_{s_coop} = P_o \{P_{SD} (\hat{T}_c + Eboff_{scoop} + RTSE + HTS + SIFS + ACK)\} + (1 - P_o) \cdot \{P_{Sr1} \cdot P_{r1D} \cdot (T_{cp} + Eboff_{scoop} + RTSE + 2headers + payload_{Sr1} + payload_{r1D} + 2SIFS + ACK)\}; \quad (C.3)$$

$$\bar{T}_{f_coop} = P_o \{(1 - P_{SD}) \cdot (\hat{T}_c + Eboff_{fcoop} + RTSE + HTS + SIFS + SIFS)\} + (1 - P_o) \cdot \{(1 - P_{Sr1}) \cdot P_{r1D} \cdot (T_{cp} + Eboff_{fcoop} + RTSE + headers + payload_{Sr1} + 2SIFS) + P_{Sr1} \cdot (1 - P_{r1D}) \cdot (T_{cp} + Eboff_{fcoop} + RTSE + 2headers + payload_{Sr1} + payload_{r1D} + 3SIFS) + (1 - P_{Sr1}) \cdot (1 - P_{r1D}) \cdot (T_{cp} + Eboff_{fcoop} + RTSE + headers + payload_{Sr1} + 2SIFS)\}; \quad (C.4)$$

Appendix C (Continued)

$$\begin{aligned}
\bar{T}_{s_2rcmac} = & (\dot{P}_2) \cdot \left\{ P_{SD} \cdot (\dot{T}_c + Ebofff_{s2rc} + RRF + SIFS + ACK) + (1 - P_{SD}) \cdot \{ P_{Sr1} \cdot P_{r1D} \cdot (\dot{T}_c + \right. \\
& Ebofff_{s2rc} + RRF + SIFS + SIFS + headers + payload_{r1D} + SIFS + ACK) \} \} + (1 - \\
& P_2) \cdot \{ P_{Sr1} \cdot P_{r1D} \cdot \{ T_{2c} + Ebofff_{s2rc} + 2headers + payload_{Sr1} + payload_{r1D} + 2SIFS + \\
& ACK \} + P_{Sr1} \cdot (1 - P_{r1D}) \{ P_{Sr2} \cdot P_{r2D} \cdot (T_{2c} + Ebofff_{s2rc} + 3headers + payload_{Sr1} + \\
& payload_{r1D} + payload_{r2D} + 4SIFS + ACK) \} + (1 - P_{Sr1}) \cdot P_{r1D} \{ P_{Sr2} \cdot P_{r2D} \cdot (T_{2c} + \\
& Ebofff_{s2rc} + 2headers + payload_{Sr1} + payload_{r2D} + 3SIFS + ACK) \} + \\
& (1 - P_{Sr1}) \cdot (1 - P_{r1D}) \{ P_{Sr2} \cdot P_{r2D} \cdot (T_{2c} + Ebofff_{s2rc} + 2headers + payload_{Sr1} + \\
& payload_{r2D} + 3SIFS + ACK) \} \}; \tag{C.5}
\end{aligned}$$

$$\begin{aligned}
\bar{T}_{f_2rcmac} = & (\dot{P}_2) \cdot \left\{ (1 - P_{SD}) \cdot \{ (1 - P_{Sr1}) \cdot P_{r1D} \cdot (\dot{T}_c + Ebofff_{f2rc} + RRF + SIFS + \right. \\
& SIFS) + P_{Sr1} \cdot (1 - P_{r1D}) \cdot (\dot{T}_c + Ebofff_{f2rc} + RRF + SIFS + SIFS + headers + \\
& payload_{r1D} + 2SIFS) + (1 - P_{Sr1}) \cdot (1 - P_{r1D}) \cdot (\dot{T}_c + Ebofff_{f2rc} + RRF + SIFS + \\
& SIFS) \} \} + (1 - P_2) \cdot \left\{ P_{Sr1} \cdot (1 - P_{r1D}) \{ (1 - P_{Sr2}) \cdot P_{r2D} \cdot (T_{2c} + Ebofff_{f2rc} + \right. \\
& 2headers + payload_{Sr1} + payload_{r1D} + 3SIFS) + P_{Sr2} \cdot (1 - P_{r2D}) \cdot (T_{2c} + \\
& Ebofff_{f2rc} + 3headers + payload_{Sr1} + payload_{r1D} + payload_{r2D} + 5SIFS) + \\
& (1 - P_{Sr2}) \cdot (1 - P_{r2D}) \cdot (T_{2c} + Ebofff_{f2rc} + 2headers + payload_{Sr1} + payload_{r1D} + \\
& 3SIFS) \} + (1 - P_{Sr1}) \cdot P_{r1D} \{ (1 - P_{Sr2}) \cdot P_{r2D} \cdot (T_{2c} + Ebofff_{f2rc} + headers + \\
& payload_{Sr1} + 3SIFS) + P_{Sr2} \cdot (1 - P_{r2D}) \cdot (T_{2c} + Ebofff_{f2rc} + 2headers + \\
& payload_{Sr1} + payload_{r2D} + 4SIFS) + (1 - P_{Sr2}) \cdot (1 - P_{r2D}) \cdot (T_{2c} + Ebofff_{f2rc} + \\
& headers + payload_{Sr1} + 3SIFS) \} + (1 - P_{Sr1}) \cdot (1 - P_{r1D}) \{ (1 - P_{Sr2}) \cdot P_{r2D} \cdot (T_{2c} + \\
& Ebofff_{f2rc} + headers + payload_{Sr1} + 3SIFS) + P_{Sr2} \cdot (1 - P_{r2D}) \cdot (T_{2c} + Ebofff_{f2rc} + \\
& 2headers + payload_{Sr1} + payload_{r2D} + 4SIFS) + (1 - P_{Sr2}) \cdot (1 - P_{r2D}) \cdot (T_{2c} + \\
& Ebofff_{f2rc} + headers + payload_{Sr1} + 3SIFS) \} \}. \tag{C.6}
\end{aligned}$$

ABOUT THE AUTHOR

Murad Khalid received his B.S. degree (SUMMA CUM LAUDE) in Electrical Engineering from the City College of the City University of New York (CUNY) in 1993 and the M.S. degree in Electrical Engineering from the City College of the City University of New York (CUNY) in 1995. He is currently pursuing his Ph.D. in Electrical Engineering Department at the University of South Florida, Tampa, Florida. His research interests include using cross layer techniques for performance enhancement in wireless ad hoc networks.